DOCTOR OF PHILOSOPHY

Dock180/Elmo proteins are critical regulators of phagocytosis,macropinocytosis and chemotaxis in Dictyostelium

Wang, Jun

Award date:
2006

Dock180/Elmo proteins are critical regulators of phagocytosis,macropinocytosis and chemotaxis in Dictyostelium

Jun Wang

2006

University of Dundee

2006

Dock180/Elmo proteins are critical regulators of phagocytosis, macropinocytosis and chemotaxis in Dictyostelium

Author: Jun Wang

Supervisor: Prof. Cornelis J Weijer FRSE

A thesis presented for the degree of
Doctor of Philosophy at the
University of Dundee, UK
February 2006

Contents

Acknowledgements

First of all, I would like to thank Prof. Kees Weijer for giving me the opportunity to do my PhD under his guidance. His analytical perusal of the manuscript is highly acknowledged. It was indeed a pleasure for me to work in his group.

I record my special thanks to Gerti Weijer for helping me in learning the molecular biological work from very beginning and organising numerous wonderful parties in her house. All of her help is really unforgettable.

I thank Dr. Dirk Dormann very much for his efficient technical assistance. He helped me out of endless problems with microscopy imaging.

To my good friend Dr. Xuesong Yang, I pay my sincere thanks for show me the interesting life in Scotland and his practical advice.

I also own my thanks to all lab colleagues and the members of the Williams, Schaap and Näthke labs for their friendship and help.

My final, and most heartfelt, acknowledgment must go to my family. Without their long lasting encouragement and support, it would be impossible to complete this work.

Jun Wang

Declarations

I certify that I am the sole author of this thesis and that I have consulted all references cited. The work of which this thesis is a record has been carried out exclusively by myself, unless indicated otherwise, and has not previously been accepted for a higher degree.

Signed: 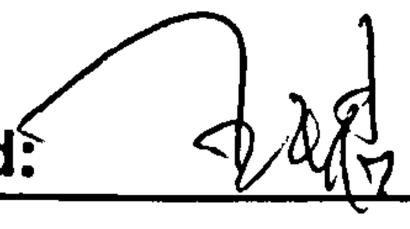 **Date:** 03/05/06

(Jun Wang)

I certify that Jun Wang has spent the equivalent of at least nine terms in research work in the Division of Cell and Developmental Biology, University of Dundee, that he has fulfilled the conditions of the Ordinance General No. 39 of the University of Dundee and is qualified to submit the accompanying thesis in application for the degree of Doctor of Philosophy.

Signed: 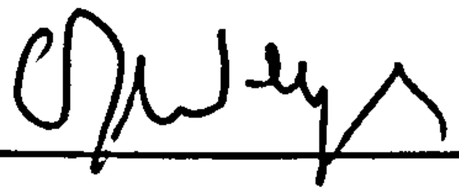 **Date:** 3/5/06

(Prof. Cornelis J. Weijer)

Summary

In this study, we report the characterization of Dock/Elmo proteins, a novel family of RacGEF's in *Dictyostelium discoideum* and describe their role in phagocytosis, macropinocytosis and cAMP mediated chemotactic cell movement. Aggregation competent *Dictyostelium* cells can detect and move up cAMP gradients. cAMP stimulation causes a transient localized increase in phosphatidyl inositol (3,4,5) tris phosphate (PIP3) concentration in the plasma membrane at the cell's leading edge. PIP3 binding domain containing RacGEF's are thought to mediate the cAMP signal through the activation of Racs to localised actin polymerization, which results in further extension of the leading edge in the direction of the cAMP gradient. However inhibition of PIP3 formation, through inhibition of PI3K activity, results only in a partial defect of chemotaxis, implying that there may exist other signalling pathways that mediate the cAMP signal to the cytoskeleton. Members of the Dock family form a novel class of Rac activators and deletion of *dock* in *Drosophila* and *C.elegans* results in chemotaxis and phagocytosis defects. We have identified the 8 *dock* genes and 4 *elmo* genes in the *Dictyostelium genome,* which we named *dockA-H* and *elmo1-4*. To investigate the role of Dock/Elmo, we generated null mutant strains (*dockA*^{null}, *dockB*^{null}, *dockA/B*^{null}, *dockC*^{null}, *dockD*^{null}, *dockG*^{null}, *dockH*^{null}, *elmo1*^{null} and elmo1/*dockB*^{null}) by gene disruption using homologous recombination.

In our study, knockout *dock* genes in *Dictyostelium* results in numerous defects. *dockA*^{null} cells show a slow chemotactic response to cAMP and reduced rate in

macropinocytosis. *dockA*^{null} slugs show poor phototaxis. *dockB*^{null} cells grow slowly in the axenic medium and are defective in chemotaxis, macropinocytosis and phagocytosis. *dockA/B* double mutant cells show stronger defects in chemotaxis than either mutant by itself. In the *dockA/B*^{null} double mutant chemotaxis is almost completely inhibited in presence of the PI3K inhibitor LY294002. *dockA*^{null}, *dockB*^{null}, *dockA/B*^{null} cells all show reduced actin polymerization upon cAMP stimulation. *dockC*^{null} cells also show poor chemotaxis to cAMP. However there is no obviously defect in chemotaxis, macropinocytosis and phagocytosis for *dockD*^{null}, *dockG*^{null}, and *dockH*^{null} cells. Although *Dictyostelium* Docks do not contain the conventional DH domain for Rac activation, we show that the DockerB domain (Docker domain of DockB protein) interacts with Rac1A in the nucleotide free state *in vitro*. The DockerA domain (Docker domain of DockA protein) preferentially interacts with RacH and RacL. Expression of Rac1A in *dockB*^{null} background can effectively rescue the defect of phagocytosis. These findings show that *Dictyostelium* Docks most likely act as RacGEF's involved in a PI3K independent chemotaxis signalling pathway and also play important roles in the regulation of endocytosis in *Dictyostelium*.

In this study we also investigated the role of Elmo1 in the regulation of cell behavior. The *elmo1*^{null} cells grow slowly in the axenic medium and are defective in chemotaxis, macropinocytosis and phagocytosis. The phenotype of *elmo1*^{null} cells is extremely similar to that of *dockB*^{null} cells. Cells of the *elmo1/dockB*^{null} double mutant did not show a much more severe phenotype than either parent stain (*elmo1*^{null} or *dockB*^{null}) by itself. These data strongly support the idea that in *Dictyostelium* Elmo1 and DockB are involved in same signalling pathways.

Our data thus strongly suggest that Dock/Elmo complexes function as RacGEF's during chemotaxis and endocytosis in *Dictyostelium*.

Chapter I Introduction

1.1. The Cytoskeleton

The actin cytoskeleton of a cell is required for cell-shape changes, cell motility and chemotaxis (Van Haastert and Devreotes, 2004), cytokinesis (Glotzer, 2005), intracellular transport processes (Rogers and Gelfand, 2000), phagocytosis and pinocytosis (Ascough, 2004; May and Machesky, 2001). The cytoskeleton is a highly dynamic structure that undergoes constant restructuring and modification in response to environmental cues.

Actin filaments are assembled by the reversible endwise polymerization of monomers. Each actin monomer needs to be activated by ATP binding before polymerisation. Polymerization stimulates ATP hydrolysis and release of inorganic phosphate (Pi). Actin filaments are polar, and the two ends have distinct biochemical properties. The fast-growing end is called the barbed or plus (+) end, and the slower-growing end is called the pointed or minus (-) end. Polymerization occurs primarily at the barbed end in cells and is tightly controlled by monomer- and filament-binding proteins that regulate the monomer pool, orchestrate the formation of filaments, organize filaments into arrays via crosslinking, and depolymerise filaments for monomer recycling (Pollard et al., 2000).

The multiplicity of actin related processes require the existence of actin in a variety of complex, dynamic structures, which are regulated by actin-binding

proteins such as Arp2/3 complex, formins. Actin-binding proteins facilitate the assembly of actin filaments into a three-dimensional meshwork by crosslinking or bundling the actin filaments, whereas others regulate filament turnover or remodel the actin cytoskeleton in response to external signals. For example, Arp2/3 is activated by an existing filament to nucleate a branch from the parent filament, with Arp2/3 at the branch point (Bailly et al., 1999; Svitkina and Borisy, 1999). This creates a dendritic network of filaments. Whereas formins nucleate from monomers alone and generate straight filaments which may sustain tension for contraction (Pring et al., 2003; Zigmond, 2004).

1.2. The *Dictyostelium discoideum* model system for cell motility

The dynamics of the actin cytoskeleton is controlled by many signalling pathways. Therefore it is advantageous to use model systems, in which the signalling networks are simpler, to establish the basic mechanisms controlling them. One such system is the social amoebae *Dictyostelium discoideum,* a soil living social amoeba that feeds on bacteria and yeast. Proteome-based eukaryotic phylogeny studies shows the divergence of Dictyostelium along the branch leading to the Metazoa soon after the plant–animal split (Eichinger et al., 2005). Despite the earlier divergence of Dictyostelium, many of its proteins are more similar to human orthologues than are those of *S. cerevisiae*, probably due to higher rates of evolutionary change along the fungal lineage. When the amoebae deplete all food, they enter a starvation phase, which results in the aggregation of hundred of thousands of cells into a hemispherical multicellular aggregate, the mound. The mound undergoes a complex morphogenesis to

produce a multicellular slug that migrates in response to light and temperature gradients to the surface of the soil, where it forms a fruiting body consisting of a stalk supporting a mass of spores. In the mound, the cells start to differentiate into prestalk and prespore cells, precursors of the stalk and spores that make up the fruiting body (Chisholm and Firtel, 2004; Weijer, 1999) (Figure 1.1). Upon the return of favourable conditions, the spore cells can germinate and each spore releases an amoeba. The purpose of this developmental cycle is to allow cells to survive starvation conditions.

Dictyostelium discoideum can be easily cultured in the laboratory on bacterial lawns or in shaking culture in an axenic medium. Manipulation of genes can be achieved through highly efficient homologous recombination or REMI (Restriction Enzyme Mediated Integration) (Kuspa and Loomis, 1992; Schiestl and Petes, 1991). *Dictyostelium* contains all the classes of actin binding proteins, that are typically are found in eukaryotes and thus can used as a convenient model for the study of the actin cytoskeleton and its dynamics (Egelhoff and Spudich, 1991; Maniak, 2001; Neuhaus and Soldati, 1999; Rupper and Cardelli, 2001).

The actin cytoskeleton has an important role in the life cycle of *Dictyostelium,* it gives shape to the cells and controls cell movement, cell division and intracellular vesicle transport (Noegel and Schleicher, 2000). Most of the signal transduction pathways that regulate Dictyostelium cell motility have homologies to those in higher organisms. Most remarkably, the ability to sense and respond to shallow gradients of extracellular signals is similar in *Dictyostelium discoideum* and mammalian neutrophils (Devreotes and Zigmond, 1988;

Krishnan and Iglesias, 2004; Parent, 2004; Weiner, 2002). In *Dictyostelium* and neutrophils the extracellular chemo-attractants bind to serpentine cell surface receptors, that couple to heterotrimeric G proteins (Jin et al., 2000; Maghazachi, 2003; Wu et al., 1995; Zheng, 2004). The downstream elements of the signalling pathway are also conserved, and include phospho-inositides, PI3K, PTEN and actin interacting proteins that control the dynamics of the actin cytoskeleton (Iijima et al., 2002). *Dictyostelium discoideum* is an attractive model system to investigate the function and control of the actin cytoskeleton and associated proteins.

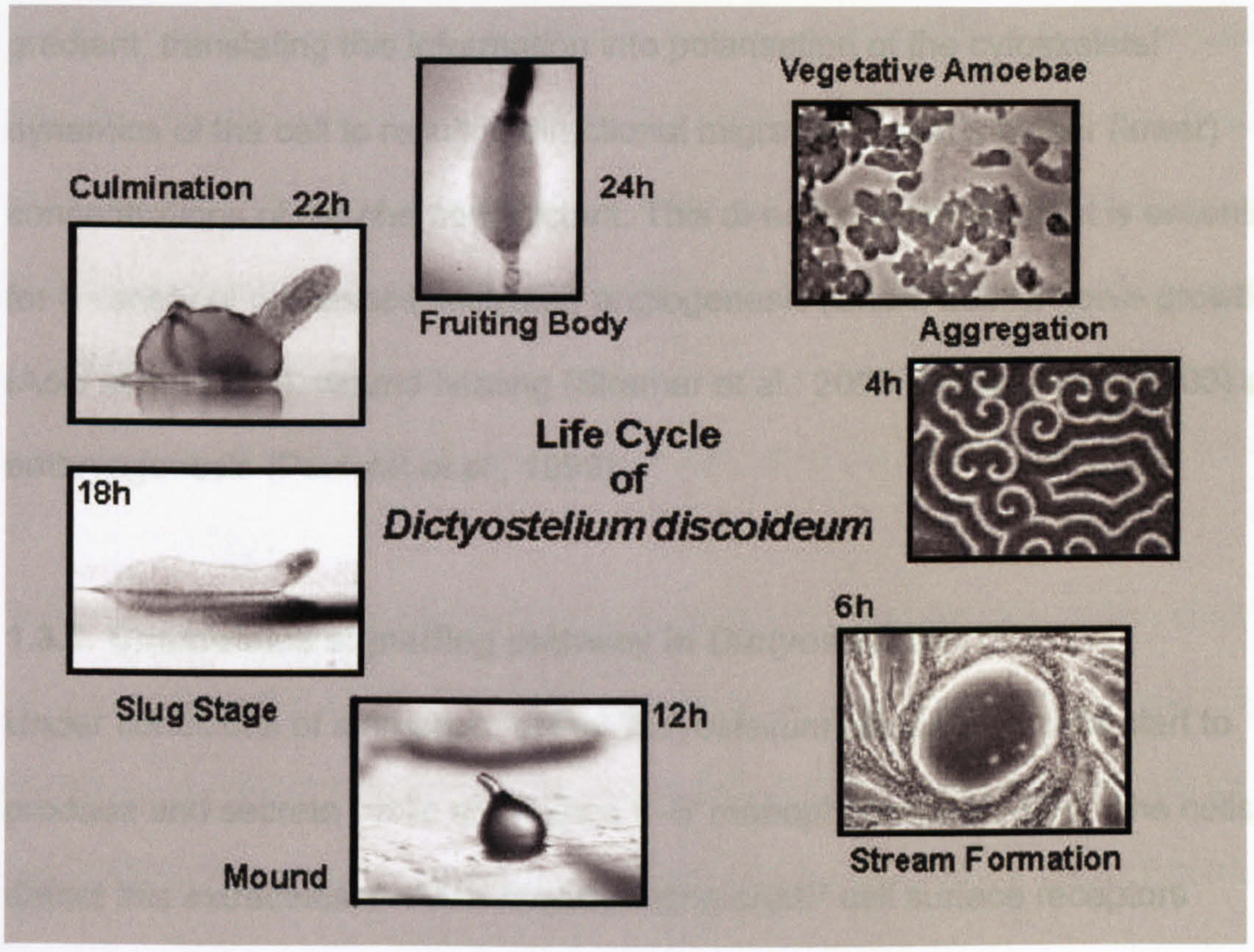

Figure 1.1 The life cycle of the social amoeba *Dictyostelium discoideum*. Amoebae feed on bacteria in the soil. When they devour all of the food and begin to starve, the cells initiate a cAMP signaling response relay, leading to aggregation and mound formation. The mound undergoes a complex morphogenesis to produce a multicellular slug that migrates in response to light and heat. Morphogenesis continues as the slug eventually culminates into the fruiting body, which is composed of a stalk supporting a spore mass. Upon the return of favorable conditions, the spore cells can germinate and each spore releases an amoeba once again. (http://www.zi.biologie.uni-muenchen.de/zoologie/dicty/dicty.html)

1.3. Chemotaxis

Directed cell movement up or down gradients of extracellular signalling molecules is known as chemotaxis. Chemotaxis involves sensing a chemical gradient, translating this information into polarisation of the cytoskeletal dynamics of the cell to result in directional migration towards higher (lower) concentrations of the chemoattractant. This directionally movement is essential for a variety of processes, including angiogenesis (Sherr, 2004), nerve growth (Aoki et al., 2005), wound healing (Stramer et al., 2005; Zegers et al., 2003) and embryogenesis (Paululat et al., 1999).

1.3.1. Chemotaxis signalling pathway in *Dictyostelium*

Under conditions of starvation, some *Dictyostelium discoideum* cells start to produce and secrete cyclic adenosine 3'-5' monophophate (cAMP). The cells detect this extracellular cAMP by serpentine cAMP cell surface receptors (cAR1-4) (Parent, 2004). Binding of cAMP to the receptors triggers two competing processes: activation of the aggregation stage-specific adenylate cyclase ACA, resulting in synthesis of cAMP; and a slower adaptation process that results in an inhibition of the activation of the adenylate cyclase (Pitt et al., 1990). The intracellular cAMP is secreted to the outside, where it can bind to the receptors of the same cells thus forming an autocatalytic feedback loop. During aggregation ACA localises in the rear of the aggregating cells, resulting in polarised cAMP secretion from the back of the cells (Comer et al., 2005; Kriebel et al., 2003) (Figure 1.2). The secreted cAMP diffuses away to activate neighbouring cells, which now in turn start to produce cAMP. The adaptation

stops the production of the cAMP and cAMP is degraded by a secreted cAMP phosphodiesterase. This results in a decrease of the cAMP concentration once cAMP synthesis stops which leads to de-adaptation of the adenylyl cyclase activation pathway (Kriebel et al., 2003; Van Haastert and Devreotes, 2004). The cells once deadapted can start to synthesize cAMP again. The processes of periodic cAMP synthesis, relay and adaptation result in cAMP wave propagation from the aggregation centre outward. The chemotactic response in the direction of higher cAMP concentrations results in the periodic movement of the cells towards the aggregation centre, in response to the outward propagating waves of cAMP. The adaptation process also prevents the cells from turning around and chasing after the cAMP waves once they have passed (Weijer, 2004).

When exposed to an attractant gradient, cells form pseudopodia in the direction of the increasing chemoattractant gradient. At the same time, pseudopod formation is suppressed elsewhere in the cell, and the uropod at the rear of the cell retracts (Devreotes and Zigmond, 1988; Pollard and Borisy, 2003; Postma et al., 2004; Ridley et al., 2003; Weiner, 2002). Resting *D. discoideum* cells extend one or two pseudopods in random directions. When chemotactic cells become polarized, they usually have only one pseudopod at any one time, which is formed close to the previous one at the leading edge. The new pseudopodia contain newly formed actin filaments, whereas at the back of the cell, the retracting uropod, is enriched in myosin II thick filaments (Figure 1.2).

Experiments have shown that the binding of chemoattractants to cell surface cAMP receptors initiates signal transduction pathways that culminate in cell polarisation and actin polymerization, which provides the driving force of directional migration via the extension of lamellipodia or pseudopodia (Postma et

al., 2004). *Dictyostelium discoideum* cells sense a cAMP gradient through serpentine cAMP cell surface receptors (cAR1-4) which are coupled to G-proteins that then transduce a signal via secondary messengers to the actin cytoskeleton (Firtel and Chung, 2000). The cARs couple to a specific G protein Ga2 containing one (Gα2) of the 11 Gα subunits found in the genome, in complex with a unique βγ complex. The βγ-complex is absolutely essential for chemotaxis (Jin et al., 1998; Wu et al., 1995). The cARs and G proteins are uniformly distributed along the cell surface without any specific spatial distribution in chemotactic cells (Jin et al., 2000; Li et al., 2003).

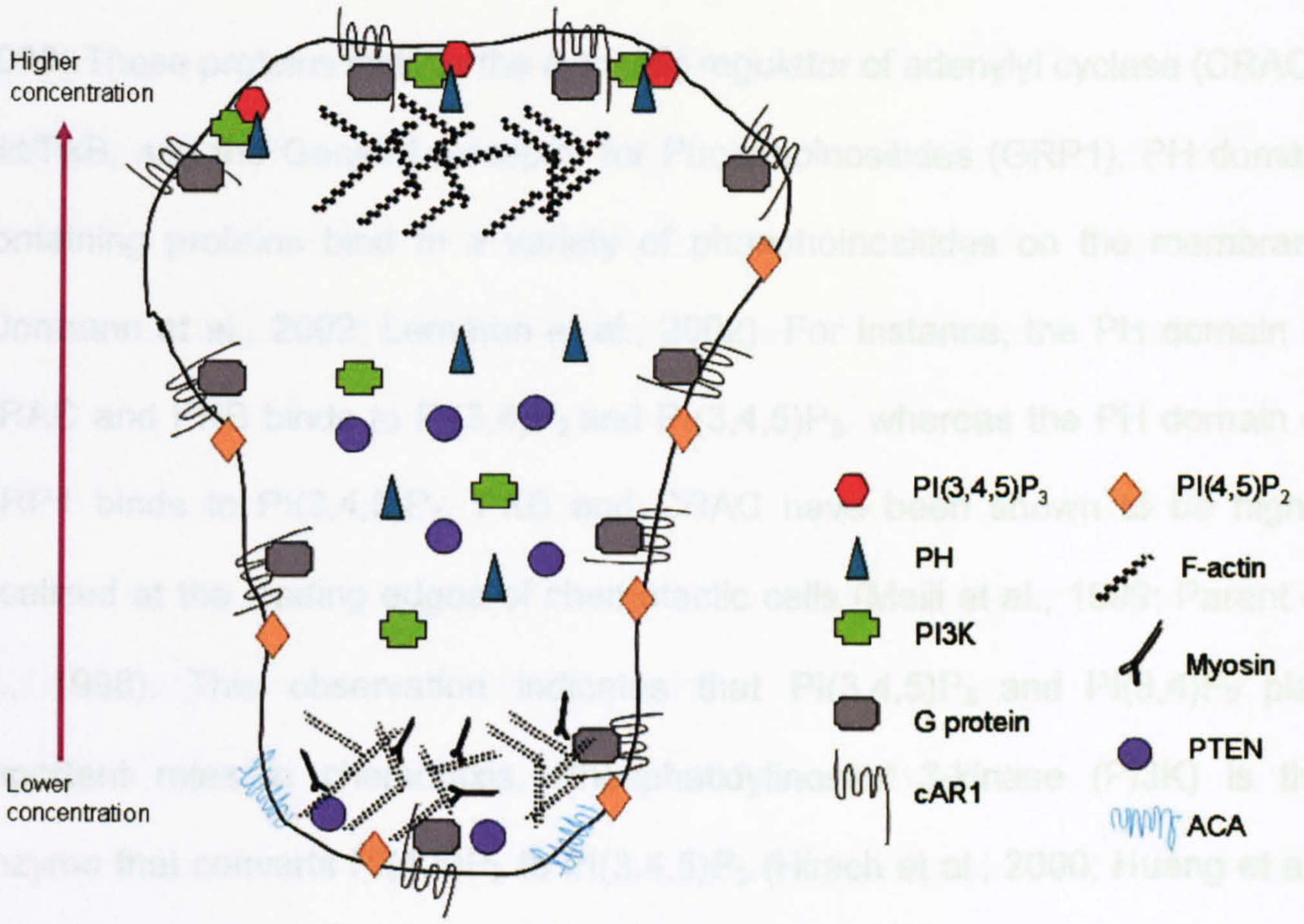

Figure 1.2. Spatial localization of components of the signaling pathway in *Dictyostelium*. The cAMP receptor cAR1 and G protein are uniformly distributed in the presence of an external cAMP gradient. PI3K, PI(3,4,5)P3, PH domain–containing proteins, and F-actin preferentially localizes to the front of the cells. PTEN, ACA, and myosin II are enriched in the back of the migrating cells. The cell is migrating toward the top of the page. (Modified from (Manahan et al., 2004).

1.3.2. Role of PI3K and PTEN

During chemotaxis, several proteins containing Pleckstrin Homology (PH) domains translocate from the cytosol to the plasma membrane, where they bind phospho-inositides (Meili et al., 1999; Parent et al., 1998; Servant et al., 2000).These proteins include the cytosolic regulator of adenylyl cyclase (CRAC), Akt/PkB, and the General Receptor for Phosphoinositides (GRP1). PH domain containing proteins bind to a variety of phosphoinositides on the membrane (Dormann et al., 2002; Lemmon et al., 2002). For instance, the PH domain of CRAC and PKB binds to $PI(3,4)P_2$ and $PI(3,4,5)P_3$, whereas the PH domain of GRP1 binds to $PI(3,4,5)P_3$. PKB and CRAC have been shown to be highly localized at the leading edges of chemotactic cells (Meili et al., 1999; Parent et al., 1998). This observation indicates that $PI(3,4,5)P_3$ and $PI(3,4)P_2$ play important roles in chemotaxis. Phosphatidylinositol 3-kinase (PI3K) is the enzyme that converts $PI(4,5)P_2$ to $PI(3,4,5)P_3$ (Hirsch et al., 2000; Huang et al., 2003; Zhou et al., 1995); the lipid 3-phosphatase PTEN reverses these reactions (Maehama and Dixon, 1998; Myers et al., 1998). In a cAMP gradient PI3K is recruited to the leading edge of the cell, whereas PTEN remains membrane associated at the trailing edge (Funamoto et al., 2002; Iijima and Devreotes, 2002; Postma et al., 2004). This spatial distribution helps to establish a steep intracellular second messenger gradient of $PI(3,4,5)P_3$. The asymmetric localisation of components of the signal pathway to the actin cytoskeleton results in localised actin polymerisation and Myosin II thick filament disassembly at the leading edge, and myosin filament assembly and contraction in the rear of the cell, processes which together mediate psuedopod extension and cell migration up the cAMP gradient (Funamoto et al., 2002; Iijima and Devreotes, 2002; Iijima

et al., 2002). *Dictyostelium discoideum* cells lacking two PI3K and leukocytes derived from mice lacking PI3Kγ have defects in polarity and show reduced efficiency of chemotaxis (Chung et al., 2001; Katanaev, 2001). Pharmacological inhibition of PI3K in *D. discoideum* amoebae and in a variety of mammalian cell types causes inhibition of chemotaxis and cell migration to varying degrees. Furthermore in a gradient of chemoattractant, cells that lack PTEN extend two or three pseudopods simultaneously, which impairs directed migration towards the chemoattractant (Iijima and Devreotes, 2002). The spatial localization of components of the signaling pathway in *Dictyostelium* is shown in Figure 1.2.

Previous studies analyzing actin polymerization dynamics in *D. discoideum* and neutrophils suggested the existence of a biphasic polymerisation response to a uniform chemo-attractant stimulus (Condeelis, 1990; Condeelis et al., 1988; Postma et al., 2003): an initial very fast large spike, followed by a more prolonged smaller second peak. In *D. discoideum* the first phase comprised at least two fold increases over the basal level, which peaked within 5-10 seconds after the addition of cAMP and ended by 20 s. The second phase was smaller and peaked between 40 and 80 s. The cells undergo a series of cell shape changes during the two phases of actin polymerization (Chen et al., 2003; Condeelis, 1990). During the first peak, cells freeze and round up, the so called cringe response. During the second phase of actin polymerization, the cells extend new pseudopods from multiple regions and start to move. Disruption of PTEN preferentially increases the second phase of the response (Chen et al., 2003). Disruption of PI3K activity (deletion of two of three *D. discoideum* PI3Ks) results in a partial defect of chemotaxis but does not block the ability of cells to sense and orient in chemotactic gradients (Buczynski et al., 1997; Funamoto et

al., 2001). LY294002, a PI3K inhibitor, has been reported to inhibit but do not block chemotaxis in *Dictyostelium discoideum*, unless unphysiologically high concentrations are used (Funamoto et al., 2001). Disruption and chemical inhibition of PI3K do not significantly affect the first rapid phase of chemoattractant-induced actin polymerization (own observations) and (Chen et al., 2003). These data indicated that actin polymerization was controlled by both PI3K dependent- and independent-signalling pathway upon cAMP stimulation in *Dictyostelium discoideum*.

1.3.3. The role of Small G proteins of the Rho family

The details of the chemotactic signalling pathway downstream of PI3K remain to be elucidated. Genetic studies have however clearly indicated that small GTPases of the Rho family (Rho, Rac & Cdc42) play a pivotal role in regulating actin polymerization for cell migration in mammals (Raftopoulou and Hall, 2004). The Rho family was grouped in three subfamilies: Cdc42, Rac and Rho. Cdc42 was shown to promote the formation of actin-rich, finger-like membrane extensions (filopodia) (Kozma et al., 1995; Nobes and Hall, 1995). Activation of Rac promotes actin polymerization at the cell periphery leading to the formation of sheet-like lamellipodial extensions and membrane ruffles. Activation of Rho promotes both the bundling of actin filaments with myosin II filaments into stress fibers and the clustering of integrins and associated proteins to form focal contacts. Evidence has accumulated to show that Rho GTPases are involved in most actin-regulated processes such as membrane trafficking (including phagocytosis, macropinocytosis and exocytosis), motility, adhesion and morphogenesis (Bokoch, 2005; Moon and Zheng, 2003; Raftopoulou and Hall, 2004). Phagocytosis mediated by the Fc receptor (FcR) has been shown to

require both Rac and Cdc42(Chimini and Chavrier, 2000; Yamauchi et al., 2004). Localization of Cdc42, Rac1 and Rac2 during receptor mediated phagocytosis were investigated by fluorescence resonance energy transfer (FRET)-based imaging methods (Hoppe and Swanson, 2004). Activation of Cdc42 occurs early and preferentially at the tips of extending pseudopodia. Rac1 activation occurs around the phagocytic cup and persists during closure; however Rac2 is active both during and after phagosome closure (Hoppe and Swanson, 2004). Dominant-negative Rac1 and Rac2 constructs inhibit chemotaxis of macrophage cell lines (Jones et al., 1998), as well as the directed migration of neutrophils (Gardiner et al., 2002) and neutrophil-like cell lines (Srinivasan et al., 2003) to chemoattractants.

In Dictyostelium the Rho family comprises 15 members. The phylogenetic analysis was performed based on the alignment of complete sets of sequences of Rho protein from fungi, plants, invertebrates and vertebrates with potential *Dictyostelium* Rho proteins (Rivero et al., 2001). Analysis showed Rac1a/b/c, RacF1/F2 and RacB are members of the Rac subfamily, and one, RacA, belongs to the RhoBTB subfamily, however there appear to be no clear homologous of the Rho and Cdc42 subfamilies in the Dictyostelium genome.

Rho family GTPases act as binary molecular switches that are turned on and off in response to a variety of extracellular stimuli. GEFs (guanine nucleotide exchange factors) and GAPs (GTPase-activating proteins) regulate small GTPases cycling between an active GTP-bound state and an inactive GDP-bound state (Figure 1.3.). Additionally, GDIs (GDP-dissociation inhibitors) have been described that capture Rho in both GTP and GDP-bound states and

allow it to cycle between cytosol and membranes. In their active state Rho GTPases interact with a multitude of effectors that relay upstream signals to cytoskeletal components, eliciting rearrangements of the actin cytoskeleton (Etienne-Manneville and Hall, 2002).

When bound to GTP, Rho GTPases undergo a conformational change that enables them to interact with downstream target molecules and transmit their signals. The activation state of Rho GTPases is controlled by GEFs, which stimulate Rho GTPases by catalyzing the exchange of GDP for GTP (Schmidt and Hall, 2002). Most known GEFs contain a Dbl homology domain in tandem with a PH domain (Braga, 2002). The Dbl homology domain is responsible for binding to Rho proteins and facilitating the exchange reaction, while the PH domain is thought to interact with lipids such as $PI(3,4,5)P_3$ and promote membrane translocation (Braga, 2002; Lim et al., 2004). Welch and co-workers demonstrated that the Rac-specific GEF P-REX-1 is recruited to the leading edge of a migrating cell by virtue of the interaction between its PH domain and PI3K generated $PI(3,4,5)P_3$ (Welch et al., 2002). This provided the first link in the signal pathway between PI3K and Rac-mediated actin polymerization. The role of the Rac-GEF Vav1 in the control of neutrophil chemotaxis was recently investigated (Kim et al., 2003). Neutrophils isolated from mice lacking Vav1 showed reduced levels of actin polymerization and displayed weaker chemotaxis for the chemoattractant fMLP (Kim et al., 2003).

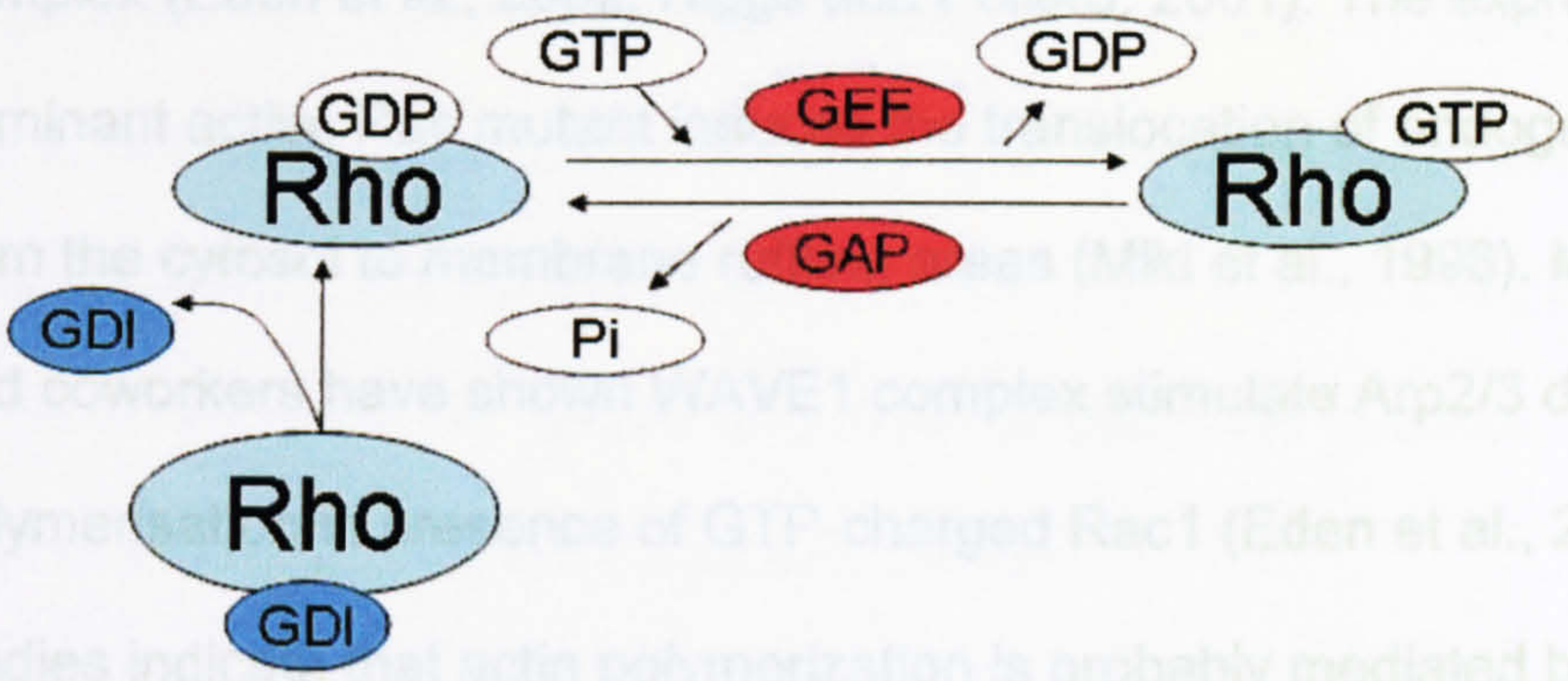

Figure 1.3 Rho GTPase cycle. Small GTPases act as molecular switches, cycling between an active GTP-bound state and inactive GDP-bound state, a process that is regulated by GEFs and GAPs. GDIs capture Rho and allow it to cycle between cytosol and membranes. (Modified from (Raftopoulou and Hall, 2004)).

It is well established that Rho-family GTPases are essential regulators of cell polarity and motility by relaying signals to Arp2/3 complex, which is composed of seven proteins that contribute to nucleate actin polymerization from existing filaments at the leading edge (Eden et al., 2002; Etienne-Manneville and Hall, 2002). Members of the Rho family of small GTPases, such as Cdc42 and Rac1, link extracellular signals and actin nucleation through pathways that include the WASP family of proteins and the actin nucleation machinery—the Arp2/3 complex (Eden et al., 2002; Higgs and Pollard, 2001). The expression of a dominant active Rac mutant induces the translocation of endogenous WAVE from the cytosol to membrane ruffling areas (Miki et al., 1998). Marc Kirschner and coworkers have shown WAVE1 complex stimulate Arp2/3 dependent actin polymerisation in presence of GTP-charged Rac1 (Eden et al., 2002). *In vitro* studies indicate that actin polymerization is probably mediated by the Arp2/3 complex, which binds to the sides of pre-existing filaments and induces the formation of branches (Bailly et al., 1999; Svitkina and Borisy, 1999).

Recent evidence indicates that activation of WAVE/SCAR proteins in *D. discoideum* enhances the production of actin-filled pseudopods (Bear et al., 1998; Blagg et al., 2003; Machesky and Insall, 1998). Disruption of SCAR in *D. Discoideum* results in less accurate directionality and slower speed during chemotaxis compared to wild type cells (Blagg et al., 2003). $scar^{null}$ cells have reduced levels of F-actin staining during vegetative growth, and abnormal cell morphology and actin distribution during chemotaxis (Bear et al., 1998).

In *D. discoideum*, identification of the RacGEF and specifc Rac involved in the chemotaxis should help to understand the components that link

$PI(3,4)P_2/PI(3,4,5)P_3$ and actin polymerization during chemotaxis.

1.4. Phagocytosis and Macropinocytosis

Phagocytosis and macropinocytosis are actin-dependent processes that result in the internalization of particles or the formation of fluid-filled macropinosomes, respectively. During the phagocytic process, cell sends out membrane projections that make contact with particles. Ingestion of the particles results in the formation of a phagosome which then fuses with lysosomes for digestion (Maniak, 2002). During the process of macropinocytosis the plasma membrane forms an invagination; liquids and material dissolved in these liquids within the area of invagination are brought into the cell.

Numerous studies have shown phagocytosis and macropinocytosis are actin-dependent processes in neutrophils and macrophages (Ascough, 2004; Cardelli, 2001; Engqvist-Goldstein and Drubin, 2003). F-actin was visualized to accumulate below the forming phagcytic cup by expressing GFP-ABD, a fusion protein of the 25kDa highly conserved actin-binding domain of filamin with the green fluorescent protein (GFP) (Pang et al., 1998). Latrunculin A that interferes with F-actin formation inhibited the protrusion of the plasma membrane and engulfment of particles and fluid, which indicates the F-actin is required for phagocytosis and macropinocytosis (de Oliveira and Mantovani, 1988).

The mechanism of phagocytosis is better understood than that underlying macropinocytosis, which is just being deciphered. Phagocytosis consists of multiple stages: (1) particle binding to the cell surface, (2) activation of a

signalling pathway that leads to remodelling of F-actin, (3) pseudopod extension to engulf the particle followed by membrane enclosure to form the phagosome, (4) the actin coat of the phagosome is removed and mature phagolysosome is generated (Cardelli, 2001) (Figure 1.4).

In mammals, binding of immunoglobulins (Igs) to foreign particles leads to the prompt clearance of those particles from the organism. The conserved Fc domain of the Igs is recognised by Fc receptors present on neutrophils and macrophages, and the opsonised particle is rapidly internalised. Complement-receptor-mediated phagocytosis is morphologically distinct from that mediated by FcRs, although both processes require actin polymerization. Complement-opsonised particles 'sink' into the phagocyte; there is minimal membrane disturbance, and internalisation does not usually lead to an inflammatory response or oxidative burst (May and Machesky, 2001).

Many actin binding, regulatory proteins (ABP, talin, WASP, Arp2/3, and Myosin), small G proteins, and phophoinositides are involved in the signalling pathway of phagocytosis. G proteins are required to convert the signals to active processes that remodel actin cytoskeleton in *Dictyostelium*. Disruption of β subunit of G proteins resulted in defect in phagocytosis and actin remodelling (Peracino et al., 1998). The model proposes that particle binding to the cell surface via an unknown receptor initiates a signaling cascade that activates phospholipase C (PLC), possibly activated through the interaction with the β subunit of the Ga2 protein. The resulting DAG and IP_3 both contribute to regulating phagocytosis, through activating Rap1 and/or RasS, and by increasing cytosolic calcium levels, respectively. Members of the Rho family are activated and play a direct role in

actin polymerization perhaps through recruitment of members of the WASP family such as SCAR.

However, in mammalian systems, inhibition of heterotrimeric G proteins does not inhibit phagocytosis (May and Machesky, 2001), which suggests that mammalian cells have made use of alternative signals to replace heterotrimeric G proteins in the process. Small GTPases, including Rac1 and Cdc42, are now firmly established as important signalling molecules downstream of Fc receptors (May et al., 2000; May and Machesky, 2001). Phagocytosis by FcRs in rat mast cells is blocked by inhibition of Rac1 or Cdc42 (Massol et al., 1998). But they are not required for complement-receptor-mediated phagocytosis (Caron and Hall, 1998).

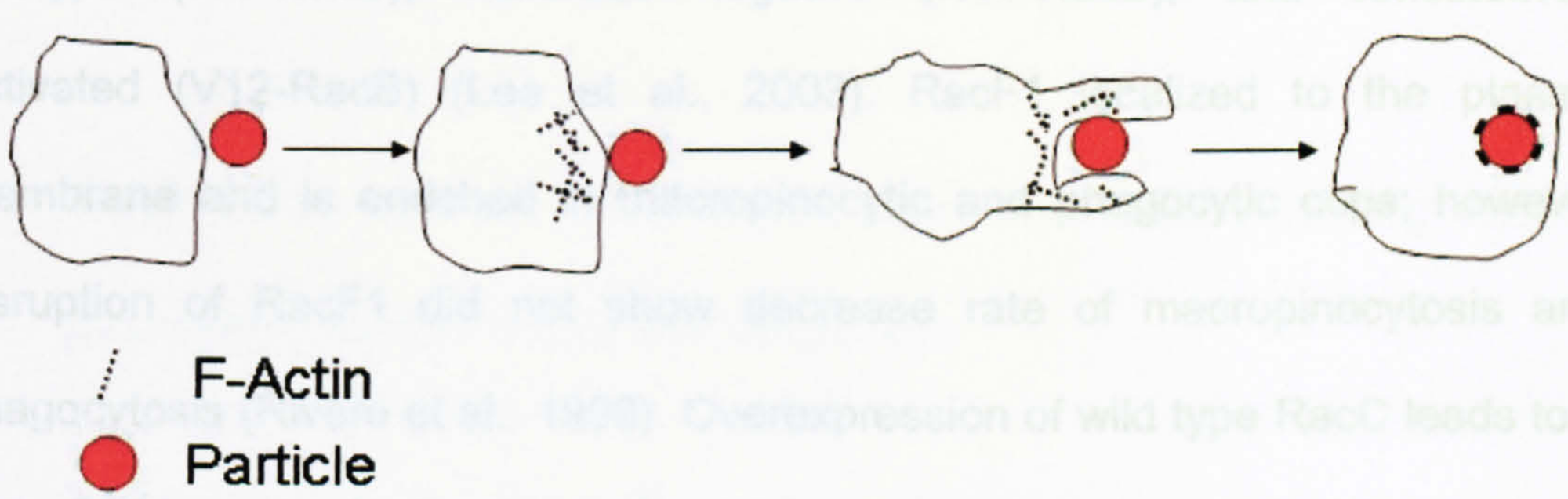

Figure 1. 4 Phagocytosis stages. (1) particle binding to the cell surface, **(2)** activation of a signalling pathway that leads to remodelling of F-actin, **(3)** pseudopod extension to engulf the particle, when the membrane is enclosed the phagosome is formed, **(4)** the actin coat of the phagosome is removed and mature phagolysosome is generated.

Rac is also important for phagocytosis in *Dictyostelium*. The Rac1-like family of proteins consists of three highly related proteins, Rac1A, Rac1B and Rac1C. Overexpression of dominant active Rac1 resulted in decreases in endocytosis and the formation of lamellopodia (Dumontier et al., 2000). Phagocytosis, endocytosis, and fluid phase efflux rates were reduced in all cell lines expressing wildtype (WT-RacB), dominant negative (N17-RacB), and constitutively activated (V12-RacB) (Lee et al., 2003). RacF1 localized to the plasma membrane and is enriched in macropinocytic and phagocytic cups; however disruption of RacF1 did not show decrease rate of macropinocytosis and phagocytosis (Rivero et al., 1999). Overexpression of wild type RacC leads to a three fold increase in phagocytosis and formation of cortical actin-rich structures (Seastone et al., 1998). These studies indicate that each of the *Dictyostelium* Rac-like GTPase functions in largely non-overlapping pathways and that a subset of these proteins might regulate phagocytosis.

It's clear that both phagocytosis and macropinocytosis require the regulation of the actin cytoskeleton. Previous evidence suggested that in *Dictyostelium* only macropinocytosis requires PI3K activity (Cardelli, 2001). Deletion of the PI3Ks, PIK1 and PIK2, reduces the rate of macropinocytosis but does not affect phagocytosis of 1μm beads (Buczynski et al., 1997). But other studies have shown in presence of PI3K inhibitor (LY294002) cells reduced the phagocytosis of yeast cells, 1μm beads and bacteria, suggesting the involvement of PI3K activity in the regulation of phagocytosis of all these particles (Dormann et al., 2004). SCAR, profilin, PH domain containing proteins, could be recruited to the plasma membrane by binding to $PI(4,5)P_2$ during the phagocytosis process (Seastone et al., 2001; Zhou et al., 2001).

Until now, many regulators have been implicated in the control of actin cytoskeleton during phagocytosis and macropinocytosis. But how extracellular signals activate Rho-family GTPases and thereby result in remodelling of the cytoskeleton is still unknown. Identification of specific RhoGEF's during these processes will help the understanding of the signalling pathways involved.

1.5. Dock/Elmo act as unconventional RacGEF's in signalling pathways to the actin cytoskeleton

1.5.1. Dock180

Mammalian Dock180 was originally identified as a 180 kDa protein has been involved the signalling pathway to lead Rac activation and promote cell migration (Cheresh et al., 1999; Kiyokawa et al., 1998a). Dock180 protein contains an SH3 domain at its extreme N terminus, a Rac interaction domain (Docker domain) and proline-rich motifs near its C terminus. Although Dock180 does not contain the conventional Dbl homology (DH) domain found in essentially all known mammalian RacGEFs (Schmidt and Hall, 2002). Dock180 contains a novel Docker domain, which specifically recognizes nucleotide-free Rac and can promote loading of GTP by Rac (Brugnera et al., 2002; Cote and Vuori, 2002). The Docker domain, which is further subdivided into two domains DHR-1 and DHR-2 by some groups, is evolutionarily strongly conserved. The Dock180 proteins have been suggested to function as unconventional Rac-GEF's, which mediate membrane ruffling and other cytoskeletal changes (Nolan et al., 1998; Reddien and Horvitz, 2000). Until recently it was believed that all Rho-GEF's contained a PH domain needed for binding localized PIP3 in the leading edge.

One group reported a steric-inhibition model for regulating the Dock180 family of GEFs (Lu et al., 2005). In this model the N-terminal SH3 domain of Dock180 binds to the distant catalytic Docker domain and negatively regulates the function of Dock180 at basal state. The SH3: Docker interaction sterically blocks Rac access to the Docker domain. ELMO, which contains a PH domain, facilitated Rac access to the Docker domain by binding to the SH3 domain of Dock180 to disrupt the SH3: Docker interaction (Figure 1.5.).

Two groups reported that the Docker binds the nucleotide free Rac and was sufficient to mediate its activation both in-vitro and in-vivo via the loading of GTP (Brugnera et al., 2002; Cote and Vuori, 2002; Grimsley et al., 2004). Whilst one group reported that the Docker domain was sufficient for Rac activation (Cote and Vuori, 2002) the other competing group found it was necessary but not sufficient (Brugnera et al., 2002). This group reported that Dock180 associated with Elmo to form a bipartite GEF (Brugnera et al., 2002). In this scenario Dock180 has the exchange activity whilst Elmo provides localisation via its PH domain (Funamoto et al., 2001; Lu et al., 2004). Whether Dock180 and its homologous are stand lone GEFs or need to be part of a protein complex to have GEF activity remains a hotly debated topic.

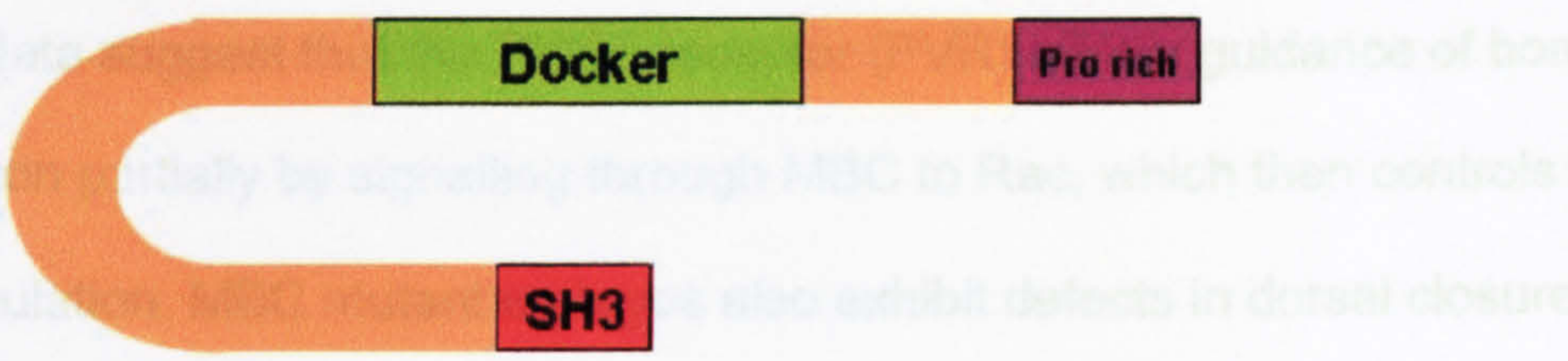

Figure 1.5. Steric-Inhibition Model for Regulation of Nucleotide Exchange via the Dock180 Family of GEFs. In this model the Docker domain of Dock180 was negatively regulated by its N-terminal SH3 domain. The SH3: Docker interaction sterically blocks Rac access to the Docker domain. ELMO1 binds to the SH3 domain of the Dock180 to disrupt the SH3: Docker interaction therefore facilitated Dock to activate the Rac. (Modificated from (Lu et al., 2005))

Mammalian Dock180 protein and its homologous in *Drosophila* Myoblast City (MBC) and *Caenorhabditis elegans* (CED-5) represent an evolutionarily conserved family of proteins involved in multiple biological processes (Cote and Vuori, 2002). The biological role of the Dock proteins is best understood in a simple multicellular organism *Drosophila* and *C.elegans* which only contain one *dock* gene each. The *Drosophila* MBC is located downstream of PVR, PDGF/VEGF factor 1 (PVF1) and activates Rac during the migration of border cells (Duchek et al., 2001). Border cell migration is a chemotactic process in *Drosophila*, which is mediated by a PDGF/VEGF signal (Duchek et al., 2001). Their data suggest that the PDGF receptor (PVR) affects guidance of border cell migration partially by signalling through MBC to Rac, which then controls F-actin accumulation. MBC mutant embryos also exhibit defects in dorsal closure and cytoskeletal organization in the migrating epidermis (Erickson et al., 1997). Furthermore CED-5, the Dock180 homologue in *C. elegans*, is required for cell-corpse engulfment during apoptosis and the migration of distal tip cells during gonal formation (Ellis et al., 1991; Wu and Horvitz, 1998). The distal tip cells (DTCs) are located at the tips of the two gonadal arms and guide the extension of each growing gonadal arm during larval development (Hedgecock et al., 1983; Kimble, 1981). In CED-5 mutants, the DTCs frequently make extra turns or stop prematurely, which results in abnormally shaped gonads (Wu and Horvitz, 1998). Mutation of CED-5 also results in defect in phagocytosis, cells show inefficient engulfment of the cell corpses (Ellis et al., 1991). The expression of human Dock180 in *C. elegans* rescued the cell-migration defect of a CED-5 mutant (Wu and Horvitz, 1998). Genetic studies suggest that CED-10 (homologous of mammalian Rac) acts downstream of the CED-5 in the genetic pathway that controls phagocytosis and cell migration (Reddien and Horvitz,

2000; Wu et al., 2001). Taken all the data above together, these results suggest the possibility that Dock180/MBC/CED-5 is an intermediate in a signal transduction pathway controlling cell migration and phagocytosis from the primary signal to the Rho family of GTPases.

Overexpression of Dock180 in mammalian cells has been reported to lead c-Jun N-terminal kinase (JNKs) activation (Dolfi et al., 1998), phagocytosis of apoptotic cells (Albert et al., 2000) and enhanced cell migration (Cheresh et al., 1999). Dock180 forms a complex with CrkII and $p130^{Cas}$ and induces cell spreading of NIH-3T3 cells (Kiyokawa et al., 1998b). Dock180 was particularly concentrated at the site of membrane spreading and at focal adhesions (Kiyokawa et al., 1998a). Expression of RacN17 significantly suppressed both cellular spreading and recruitment of CrkII, $p130^{Cas}$ and Dock180 to focal adhesions (Kiyokawa et al., 1998a). These results demonstrated that Rac1 is required for the Dock180 induced morphological change and also for the recruitment of Dock180 to sites of membrane spreading.

Dock2 is one member of the Dock180 protein family in mammalian. It has been implicated play an important role in the chemotaxis of lymphocytes (Fukui et al., 2001; Reif and Cyster, 2002). Dock2-deficient mice exhibited migration defects of T and B lymphocytes. In $Dock2^{-/-}$ mice lymphocytes, chemokine-induced Rac activation and actin polymerization were almost totally abolished (Fukui et al., 2001). Elmo1 is the mammalian orthologue of the *C.elegans* gene, CED-12, which has been shown to functionally cooperate with Dock180 activated Rac during phagocytosis and cell migration (Gumienny et al., 2001; Wu et al., 2001; Zhou et al., 2001). In lymphocytes Elmo1 has been implicated in association with

Dock2, which is critical for Dock2-mediated Rac activation (Sanui et al., 2003). Dock2 mediated efficient lymphocyte migration in a largely PI3K-independent manner, although a minor, PI3K-dependent pathway for migration was observed in wild-type and Dock2-deficient lymphocytes (Nombela-Arrieta et al., 2004). PI3K inhibitor, Wortmannin, only reduced control wild type lymphocyte cell migration by 30%; however Wortmannin treatment abrogated the residual migration of Dock2-deficient cells' (Nombela-Arrieta et al., 2004).

1.5.2. ELMO

Three Elmo proteins have been reported in mammals. They do not appear to contain any obvious catalytic domains but have three recognizable features near the C-terminus: PH domain, a putative leucine zipper motif and a proline-rich motif (Yin et al., 2004). Elmo1 forms a complex with Dock180 and when these two proteins are co-expressed, a Rac-GEF activity is present in Elmo1 immmunoprecipitates (Braga, 2002; Brugnera et al., 2002). However when expressed on its own Elmo1 cannot activate Rac *in vitro* which precluded Elmo1 from being the GEF itself. Recent evidence suggests that the Dock180-Elmo1 complex acts as a bipartite RacGEF (Braga, 2002; Brugnera et al., 2002). Interaction with Rac is primarily mediated through Dock180 while Elmo1 potentiates the Dock180-Rac interaction. In this way the tandem Dbl and PH domains in the Dbl family of GEF's is spread between two distinct proteins (Brugnera et al., 2002). It has been suggested that the PH domain of Elmo binds the Dock180-Rac complex *in trans* and so stabilizes Rac in the nucleotide-free transition state (Lu et al., 2004) (Figure 1.5.).

1.6. Aim of the work presented in this thesis

In *Dictyostelium* Inhibition of PI3K does not completely block chemotaxis; therefore there may exist parallel signalling pathways to the actin cytoskeleton. Some of which may be Dock mediated as it has been shown to be involved in chemotaxis other organisms. Analysis of the *D. discoideum* genome database identified at least eight Dock (DockA, B, C, D, E, F, G and H) and four putative Elmo (Elmo1~4) homologous through their evolutionary conserved Docker and Duf609 domains respectively. The Duf609 domain of approximately 160 amino acids is a conserved domain found in a number of eukaryotic proteins including Ced-12, human Elmo1, and human Elmo2. Given the high degree of conservation in Dock/Elmo proteins from different species it is likely that these proteins have a role in actin polymerization and cell migration in *D. discoideum*. The experiments in this thesis attempt to elucidate the role of Dock/Elmo homologous in regulation of cellular behaviour by generating knockout mutants in *Dictyostelium discoideum*. The phenotype of these mutants has been studied, with emphasis on actin dependent processes; F-actin polymerization, endocytosis, motility and chemotaxis.

From our studies of *dock* knockout mutants we have found that *dock* mutant cells are defective in growth, pinocytosis, phagocytosis, chemotaxis and phototaxis. Interestingly, $dockA^{null}$, $dockB^{null}$ and $dockA/B^{null}$ mutants show altered actin polymerization responses to cAMP stimulation from wild type cell in the presence of PI3K inhibitor. In collaboration with Dr Francisco Rivero, Dept of Biochemistry Cologne, we have shown that DockB interacts preferentially with the Rac1A in the nucleotide-free state; DockA interacts weakly with RacH and

RacL. We have expressed Rac1A in a *dockB*^{null} background to show that it rescues the phagocytosis defect. All the data indicate Dock may act as unconventional RacGEF's in phagocytosis, macropinocytosis and chemotaxis acting in parallel to the PI3K pathway. Disruption of *elmo1* results in similar phenotype as that of the *dockB*^{null} strain, which implicates this protein as a critical component in multiple cellular processes involving the reorganisation of the actin cytoskeleton. However the exact function of Elmo1 and its role in activating Rac when complexed with members of the Dock superfamily of proteins remains unknown.

The experiments presented in this thesis have defined important roles for members of the Dock family and Elmo1 in *Dictyostelium discoideum* in the control of cell behaviour through their effects on the dynamics of the actin cytoskeleton.

Chapter II Materials and Methods

Cells and development conditions

Cells were grown in HL5 medium according to standard conditions (Sussman, 1987). For experiments, cells were harvested from shaking cultures at a density between 2~5.0x10^6cells/ml. They were harvested by centrifugation at 2000rpm (Jouan B 3.11 Centrifuge) for 2min and wash twice in KK2 before plating out on 1% KK2 or H_2O agar plates at density of 5x10^5cells/cm^2 and incubated at 21°C for various periods of time or kept in 8°C incubator overnight for experiments to be performed the next day.

Growth on SB agar plates

Dictyostelium cells were plated onto SB agar plates overlaid with *Klebsiella aerogenes* and incubated at 22°C for 3-4 days until *Dictyostelium* plaques appeared on the bacterial lawns. Single plaques obtained after incubation at 22°C for 3-4 days were picked up with sterile pipette tips, transferred to 24 well plates containing 1ml HL5 medium supplemented with penicillin/streptomycin at a concentration of 50unit/ml penicillin and 50µg/ml streptomycin to get rid of the bacteria and any other appropriate selective antibiotic (depending upon mutant).

D. discoideum transformation

The electroporation method for transformation of *Dictyostelium* cells used was

as described by de Hostos (de Hostos et al., 1993). Cells were harvested from shaking cultures (in HL5 medium) at a density between 2~5.0x10^6 cells/ml and cooled on ice for between ~10min. Cells were spun down by centrifugation at 2000rpm (Eppendorf 5810 R centrifuge) at 4°C for ~2 minutes and washed s twice in cold sterilized EP buffer (20mM Hepes, 5mM $NaHCO_3$, 1mM NaH_2PO_4, 4M KCl, 5M NaCl, 1M $MgCl_2$, pH 7.0). Cells were re-suspended to 5.0x10^7 cells in 90µl ice cold EP buffer). Cells were mixed with 20~25µg plasmid DNA. The cell-DNA mixture was transferred to a sterile, ice cold, 1mm electroporation cuvette and electroporated 0.65kV and 25µF twice -5s apart in a Biorad Genepulser II. The cells were incubated in the cuvette on ice for a further 5min before transferring to a sterile 10cm diameter Petri dish containing 10ml of HL5 medium. Cells were allowed to recover overnight before adding the drug used for selection (G418 10µg/ml, Hygromycin 50µg/ml or Blasticidin 7.5µg/ml).

Growth assay

Dictyostelium wild type-AX2 and *dock* mutant strains were grown axenically in HL5 medium at 22°C with rotary shaking at 125rpm. At various times the cell density was measured by counting in a hemocytometer to investigate to the growth of the cells.

E. coli transformation and clone selection

The bacterium *E. coli* was used for the amplification of plasmid vectors. For *E. coli* transformation, 0.5-5ng of plasmid DNA was added to 50µl of XL1-blue chemically competent *E. coli* bacteria prepared as described below. The mixture

incubated on ice for 20minutes. The cells were then given a heat shock for 1.5min at 42°C and transferred immediately to ice before being shaken in 200µl LB medium (1%(w/v) Bacto-peptone, 0.5%(w/v) Bacto-Yeast extract (both Oxoid, Hampshire, UK), 0.2M NaCl, autoclaved) at 37°C for 30 minutes. The cells were then spread on LB-agar plates containing a selectable marker and incubated overnight at 37°C. Clones containing plasmid vectors were then used to inoculate larger volumes of LB medium containing a selectable marker which were then were shaken overnight at 37°C to facilitate bacterial growth and plasmids were then isolated as described below.

Preparation of chemical competent *E. coli* cells

An overnight grown culture of *E.coli* (1ml) was inoculated into 100ml LB medium and incubated at 37°C, with shaking 250rpm until an OD600 of 0.5-0.6 was obtained. The bacteria were then pelleted at 4°C for 15min at 4,000rpm (Beckman Avanti J25, rotor JA-25.50) and the bacterial pellet was resuspended in 5ml of ice-cold TFB I buffer (30mM KOAc, 50mM $MnCl_2$, 100mM KCl, 10mM $CaCl_2$, 15% (v/v) glycerol, pH 5.8) and incubated on ice for 5min. The bacterial cells were again pelleted and resuspended in 2ml of ice-cold TFB II buffer (10mM MOPS, 75mM $CaCl_2$, 10mM KCl, 15% glycerol, pH 7.0) and then aliquoted 50µl/tube. The aliquots were then quickly frozen in a dry ice bath and immediately stored at -80°C.

Purification of plasmid DNA

In general, for small cultures (600µl) of *E. coli* transformants, the alkaline lysis method was used to extract plasmid DNA. This method is good for screening a large number of clones simultaneously for the desired recombinant plasmid. Briefly, single transformants were picked up from the culture plate and were grown overnight in 1ml of LB media containing suitable antibiotic. Next day, the overnight grown *E. coli* cells were pelleted by centrifugation at 12,000rpm in a microcentrifuge for 30sec. The pellet was then re-suspended completely in 300µl buffer P1 (50mM TrisHCL, 10mM EDTA, pH 8.0) containing RNase A at 1µg/ml and the suspension was mixed with 300µl P2 buffer (200mM NaOH, 1%SDS) and 300µl P3 buffer (3M KOAc pH 5.5), respectively. The mixture was centrifuged at 12.000 rpm for 15min at room temperature. The plasmid DNA present in the supernatant was precipitated by adding 700µl of isopropanol and mixed completely. The precipitated DNA was pelleted in the Eppendorf centrifuge at 12,000rpm for 20min and the DNA pellet was washed with 70% ethanol, dried in the fume hood and finally resuspended in 50µl TE, pH 8.0.

Alternatively, for pure plasmid preparations in small and large scales, kits were provided by Qiagen (Qiagen Mini- and Midi- Prep kit). These follow basically the same approach: first overnight culture of bacteria containing the plasmid is pelleted and the cells are lysed by alkaline lysis. Followed by neutralisation and separation of the genomic DNA and cell walls by centrifugation, the supernatant containing the plasmid DNA is then adsorbed on a silica matrix, washed with ethanol, and then plasmid DNA eluted into TE, pH 8.0.

Recovery of DNA fragments from agarose gel

DNA fragments from restriction enzyme digests or from PCR reactions were separated by agarose gel electrophoresis in TBE gels and the gel piece containing the desired DNA fragment was carefully and quickly excised while observing the ethidium bromide stained gel under a UV transilluminator. The DNA fragment was then purified from the excised gel piece using the Qiagen gel extraction kit, following the protocol provided by the manufacturer.

Digestion with restriction enzymes

All restriction enzymes were obtained from NEB, Promega or Roche and the digestions were performed in the buffer systems and temperature conditions as suggested by the manufacturers. The plasmid DNA was digested for 1-2 h genomic DNA was digested at 37°C for 12-16h.

Generation of blunt ends in linearised plasmid DNA

For many cloning experiments, it was necessary to convert the 5' or 3' extensions generated by restriction endonucleases into blunt ends. Repair of 5' extensions was carried out by polymerase activity of the Klenow fragment, whereas repair of 3' extensions was carried out by the 3' to 5' exonuclease activity of the Klenow fragment.

Reaction-mix for 5' extensions:

1-4µg linearised DNA

5µl 10x Klenow buffer

1µl 50x dNTP-mix (each 4mM)

2U Klenow fragment

Add H_2O to make 50µl final volume

Reaction-mix for 3' extensions:

1-4µg linearised DNA

5µl 10x Klenow buffer

2U Klenow fragment

Add H_2O to make 50µl final volume

The reaction was carried out at 16°C for 1hour. After incubation, the reaction was immediately stopped by purification using Qiagen Gel extraction kit.

Dephosphorylation of DNA fragments

To avoid self-ligation of the vector having blunt ends or that has been digested with a single restriction enzyme, 5' ends of the linearised plasmids were dephosphorylated by Shrimp Alkaline Phosphatase (SAP, Promega). Briefly, in a 50µl reaction volume, 1-5µg of the linearised vector-DNA was incubated with 1unit/µgDNA Shrimp Alkaline Phosphatase (SAP) in SAP-buffer (provided by the manufacturer) at 37°C for 2 hours. After 2 hours a further 1µl (2units) of SAP was added and the dephosphorylation reaction incubated at 37°C for a further 16 hours. The reaction was heat inactivated at 65°C for 20min and purified again using the Quiagen Gel Extraction kit.

Ligating DNA fragments

DNA fragment and the appropriate linearised plasmid were mixed in approximately equimolar amounts. T4 DNA ligase (Promega) and ATP were added as indicated below and the ligation reaction was left overnight at 20°C.

Ligation reaction:

Linearised vector DNA (3kb, 200-400ng)

DNA-fragment (1kb, 200-400ng 1:3 molar ratio of vector: insert DNA)

2µl 10x Ligation buffer

1.5unit T4 ligase

Add H_2O to make 20 µl

Glycerol stock of bacterial culture

Glycerol stocks of all the bacterial strains/transformants were prepared for long-term storage. The culture was grown overnight in LB medium with or without the selective antibiotic (depend upon the bacterial transformant). 750µl overnight grown culture was add 250µl 65% glycerol in a 1.5ml microcentrifuge tube, mixed well by vortexing and the tube was frozen on dry ice and stored at –80°C.

Gene inactivation

Cloning of *dock* fragments

To clone the *dock* genes a piece of the *dock* gene sequence was amplified from

genomic DNA from *D. discoideum* AX2 wild type strain.

PCR reaction mixture:

1µl Ax2 genomic DNA (1µg/ml)

1µl Forward primer (20µg/ml)

1µl Reverse primer (20µg/ml)

2µl 2.5mM dNTPs

2µl 10x Pfu buffer (Promega)

1µl Taq: Pfu mixture (4units Taq: 0.6unit Pfu)

Add H_2O to final volume 20µl

The PCR reaction was preheated to 95°C for 10 minutes to denature the DNA before the addition of 1µl Taq:Pfu polymerase (4units Taq: 0.6unit Pfu) followed by 35 cycles of 95°C for 30 seconds, 54°C for 30 seconds and 64°C for 3 minutes.

To amplify the *dockA* (DDB0201649) sequence 1361-4205bp the following primers were used

Forward primer 5'- GAA TCC AAA TGA AAG AAT TAG AAC AAT CTT -3'

Reverse primer 5'- TAC TAA AAT GGA AAT GTA ATA ATT GGA AAA -3'

To amplify the *dockB* (DDB0218629) sequence 2622-4621bp the following primers were used

Forward primer 5'- CGG ATT CCC AAC CTT TAC CT -3'

Reverse primer 5'- GCA ATC ACA TGG ATC ATT GG -3'

To amplify the *dockC* (DDB0191032) sequence 5245-6755bp the following primers were used

Forward primer 5'- AAA AGA ATT GAA AGT AAA ACG ATT GAA -3'

Reverse primer 5'- CCC TTT GAA GTT TTG GGA AA -3'

To amplify the *dockD* (DDB0217599) 4613-6658bp the following primers were used

Forward primer 5'- GCA GAT ATC ACT GAA AAA CGT TTA CTC A -3'

Reverse primer 5'- CTA TTC TTT TCA TAG AGT GGC ATT AGG A -3'

dockG (DDB0190104) starts from the 6bp before the start codon for DockG and finished at 1922bp. This sequence was amplified by the primers below.

Forward primer 5'- ATA AAA GAT GTC ATC ACC AGA TTT ACC ACC -3'

Reverse primer 5'- ATT GTG CCA ATA ATG CAT CAT TCT TTT -3'

To amplify the *dockH* (DDB0184155) sequence 727 -2737bp following primers were used

Forward primer 5'- CAA CAC CAC AAA CAC CTC AAC AAA A -3'

Reverse primer 5'- ATG ATT CAA TCG CAT TCT CTA ATG G -3'

PCR products were visualised on 0.6% agarose gels. The products were excised from the gel and were purified using the Qiagen Gel Extraction Kit. PCR fragments were ligated into a pCR-Blunt II-TOPO vector following protocols from the supplier (Invitogen).

The ligation reaction was transformed into one-shot electrocomp *E.coli* cells (Invitrogen) by a single electroporation pulse of 1.5mv (25µF capacitance) using a Biorad gene pulser II (for details see D. discoideum transformation). The cells were then incubated for 1hour at 37°C with 250µl LB medium before plating on LB/kanamycin (50µg/ml) agar plates. Followed by incubation at 37°C for 16 hours. Colonies were selected and cultured in shaken culture in 1ml LB/kanamycin (50µg/ml) medium for 16 hours at 37°C.

Plasmid DNA was purified from these cultures using the Qiagen Mini-prep kit according to the manufacturer's instructions and analysed for the presence of the Dock inserts by restriction analysis with EcoRI (0.5µg DNA in a final volume of 10µl incubated at 37°C for a minimum of 2 hours). Restriction fragments were visualised on a 0.6% agarose gel. The constructs were confirmed by restriction digest using other enzyme upon the restriction sites inside the insert.

Generating *dock* gene disruption constructs

The Dock /TOPO II Blunt PCR vector was linearised (37°C for a minimum of 2 hours) with different unique restriction enzyme within *dock* inserts, BaeI for DockA, HpaI for DockB, BstBI for DockC, PacI for DockD, ClaI for DockG and PacI for DockH. The linearised plasmids were purified using the Quiagen Gel Extraction Kit and 5' overhangs made blunt by incubation with 2units Klenow

fragment and 40μM dNTP's at 37°C for 30min. The reaction was heat inactivated at 75°C for 10min before dephosphorylation of the restricted ends by the addition of 2units of Shrimp Alkaline Phosphatase (SAP) and incubation at 37°C for 2 hours. After 2 hours a further 2units of SAP was added and the dephosphorylation reaction incubated at 37°C for a further 16 hours. The reaction was heat inactivated at 65°C for 20min and purified again using the Qiagen Gel Extraction kit.

The linearised *dock* /TOPO II blunt vector was ligated to an excess of Blasticidin resistance cassettes (BSR) or Hygromycin resistance cassettes with DNA ligase at 16°C for 16 hours. We generated 8 gene disruption constructs: *dockA/BSR*, *dockB/BSR*, *dockC/BSR*, *dockD/Cre-BSR*, *dockG/Cre-BSR*, *dockH/Cre-BSR*, *dockA/Hyg* and *dockB/Hyg*. BSR cassettes were cut from pBlueBSR by HindIII and BamHI; Cre-BSR cassettes were cut from pLPBLP by SmaI, which contained loxp site can be used to generate multiple mutants using one single selectable marker (Faix et al., 2004); Hyg cassettes were cut from pHygAK-REMI/TOPO by XbaI and SacI. The *dock* gene disruption constructs were amplified from plasmid DNA by PCR using the *dock* primers and the conditions previously described.

Cloning of *elmo1* fragment

Due to low efficiency of blunt end ligation, we cloned two piece fragment of *elmo1* gene into the pLPBLP vector on Cre-BSR cassette' both sides by sticky end ligation instead of blunt end ligation.

Two regions of the *elmo1* gene sequence were amplified using genomic DNA

from *D. discoideum* AX2 wild type strain. The first sequence, Insert 1, contains 1000bp upstream of the *elmo1* start codon and the first 29bp of the *elmo1* coding sequence. This sequence is delimited by the primers below.

Forward primer 5'- AGT CGA CAT ACT GAT TAT CAT CAA GTT G -3'

Reverse primer 5'- AAA GCT TCT TTC TTG GAA TGT AAC TTT -3'

The second sequence, Insert 2, start from 1289bp to 2212bp. The insert2 was amplified incorporates 923bp fragment by the primers below.

Forward primer 5'- AAA AGG ATC CTA TCT GAA CAA TGG AAA CAA -3'

Reverse primer 5'- AAA ACC TAG TTT GTT GGA ATT GAT TGA TTT -3'

The PCR reaction for both sequences was preheated to 95°C for 10 minutes before the addition of 1µl Taq:Pfu (4units Taq: 0.6unit Pfu) followed by 35 cycles of 95°C for 30 seconds, 54°C for 30 seconds and 64°C for 3 minutes.

Cloning of *elmo1* Insert 1

PCR products were visualised on an ethidium bromide 0.6% agarose gels. A 1kb product was excised from the gel and was purified using the Qiagen Gel Extraction Kit. This PCR product and the pLPBLP plasmid were digested with HindIII and SalI for 2 hours at 37°C. The digest products were purified using the Qiagen Gel Extraction Kit and the PCR product was ligated into the linearised vector with T4 DNA ligase (Promega) at room temperature for 1 hour. The ligation reaction was transformed into 100µl *E. coli* XL-Blue chemical competent cells by a 90sec heat shock at 42°C. Transformed cells were then incubated with

300µl of LB medium at 37°C for 15min prior to plating on LB/ampicillin (50µg/ml) agar plates and incubation overnight at 37°C.

Transformant colonies were cultured in 1ml LB/ampicillin (100µg/ml) media at 37°C for 16 hours. Plasmid DNA was purified using a mini-prep protocol and analysed for the presence of *elmo1* Insert 1 by restriction analysis with HindIII and KpnI at 37°C for 2 hours. Restriction digests were visualized on ethidium bromide 0.6% agarose gels.

Cloning of *elmo1* Insert 2

PCR products were visualised on ethidium bromide 0.6% agarose gels. A ~1kb product was excised from the gel and purified using the Qiagen Gel Extraction Kit. This fragment was ligated into pLPBLP plasmid following digestion with BamHI and SpeI according to the protocol described above. Restriction analysis was performed on the plasmid DNA isolated from transformant colonies using BamHII and SpeI and was visualized on ethidium bromide 0.6% agarose gels.

Generation of the *elmo1* knockout construct

Plasmids containing *elmo1* Insert 2 were purified with the Qiagen Gel Extraction Kit and were pooled together before being digested with BamHI and NotI in a final volume of 200µl for 2 hours at 37°C. The restriction digests were visualised on ethidium bromide 0.6% agarose gels. The ~1kb Insert 2 band was excised and purified using the Qiagen Gel Extraction Kit. The pLPBLP plasmid containing Insert 1 was also digested with BamHI and NotI. Purified *elmo1* Insert 2 was ligated into the linearised vector with T4 DNA ligase at room temperature for 1 hour. The ligation reaction was transformed into *E. coli* XL-Blue according

to the protocol described above. Restriction analysis was performed on the plasmid DNA isolated from transformant colonies using NotI and KpnI and was visualized on ethidium bromide 0.6% agarose gels.

This *elmo1* construct was amplified from plasmid DNA by PCR using the *elmo1* Insert 1 forward primer and the *elmo1* Insert 2 reverse primer. The PCR reaction conditions used were as previously described but with an increased extension time of 6 min.

Isolation of genomic DNA from *Dictyostelium* cells

Genomic DNA from *Dictyostelium* was prepared according to the method (Nellen et al., 1987) with slight modifications. The pellet of 1 x 10^8 *Dictyostelium* cells grown in shaking suspension was washed twice with ice-cold KK2 buffer. The pellet of *Dictyostelium* cells was finally resuspended in 1ml cold HMN buffer (10mM $MgCl_2$, 10mM NaCl, 30mM HEPES pH 7.5, 10% sucrose, 0.5% Nonidet P40). The nuclei fraction was obtained by centrifugation at 6,000rpm for 5mins. The nuclear pellet obtained was carefully resuspended in 1ml TE, pH 8.0, with 0.5% SDS and 0.1mg/ml proteinase K and incubated at 56°C for 1h and then 37°C incubation overnight. The genomic DNA was extracted twice with phenol/chloroform (1:1 v/v), precipitated by adding 2.5 vol. 96% ethanol and 1/10 vol. 3M sodium acetate, pH 5.2. The DNA precipitate was carefully spooled with a Pasteur pipette, washed with 70% ethanol, air-dried and dissolved in the desired volume of TE, pH 8.0.

Alternatively, for rapid genomic DNA preparations in small scales, kits were provided by Sigma (Sigma genelute mammalian genomic DNA kit, G1N70). The pellet of 5 x 10^6 *Dictyostelium* cells grown in shaking suspension was washed twice with ice-cold KK2 buffer. The pellet of *Dictyostelium* cells was finally re-suspended in 1ml cold HMN buffer (10mM $MgCl_2$, 10mM NaCl, 30mM HEPES pH 7.5, 10% sucrose, 0.5% Nonidet P40) and incubated on ice for 5mins. The nuclei fraction was obtained by centrifugation at 6,000rpm for 5mins. The nuclear pellet obtained was carefully re-suspended in 50µl HMN buffer, 0.4mg proteinase K, 200µl resuspension solution and 200µl lysis solution (supplied by manufacturer). Incubate the mixture at 70°C for 10mins. Add 500µl of the Column Preparation Solution (supplied by manufacturer) to each pre-assembled GenElute Miniprep. Binding Column and centrifuge at 12,000 x *g* for 1 minute. Discard flow-through liquid. Add 200µl of 100% ethanol to the lysate; mix thoroughly by vortexing 5-10 seconds. Transfer the entire contents of the tube into the treated binding column. Centrifuge at 6500 x *g* for 1 minute. Add 500µl of Wash Solution (supplied by manufacturer) to the binding column and centrifuge for 1 minute at 6,500 x *g*. Add another 500µl of Wash Solution to the binding column; centrifuge for 3 minutes at maximum speed (12,000-16,000 x *g*) to dry the binding column. Pipette 50µl of the Elution Solution (supplied by manufacturer) directly into the center of the binding column; centrifuge for 1 minute at 6,500 x *g* to elute the DNA.

Southern blotting

Southern blotting (Southern, 1975) is a technique used to transfer DNA from its position in an agarose gel to a nitrocellulose/nylon membrane. After transfer, the

membrane can be hybridised with a probe to identify specific fragments. The ethidium bromide stained agarose gel was photographed under UV light to document migration of DNA fragments with respect to the DNA-size marker. DNA was depurinated by incubating the gel in 2 vol. of 0.25M HCl for 20min at room temperature with gentle shaking to fragment large pieces of DNA to facilitate the transfer out of the agarose gel. The gel was rinsed in deionised H_2O to remove excess HCl and was then incubated in 2 vol. of denaturation solution (0.5M NaOH, 1.5M NaCl) for 30min in order to denature the DNA. Now the transfer was performed by capillary transfer technique. Briefly, the gel was transferred directly from the denaturation solution to a buffer reservoir containing a supporting wick (made up of Whatman 3MM paper) and 10x SSC. A dry nylon membrane (Biodyne B membrane, Pall) of the same size as the gel was then directly placed on the alkaline gel. Three pieces of Whatman 3MM paper followed by blotting pads, all cut to the same size as the gel, were placed on top of the nylon membrane. Allow the DNA to transfer to the membrane overnight. Next day, positions of the wells and the orientation of the membrane were marked before removing the membrane from the gel surface. The transferred DNA was crosslinked onto the membrane by UV 120mJ/cm^2 for 2mins. After crosslinking, the membrane was hybridised with a desired probe. The signal was detected by Gene Images™ CDP-Star™ Detection Kit (Amersham Bioscience) following supplied protocol.

Labelling of DNA probes

DNA probes used for southern blotting were obtained by purification of PCR fragments. 0.5µl DNA (~2µg) was diluted in 20µl H_2O and denatured at 100°C for

5mins. Snap the tube cool on ice and add 30µl labelling mixture as below. Incubate the tube in dark at 37°C for one hour. Store the probes in -20°C.

Labelling mixture (all reagents were supplied by the Gene Images™ CDP-Star™ Detection Kit (Amersham Bioscience)):

14µl H_2O

10µl nucleotide mix

5µl random primer

1µl Klenow

Total volume was 50µl.

Before using, labelled probes were denatured at 100°C for 5 minutes.

Isolation of total RNA from *Dictyostelium* Cells

$5x10^6$ cells were inoculated into the small Petri dishes (diameter 3.5cm), containing 1% Agar dissolved in KK2. The cells were allowed to develop to different stages by incubation at 22°C. RNA from cells at different developmental stages was isolated using the Qiagen RNeasy Mini kit (QIAGEN Cat. No.74104). $5x10^6$ cells from each different stage were spun down by the benchtop centrifuge at 500g for 3mins. The pellet was resuspended in 350µl Buffer RLT supplied by the kit. At this step, the cell suspension can be stored in -80°C for two weeks. 70µl cell suspension in Buffer RLT was mixed with equal amount 70% RNase free ethanol. Apply the mixture to RNeasy Mini column suppied by the kit and 10,000rpm spin 15secs on benchtop centrifuge. 350µl Buffer RW1 was applied to column and 10,000rpm spin 15sec. To avoid the

genomic DNA contamination, pipet 80µl DNase I incubation mix (supplied by RNase-Free DNase Set cat. no. 79254) directly onto the RNeasy column and place on the benchtop (20–30°C) for 15min. 350µl Buffer RW1 was added to the column and 10,000rpm spin 15sec.Transfer the column to new 2ml collection tube and wash the column twice by 500µl Buffer RPE twice. Discard the flow through and transfer the column to new 1.5ml eppendorf tube. 30µl RNease free water to elute RNA from the column with 14,000rpm 15sec by benchtop centrifuge. Store the RNA in -80°C.

The concentration of RNA was determined by measuring the OD260 of the solution using a spectrophotometer. 1 OD260 = 40µg/µl RNA

cDNA synthesis

Dilute 2µg total RNA in 50µl RNase free water. Snap cool on ice after 10mins heating. Add 30µl 1x Reverse transcription mixture. Incubate at 37°C for 1hour, followed by 30min at 56°C. Store 5µl aliquots at -80°C for two weeks.

1X Reverse transcription mixture:

3µl 0.2µg/µl Random Hexamer

2µl 25mM dNTPs

8µl H_2O

16µl 5x Buffer

1µl Reverse Transcriptase (Promega)

RT PCR

The expression of some of the dock and *elmo1* genes was detected using PCR of cDNA samples made as described above

The following primers were used to detect the expression of the specific genes

dockA:

Forward primer 5'- AAG AAC AAA TTG GAT GGT ATA GTG G -3'

Reverse primer 5'- CGA TCA CGT AAA TCA TAG GTA ATC T -3'

Excepted product size: 490 bps from genomic DNA template

354 bps from cDNA template

dockB:

Forward primer 5'- AAC TCA ATT AAA TCG CGT TAT GGT G -3'

Reverse primer 5'- GGC AGA CAT TTT CTC TTG AAG ATT TTG -3'

Excepted product size: 345 bps from genomic DNA and cDNA template

dockC:

Forward primer 5'- ATC ATT TAT TAA CAA TTC AAT TAC AAA ATC -3'

Reverse primer 5'- CAC CAC CAT TTA CAC TAT CAA TTA AAC G -3'

Excepted product size: 369 bps from genomic DNA template

282 bps from cDNA template

elmo1:

Forward primer 5'- TCT TTA TTT TTA TCA TCT GGT CAA TTA GTT -3'

Reverse primer 5'- CTG TCG ATG TCA TTG ATG TAA TAG TAA ACT C -3'

Excepted product size: 603 bps from genomic DNA template

516 bps from cDNA template

IG7:

Forward primer 5'- TTA CAT TTA TTA GAC CCG AAA CCA AGC G -3'

Reverse primer 5'- TTC CCT TTA GAC CTA TGG ACC TTA GCG -3'

Excepted product size: 368 bps from genomic DNA and cDNA template

The PCR reaction for was preheated to 94°C for 4min followed by 25 cycles of 94°C for 30sec, 52°C for 30sec and 64°C for 1min.

PCR reaction mixture:

5µl cDNA

1µl Forward primer (20µg/ml)

1µl Reverse primer (20µg/ml)

2µl 2.5mM dNTPs

2µl 10x Pfu buffer (Promega)

1µl Taq:Pfu mixture (4units Taq: 0.6unit Pfu)

Add H_2O to final volume 20µl

cDNAs were normalized using PCR of the constitutively expressed IG7 gene . The PCR product (368 bps) were visualised on 1% agarose gels. The amount of the templates were normalised by the florescence density on the agarose gel. Until PCR products by using IG7 primers with normalised template were in the similar florescence density. The normalised templates were run the PCR by

specific primers to determine gene expression.

Cloning of Docker domain constructs and expression in cells

To clone the Docker domains from DockA and DockB protein, DockerA and DockerB respectively, were amplified these segments from genomic DNA by PCR using the primers below.

To amplify the DockerA from DDB0201649 sequence 5286-8910bp the following primers were used

Forward primer 5'- AAG GAT CCT TAG AGA GTG AAA TCA TTC AAA CCA AT -3'

Reverse primer 5'- ACT CGA GTT AAT TTT TGT CTT GAA TTT TTC ATT GT -3'

To amplify the DockerB from DDB0218629 sequence 4066-5783bp the following primers were used

Forward primer 5'- CCA CTT GGA TCC TGT GAA TTT AAA GAA TAT AAA TCA TTC ATC -3'

Reverse primer 5'- TTT TAT CTC GAG GTT CCA ATT CAT TTC TCA TTC TTG T -3'

The PCR reaction for both sequences was preheated to 95°C for 10min before the addition of 1µl Taq:Pfu (4units Taq: 0.6unit Pfu) followed by 35 cycles of 95°C for 30 sec, 54°C for 30sec and 64°C for 3min.

PCR reaction mixture:

1µl Ax2 genomic DNA (1µg/ml)

1µl Forward primer (20µg/ml)

1µl Reverse primer (20µg/ml)

2µl 2.5mM dNTPs

2µl 10x Pfu buffer (Promega)

1µl Taq:Pfu mixture (4units Taq: 0.6unit Pfu)

Add H_2O to final volume 20µl

The PCR fragments and GFP expression vector PB17s were digested by BamHI and XhoI. Purified Docker domain fragments were ligated into the linearised PB17s vector. Positive plasmid DNA was transfect wildtype Dictyostelium by the electroporation.

Synergy experiments

Cells from different strains were harvested and washed twice in KK2. Mix 90% cells with 10% Ax2 A15LacZ cells (total $5x10^6$ cells). Resuspend the mixture in 30µl KK2. Place 10µl cell suspension mixture on one square piece of nitrocellulose filter. Incubate filters on KK2 agar dish at 22°C for development. Submerge the filters in 0.25% glutaraldehyde to fix the cells for 10mins. Remove the fixative carefully and wash twice in KK2. Pipette 1ml of β galatosidase staining solution on the filter until the blue colour is sufficiently developed (1-5 hours). Wash the filters twice in Z-buffer. Mount the filter on a microscope slide in 80% glycerol.

GFP Synergy experiment

Harvested cells and wash twice in KK2. Mix 5% GFP expressing cells from different strains with 95% Ax2 cells. Resuspend $5x10^6$cell mixture in a 30µl KK2. Drop 10µl cell suspension on a 1% KK2 agar plate and leave it to air dry for 10mins. Incubate the plates for the desired time at 22°C. Photograph the phenotypes at different time points.

Phototaxis assay

$3x10^6$ cells were resuspended in 30µl H_2O and inoculated into the Petri dish containing 1% Agar dissolved in H_2O. The drops were placed 1cm from the plate's periphery. The Petri dishes were incubated in a box with a lateral hole, 3mm in diameter, opposite the inoculation point, as a unidirectional light source. Temperature was kept constant at 22 °C. Approximately 72 h after inoculation, slime trails were blotted onto a clear transparency film and stained with Coomassie Blue for 30 minutes followed by destaing in 7% acetic acid (Fisher *et al.* 1981).

Macropinocytosis assay

For measuring fluid-phase uptake, a modification of the previously published phagocytosis assay (Hacker et al., 1997) was developed. Samples (1ml) of $2x10^7$ cells were shaken in 2ml tube on benchtop vortex. TRITC-dextran (Sigma) was added to a final density of 1mg/ml. Samples of 50µl were withdrawn at

intervals and added 5µl 1% azide to the sample to inhibit the cell metabolism. Cells were pelletd by centriguation for 6sec in an Eppendorf benchtop centrifuge (14,000 rpm). The cell was washed in KK2 buffer and spun for 6sec in an Eppendorf benchtop centrifuge again. The cell pellet was resuspended in 100µl of KK2 buffter containing 0.1% Tween20. The relative fluorescence intensity was immediately measured in 100µl volume in a 96 well plate (Greiner cellstar 96 flat bottom) in a CytoFluor Multi-Well Plate Reader series 4000 using 488nm light for excitation and recording emission at 520nm.

Phagocytosis assay

AX2 and the mutant cell lines were grown to densities up to $5x10^6$ cells/ml, harvested, washed, and resuspended in KK2 buffer to a density of $2x10^7$cells/ml in a 2ml tube. 120ul Tetramethyl rhodamine isothiocyanate (TRITC)-labelled yeast were added to 1.5ml of the cell suspension. Samples of 200µl were withdrawn at 0, 15, 30, 45, 60, 90 and 120min and added to 1ml cold KK2. Then 100µl trypan blue solution (20mg/ml dissolved in 20mM sodium citrate containing 150mM NaCl; Merck, Darmstadt, Germany), which quenches the fluorescence of noninternalized yeast cells was added to the sample. After 5mins of agitated incubation, cells were spun and the supernatant was removed carefully. After resuspension of the pellet in 100µl cold KK2 buffer, the fluorescence was measured in 100µl volume in a 96 well plate (Greiner cellstar 96 flat bottom) in a CytoFluor Multi-Well Plate Reader series 4000 using 530nm light for excitation and recording emission at 580nm.

Fluorescent labelling of yeast

5g yeast was resuspended in 50ml PBS in 100 ml flask. Waterbath the flask in boiling water for 30min with stirring. The cell pellet was collected by 4000rpm centrifuge (Eppendorf 5810 R centrifuge) and washed 5 times with PBS and twice in KK2. Adjust the concentration of cell particles to $1x10^9$particles/ml. For labelling, resuspend the pellet of 2×10^{10} particles in 20ml 50mM Na_2HPO_4 pH 9.2. Add 2mg TRITC, incubate 30 minutes at 37°C on a rotary shaker. Wash twice in 50mM Na_2HPO_4 pH 9.2 and four times in KK2. Aliquoted of $1x10^9$ particles/ml at -20°C.

Actin measurement by Flow Cytometry

Harvest cells and wash twice in KK2. Resuspend cells at $1x10^7$/ml. 200µl cell resuspension to one FACS tube (Falcon 12x75mm 5ml round-bottom tubes cat. No. 2054) ($2x10^6$ cells per tube) total four tubes for one stain, one for control, the rest three are staining samples. Fix the cells in fresh 4% paraformaldehyde in H_2O 15mins. Wash the pellet twice in KK2. Remove the supernatant and resuspended the pellet in 1ml 0.1% Triton X-100 in PBS on ice 5mins. Wash the pellet twice in KK2. Resuspend the pellet in 200µl KK2, add 1µl Alexa phalloidin 488 (from molecular probes A12379) (300units in 1.5ml Methanol) to each staining tube RT 30mins. Wash the cells by KK2, Resuspend pellet in 1ml KK2. Run the samples in Flow Cytometry.

Chemotaxis Assays

AX2 and the mutant cell lines were grown to densities below $5x10^6$ cells/ml, harvested, washed, and resuspended in KK2 buffer to a density of $2x10^7$cells/ml and pulsed with 30nM cAMP for 5 hours at 6mins intervals.

One Drop Chemotaxis Assay: (Van Haastert et al., 1982)

200µl cell suspension was spun down and the pellet resuspended in 20µl KK2 buffer. The cells were laid out as a line of little drops (0.1µl) on $1x10^{-8}$M cAMP containing 1% KK2 agar plates. The drops were allowed to dry in a couple of minutes and the results were scored every 10min by inspection of the drops under a dissection microscope. For every time point the percentage drops showing a positive response (Figure 2.1 B) is recorded for each strain.

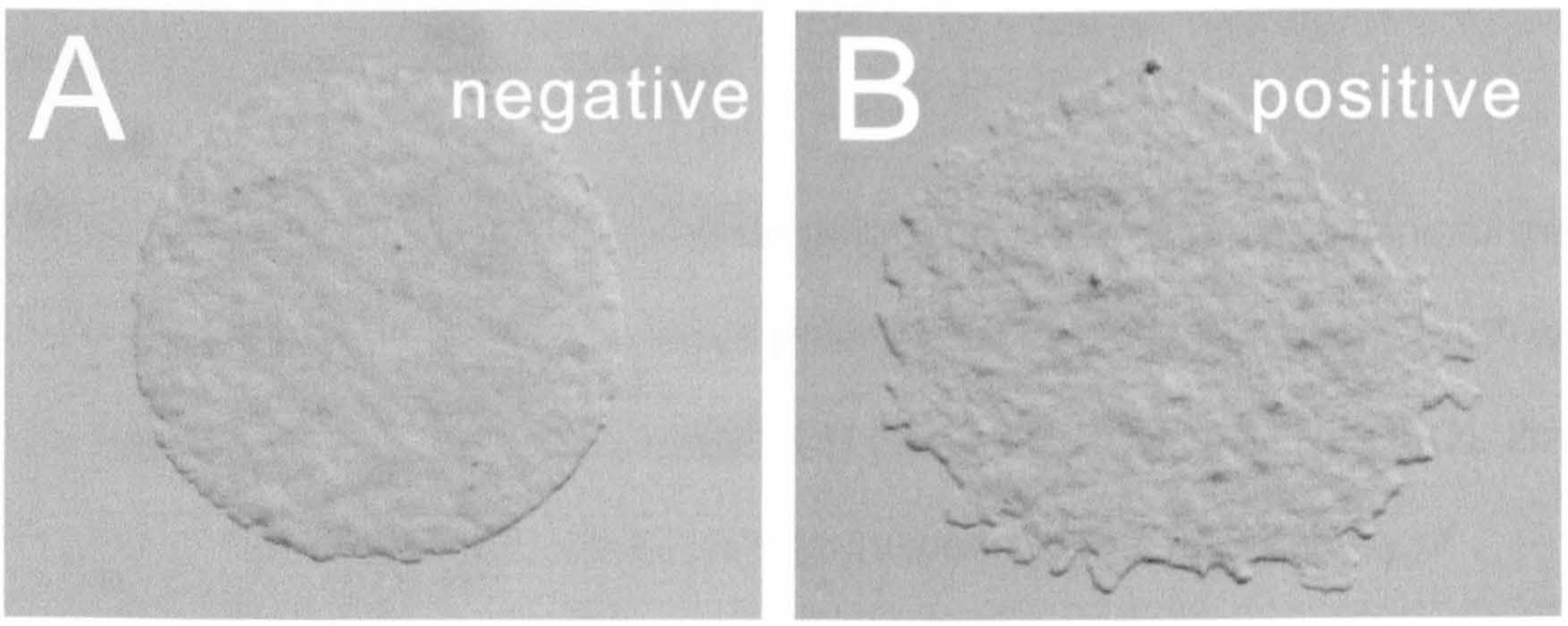

Figure 2.1 One Drop Chemotaxis. Figure A is negative response. **Figure B** is positive chemotaxis to 10^{-8}M cAMP after 30mins.

Two Drop Chemotaxis Assay: (Van Haastert et al., 1982)

Cell suspension was laid out as a line on 1% KK2 agar plate. $1x10^{-5}$M cAMP solution (0.1ul) was laid out as small drops 100µm from cell drops on the agar

plate. The results were scored every 15min by inspection of the drops under a dissection microscope. A chemotactic reaction was considered positive when the half of the cell drop closest to the cAMP contained at least twice as many cells as the opposite half.

Needle Chemotaxis Assay

Chemotaxis analysis was performed as described previously (Gerisch et al., 1975). AX2 and the mutant cell lines were grown to densities below $5x10^6$ cells/ml, harvested, washed, and resuspended in KK2 buffer to a density of $2x10^7$cells/ml and pulsed with 30nM cAMP for 5 hours at 6mins intervals. An Eppendorf Patchman micromanipulator with a glass capillary needle filled with $1x10^{-4}$M cAMP solution was brought into the field of view of confocal microscope. The response of the cells was recorded by time-lapse video.

Actin polymerization assay

To measure the cAMP-stimulated actin polymerisation response, a miniaturized and adapted version of the procedure described previously(Kim et al., 1997) was used. Growing cells were washed with DB (5mM KH_2PO_4, 5mM Na_2HPO_4, 2mM $MgSO_4$, and 0.4mM $CaCl_2$, ph6.2) and re-suspended to a final density of $1x10^7$cells/ml. The cells were then developed in suspension with 30nM cAMP pluse every 6min for 4 hours on a horizontal shaker rotating at 160rpm. Next, 3mM caffeine was added, the cells shaken for further 20min to interrupt the cAMP oscillations then washed twice in phosphate-magnesium (PM) buffer (5mM KH_2PO_4 pH6.5, 5mM Na_2HPO_4, 2mM $MgSO_4$) to remove the caffeine,

re-suspended to $3.3x10^7$cells/ml and shaken on a horizontal shaker at 850rpm for 10min. At t=0, the cells were stimulated with 1mM cAMP then 20ul samples were taken at two second intervals and added to fixing solution (3.7% formaldehyde, 0.1% Triton, 250nM TRITC-Phalloidin, 20mM KPO4, 10mM PIPES, 5mM EGTA, 2mM MgCl2, pH 6.8). After staining for 1hour, in the dark, on a room temperature centrifuge the fixed cells were pelleted by centrifugation at 14,000rpm for 3min, re-suspended in 500µl methanol and mixed for one hour on a horizontal shaker (in the dark) to extract the phalloidin. After centrifugation to clear the methanol/phalloidin mix, 100µl of the supernatant was transferred to a 96 well plate (Greiner cellstar 96 flat bottom) for determination of the rhodamine fluorescence on CytoFluor Multi-Well Plate Reader series 4000 using 530nm light for excitation and recording emission at 580nm.

Generation of GST fusions of Rho GTPases

DNA fragments encoding Dictyostelium Rho GTPases were amplified by PCR using specific oligonucleotide primers that introduced restriction sites suitable for cloning into pGEX vectors (Amersham Pharmacia Biotech). For RacA, only the GTPase domain was cloned. All constructs were verified by sequencing. Vectors were introduced into XL-1 blue *E. coli* cells.

GTPase binding assays

Expression of GST fusions of Rho GTPases was performed at room temperature for 5 hours after induction with 0.5mM IPTG. Bacteria were lysed in a buffer containing 50mM Tris, pH 8, 300mM NaCl, 10mM $MgCl_2$, 4mM DTT, 1mM

phenylmethylsulfonyl fluoride, complete protease inhibitor cocktail (Roche) and 0.1mg/ml lysozyme. After sonication, bacterial lysates were cleared by centrifugation at 25,000xg for 1 hour at 4°C. Supernatants were shock-frozen in liquid nitrogen and stored at -80°C. For binding to glutathione-sepharose (Amersham Pharmacia Biotech), lysates were incubated with beads for 60minutes at 4°C. Beads were washed extensively in a buffer containing 50mM Tris, pH 8, 1M NaCl, 10mM $MgCl_2$ and 4mM DTT followed by equilibration in Dock lysis buffer.

Dictyostelium cells expressing GFP-tagged DockerA or DockerB were lysed in Dock lysis buffer (25mM Tris, pH 7.5, 150mM NaCl, 5mM EDTA, 0.5% Triton X-100, 1mM NaF, 0.5mM Na_3VO_4 (sodium orthovanadate) and complete protease inhibitor cocktail). Lysates were clarified by centrifugation at 14,000xg for 5 minutes. Clarified lysates were shock-frozen in liquid nitrogen and stored at -80°C. 1ml cell lysate (equivalent to 4 x 107 cells) was incubated with the indicated GST fusion proteins pre-bound to glutathione-sepharose for 60 minutes at 4°C. Beads were washed extensively with Dock lysis buffer and proteins were eluted from the beads with SDS sample buffer. GFP-Docker fusions and GST fusions were detected by immunoblotting using anti-GFP monoclonal antibody K3-184-2 (Noegel et al., 2004) and anti-GST polyclonal antibody, respectively, followed by enhanced chemoluminescence.

For nucleotide loading, GST-Rac1A pre-bound to gluathione-sepharose beads was incubated for 60min at 4°C with a 10-fold molar excess GDP or GTPγS. The reaction was then stopped by addition of $MgCl_2$ to a final concentration of 15mM prior to incubation with *Dictyostelium* lysates supplemented with 15mM $MgCl_2$.

SOLUTIONS:

HL5 Medium (per litre) (pH 6.3)

15.4g Glucose, 14.3g Oxoid Bacto-Peptone, 7.15g Oxoid-Yeast Extract, 0.52g Na_2HPO_4, 0.48g KH_2PO_4 in H_2O then autoclave for less than 15 minutes.

SB plates (per litre) (pH 7.0)

5g Glucose, 5g Bacto-Peptone, 0.5g Bacto-Yeast Extract, 2.3g KH_2PO_4, 1.3g K_2HPO_4, 15g Agar in H_2O then autoclave for less than 15 minutes.

LB medium (per litre) (pH 7.0)

10g Bacto-Peptone, 5g Bacto-Yeast Extract, 10g NaCl in H_2O adjust to pH 7.0 with NaOH

Autoclave for less than 15 minutes

LB plates (per litre)

LB medium, 15g Agar, (selection-100µg/ml Ampicillin)

KK2 Buffer (pH 6.8)

20mM KH_2PO_4

20mM K_2HPO_4

DB Buffer (pH 6.2)

5mM KH_2PO_4

5mM Na_2HPO_4

2mM $MgSO_4$

0.2mM $CaCl_2$

EP Buffer (pH 7.0)

20mM Hepes

5mM $NaHCO_3$

1mM NaH_2PO_4

4M KCl

5M NaCl

1M $MgCl_2$

Adjust pH to 7.0 then autoclave

TFB I Buffer (pH 5.8)

30mM KOAc

50mM $MnCl_2$

100mM KCl

10mM $CaCl_2$

15% (v/v) glycerol

Adjust pH to 5.8 by H-acetate

TFB II Buffer (pH 7.0)

10mM MOPS

75mM $CaCl_2$

10mM KCl

15% (v/v) glycerol

Adjust pH to 7 by NaOH

P1 Buffer (pH 8.0)

50mM TrisHCL

10mM EDTA

Adjust pH to 8.0 by HCL

P2 Buffer

200mM NaOH

1% SDS

P3 Buffer (pH 5.5)

3M KOAc

Adjust pH to 5.5 by acetic acid

6x DNA loading buffer

Dissolve 4g sucrose and 2.5mg Bromophenol blue in a 6ml solution of TE buffer.

Once dissolved, bring up to a final volume of 10 ml with TE buffer.

Southern Blot Denaturing buffer

1.5 M NaCl

0.5M NaOH

Southern Blot Neturalizing buffer (pH 7.0)

0.5M Tris-HCL

1.5M NaCl

Southern Blot Hybridization buffer (100ml)

1:20 diluted liquid block

0.1% (W/V) SDS

5% (W/V) dextran sulphate

in 5X SSC

20x SSC

0.3M Na(3)citrate (tri-sodium citrate) , 3M NaCl

Southern wash solution 1

1x SSC

0.1% SDS

Southern wash solution 2

0.5x SSC

0.1% SDS

Buffer A for southern (pH 9.5)

300mM NaCl

100mM TrisHCl

pH 9.5 then autoclave

Wash buffer for Gene images CDP-Star detection module

0.3% (v/v) Tween 20 in buffer A

Southern Antibody solution (10ml)

0.5% (W/V) BSA (Albumin, Bovine) 0.05g in 10ml buffer A then add 1.5ul antifluorescein-AP to the fresh solution

HMN buffer (pH 7.5)

10mM $MgCl_2$

10mM NaCl

30mM HEPES

10% sucrose

0.5% Nonidet P40

STE buffer (pH 8)

100mM TrisHCl

150mM Nacl

1mM EDTA

5mM DTT

Fixative solution for lacZ staining (Synergy experiment)

0.25% Glutaraldehyde

2% Tween 20

In Z-buffer

Z-buffer (pH 7.0)

10mM KCl

40mM NaH_2PO_4

60mM NaH_2PO_4

1mM $MgSO_4$

β galactosidase staining solution

1mM Xgal

5mM $K_3Fe(CN)_6$

5mM $K_4Fe(CN)_6$

1mM EGTA

In Z-buffer

Chapter III Investigation into the role of *dockA* and *dockB* genes

3.1. Introduction

Aggregation competent Dictyostelium cells respond by chemotaxis to cAMP gradients. cAMP stimulation causes a transient localized increase in PIP3 concentration in the plasma membrane. PIP3 binding domain containing Rac GEF's are thought to mediate the cAMP signal through the activation of Rac's which ultimately result in actin polymerization and movement. Inhibition of PIP3 formation however results only in a partial loss of chemotaxis, implying that there may exist other signalling pathways that mediate the cAMP signal. The Dock180 proteins have been suggested to function as unconventional Rac-GEF's, which mediate membrane ruffling, phagocytosis and chemotaxis(Duchek et al., 2001; Kiyokawa et al., 1998a; Kiyokawa et al., 1998b; Nolan et al., 1998; Wu and Horvitz, 1998). Dock180 contains a novel domain, termed Docker domain, which specifically recognizes nucleotide-free Rac and can promote loading of GTP by Rac in vitro (Brugnera et al., 2002; Cote and Vuori, 2002).

We have identified the 8 *dock* genes in *Dictyostelium,* which we named *dockA*, *B*, *C, D, E, F, G* and *H*. The aim of this study is to gain insight into the role of Dock proteins especially DockA and DockB in *Dictyostelium* by generating knockout mutants. Our data suggest that *dockA* and *dockB* are involved in growth, endocytosis and phototaxis. d*ockA*^{null}, *dockB*^{null} and *dockA/B*^{null} cells show reduced chemotaxis when compared to wild type cells, both in the absence and

presence of a PI3 Kinase inhibitor LY294002. d*ockA*^{null}, *dockB*^{null} and *dockA/B*^{null} mutants all show altered cAMP stimulated actin polymerization responses. These data support the notion that *dock*A and *dockB* are involved in the control of cAMP induced the actin polymerization necessary for efficient chemotaxis.

3.2. Results

3.2.1. *Dictyostelium dock* genes

In order to investigate whether *Dictyostelium* contained *dock* genes that could be involved in the regulation of the actin cytoskeleton, we performed a Blast search using the human Dock180 protein sequence as query sequence (Altschul et al., 1990). We identified 8 *dock* genes in *Dictyostelium*, which we called *dockA, B, C, D, E, F, G,* and *H*. Using each of the *Dictyostelium* Dock protein sequence as query sequence to do Blast search again, we could not find more dock genes in current genome database. Human Dock180 is a large protein of 1866 amino acids, and contains an SH3 domain at its extreme N terminus, a Docker domain and proline-rich motifs near its C terminus (Cote and Vuori, 2002). *Dictyostelium discoideum* Dock proteins are around 2000 amino acids length and all the proteins contain a Docker domain near their C-terminus, except DockH which has its Docker domain in the middle of the protein (Figure 3.1).

DockA and DockB both contain a SH3 domain in their N-termini. No significant domain information was found in the remaining parts of the Dock proteins by blasting against the SMART or PFAM database. Amino-acid sequences of Dock-related proteins from mammalian, *Drosophila, C. elegans and Dictyostelium discoideum* were aligned by Vector NTI Clustal W package. The

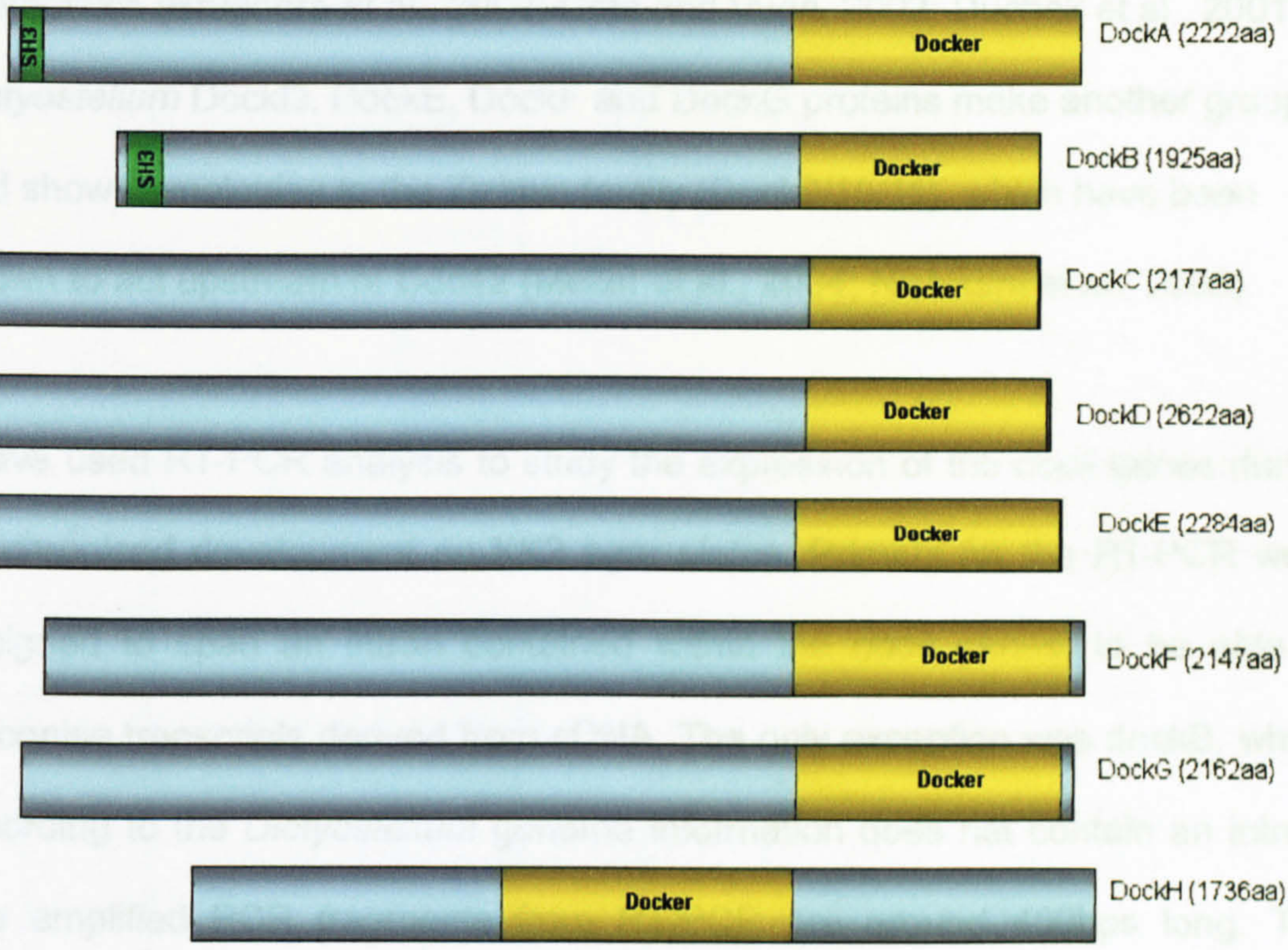

Figure 3.1 *Dictyostelium discoideum* Dock proteins. *Dictyostelium* Dock proteins are in around 2k amino acids length and all the proteins contain a C-terminal Docker domain, except DockH has its Docker domain in the middle of the protein. DockA and DockB both contain a SH3 domain at their N-terminus. No significant conserved domain information was found in the rest of the Dock proteins by using the protein blast against SMART or PFAM database.

final output tree was generated with MEGA (Figure 3.2). DockA, B and C of *Dictyostelium* proteins show a closer relationship to mammalian Dock180, MBC and CED-5, which were shown to act as RacGEF's during phagocytosis and chemotaxis (Brugnera et al., 2002; Cote and Vuori, 2002; Duchek et al., 2001). *Dictyostelium* DockD, DockE, DockF and DockG proteins make another group and show homologies to the Zizimin family (Dock9/10/11), which have been shown to act upstream of Cdc42 (Meller et al., 2004; Nishikimi et al., 2005).

I have used RT-PCR analysis to study the expression of the *dock* genes during synchronised development on KK2 agar plates. Primers for the RT-PCR were designed to span an intron contained within the *dock* genes, to be able to recognise transcripts derived from cDNA. The only exception was dockB, which according to the *Dictyostelium* genome information does not contain an intron. The amplified PCR fragments from RT-PCR are around 400bps long. The expression patterns are shown in Figure 3.3. The expression of the ribosomal gene IG7 was used as a normalisation control. The *dock* genes display similar patterns of developmental regulation. *dockA* is expressed during all the stages of development. In-Situ Hybridization data from *Dictyostelium* cDNA project indicated that *dockA* is expressed specifically in prestalk cells in the slug stage of development (Figure 3.4). We managed to amplify a specific *dockB* fragment from cDNA treated with RNAse free DNAse I. *dockB* fragment is seen to be present from 0~20 hours of development and expression decreases at 24 hours. These results suggest that *dockA* and *dockB* are required during growth and development of *Dictyostelium discoideum*.

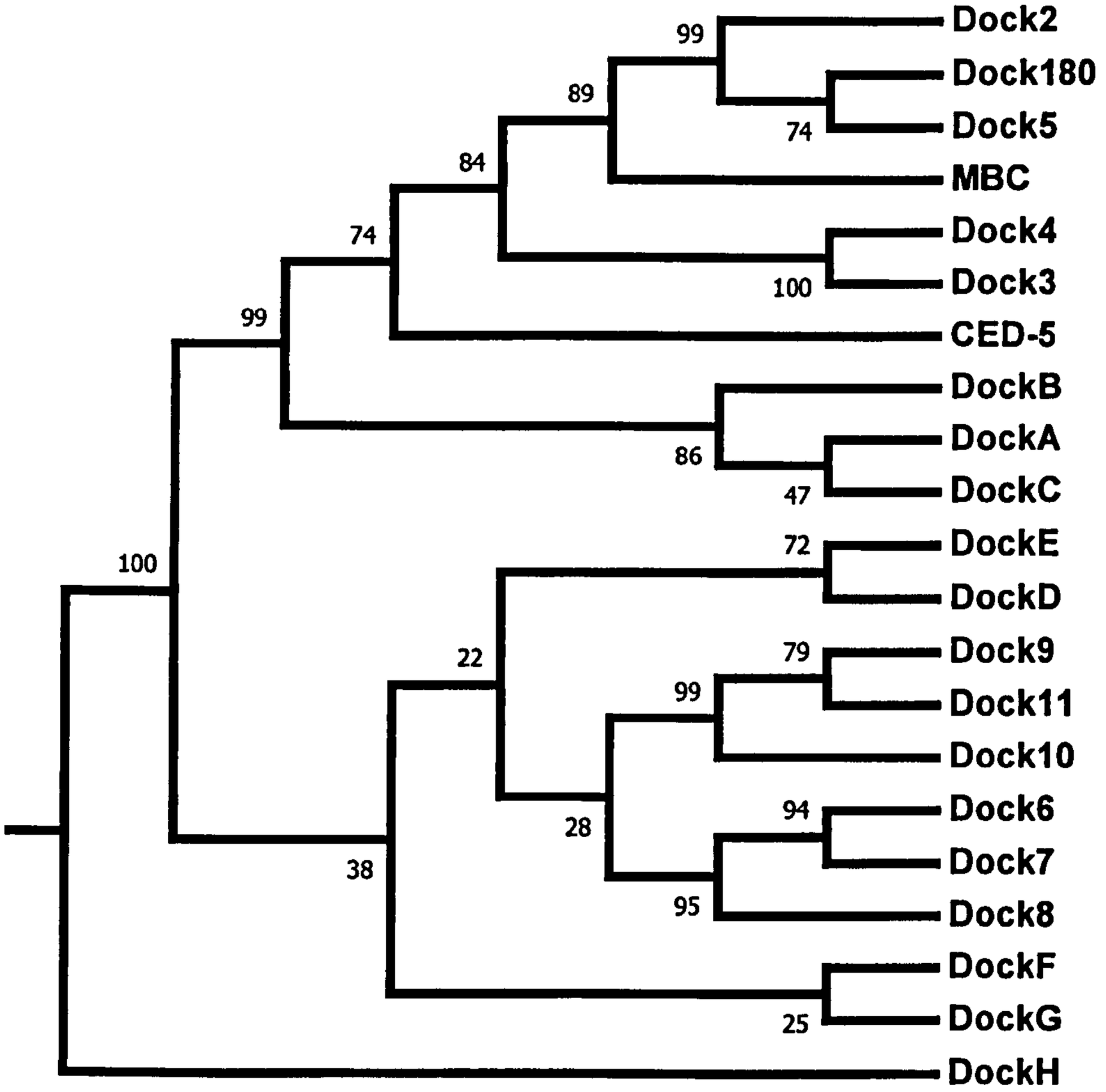

Figure 3.2 Phylogenetic tree of Dock-related proteins. Amino-acid sequences that cover the region of the Docker domains of the indicated human, *Drosophila*, *C. elegans* and *Dictyostelium* family members were aligned with ClustalW. The tree was derived by neighbor-joining analysis applied to pairwise sequence distances calculated with the PHYLIP package to generate unrooted trees. The final output was generated with MEGA. The number at each node represents the percentage of bootstrap replicates (out of 100). *Dictyostelium* DockA, B and C show relatively close to Mammalian Dock180, Dock2, *Drosophila* MBC, and *C.elegans* CED-5. DockD, DockE, DockF and DockG proteins in *Dictyostelium* make another group with Dock9/10/11 family.

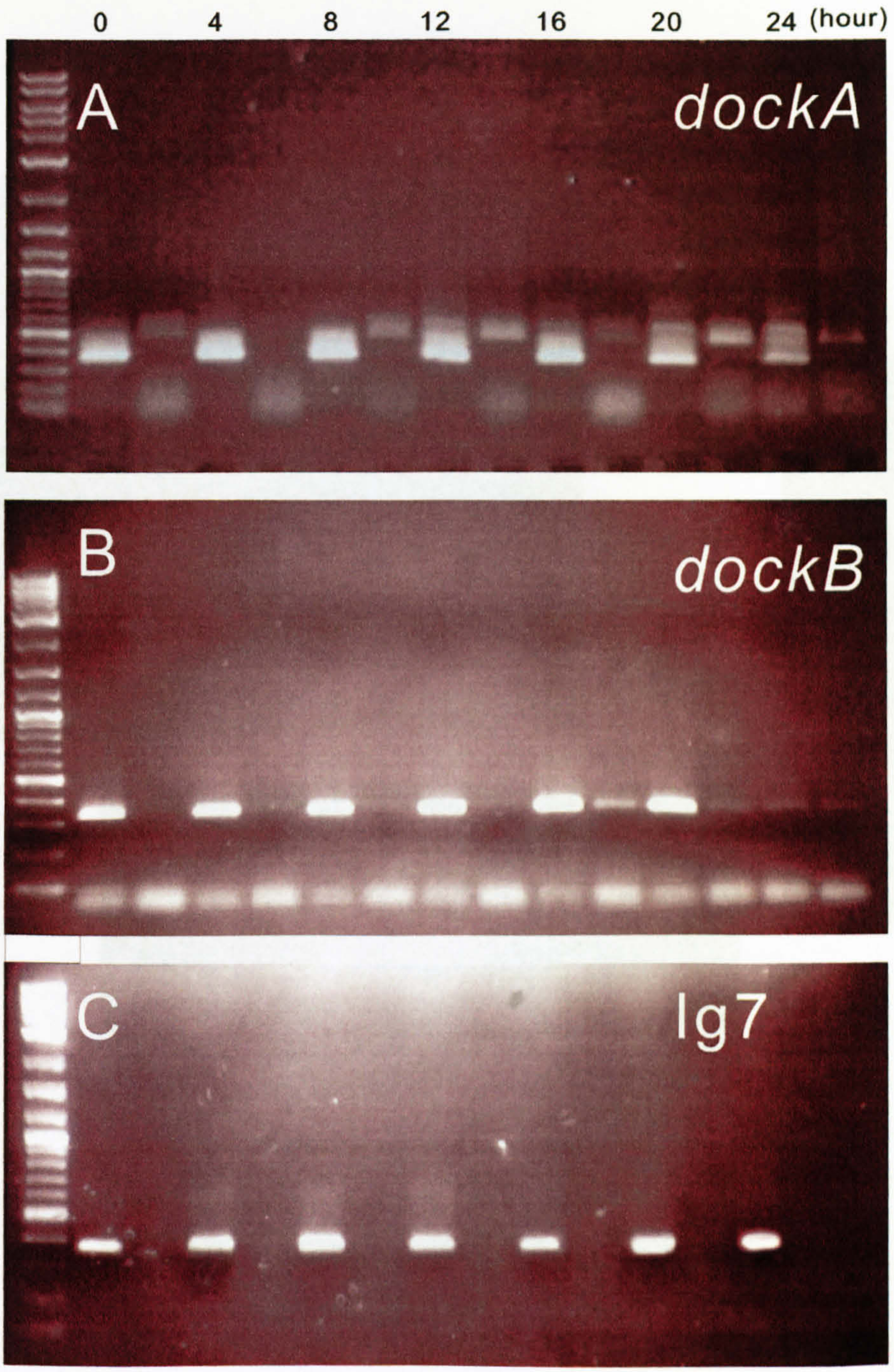

Figure 3.3 *dockA* and *dockB* expression profile during growth and development. **(A)** RT-PCR primers for *dockA* were designed to flank an intron. Therefore the specific fragment amplified from cDNA is 363bp, which is 127bp smaller than the fragment piece amplified from contaminating genomic DNA. RT-PCR products shown are taken every 4 hours during development from 0 hrs to 24 hrs (left to right). *dockA* is expressed during all the stages of growth and development. **(B)** After treating the cDNA with RNAse free DNAseI to get rid of the contaminated genomic DNA, a specific *dockB* fragment is seen to be present from 0~20 hours of development and expression decreases at 24 hours. **(C)** Expression of the ribosomal gene IG7 was run as a normalisation control. In parallel we load the PCR products by using cDNA which was transcribed in the absence of reverse transcriptase. These data were reproducible in 6 independent RT PCR reactions from three independent cDNA templates.

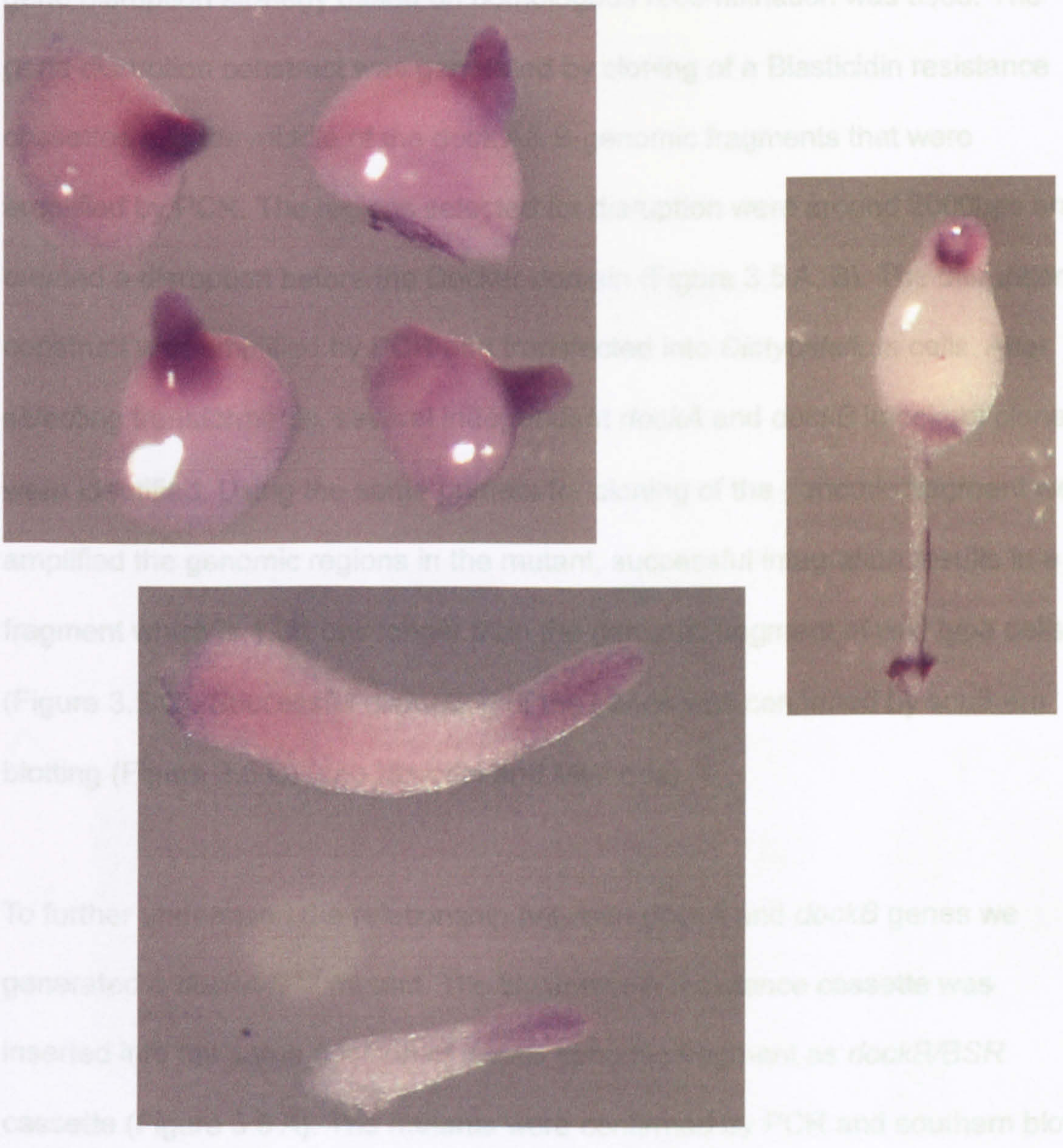

Figure 3.4 *In situ* hybridization of *dockA*. The In-Situ Hybridization data from *Dictyostelium* cDNA project show that *dockA* is expressed specifically in prestalk cells. (http://dictycdb.biol.tsukuba.ac.jp/cDNAproject.html)

3.2.2. Generation of *dockA* and *dockB* null mutants by the homologous recombination

To investigate the role of the *dockA&B* genes in the regulation of *Dictyostelium*, a gene disruption strategy based on homologous recombination was used. The gene disruption construct was generated by cloning of a Blasticidin resistance cassettes into the middle of the dock A& B genomic fragments that were amplified by PCR. The regions selected for disruption were around 2000bps and created a disruption before the Docker domain (Figure 3.5 A, B). The disruption construct was amplified by PCR and transfected into *Dictyostelium* cells. After selecting transformants, several independent *dockA* and *dockB* knockout clones were identified. Using the same primers for cloning of the genomic fragment we amplified the genomic regions in the mutant, successful integration results in a fragment which is 1.3K bps longer than the genomic fragment of wild type cells (Figure 3.5 C). Successful disruption of the genes was confirmed by southern blotting (Figure 3.5 D) (see Material and Methods).

To further understand the relationship between *dockA* and *dockB* genes we generated a *dockA/B*^{null} mutant. The Hygromycin resistance cassette was inserted into the same position of *dockB* genomic fragment as *dockB/BSR* cassette (Figure 3.6 A). The mutants were confirmed by PCR and southern blot (Figure 3.6 B C)

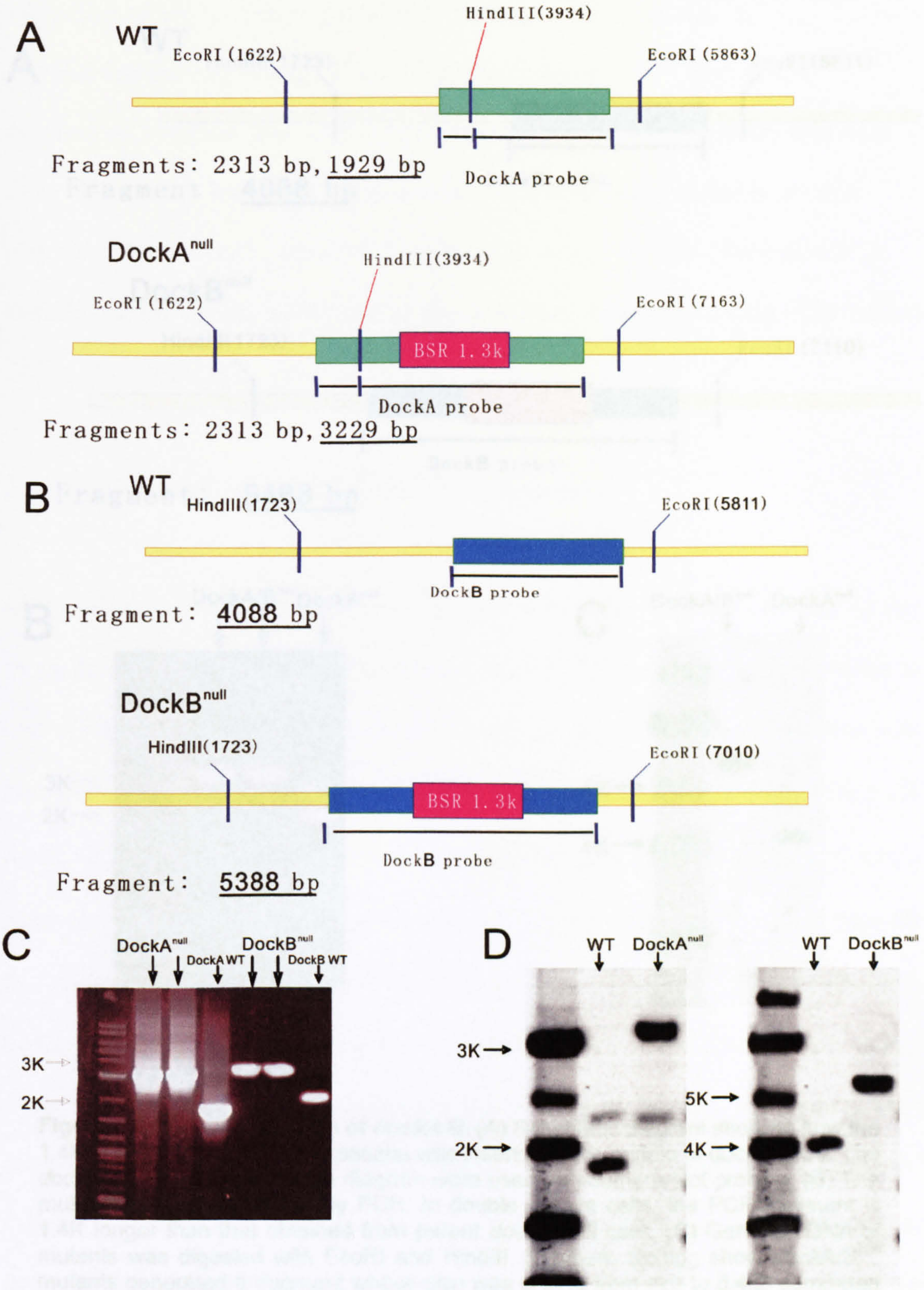

Figure 3.5 Gene inactivation of *dockA* and *dockB*. **(A)(B)** Schematic diagrams showing how the 1.3kb Blasticidin resistance cassette was inserted in the middle of *dockA* and *dockB* genes. *dockA* and *dockB* probes indicated in the diagram were used for southern blot probing. **(C)** The mutant strains were tested by PCR. In the knockout strains the PCR product amplified is 1.3K longer than that of wild type cells. **(D)** The genomic DNA of mutants was digested by EcoRI and HindIII. Southern blotting show that the *dockA* mutant generates a fragment of 3.2K bps compare to wild type cells where the fragment is 1.9kb, whereas *dockB* null cells generated a fragment that was shifted from 4kb to 5.3kb.

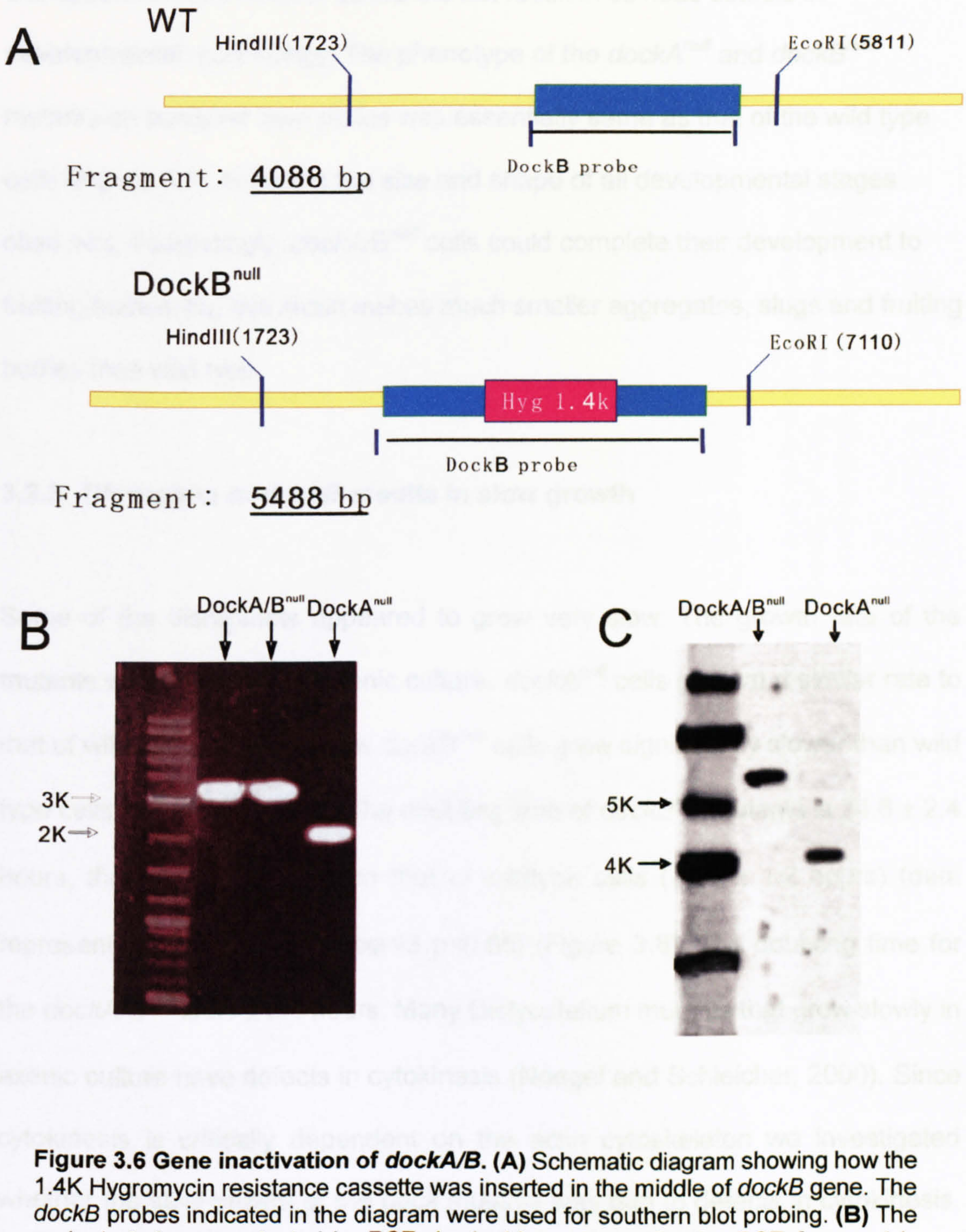

Figure 3.6 Gene inactivation of *dockA/B*. (A) Schematic diagram showing how the 1.4K Hygromycin resistance cassette was inserted in the middle of *dockB* gene. The *dockB* probes indicated in the diagram were used for southern blot probing. **(B)** The mutant strains were tested by PCR. In double mutant cells, the PCR fragment is 1.4K longer than that obtained from parent *dockA* null cells. **(C)** Genomic DNA of mutants was digested with EcoRI and HindIII. Southern blotting show *dockA/B*^{null} mutants generated a fragment whose size was shifted from 4kb to 5.4kb compared to *dockA*^{null} cells.

Disruption of *dockA* and or *dockB* did not result in obvious defects in developmental morphology. The phenotype of the *dockA*^{null} and *dockB*^{null} mutants on bacterial lawn plates was essentially same as that of the wild type cells (Figure 3.7), including the size and shape of all developmental stages observed. Interestingly, *dockA/B*^{null} cells could complete their development to fruiting bodies; but this strain makes much smaller aggregates, slugs and fruiting bodies than wild type.

3.2.3. Disruption of *dockB* results in slow growth

Some of the disruptants appeared to grow very slow. The growth rate of the mutants was measured in axenic culture. *dockA*^{null} cells grew at a similar rate to that of wild type cells, while the *dockB*^{null} cells grew significantly slower than wild type cells in axenic medium. The doubling time of *dockB*^{null} mutants is 24.6 ± 2.4 hours, three times longer than that of wildtype cells (7.37 ± 1.2 hours) (data represents mean ± SD, number=3 $p<0.05$) (Figure 3.8). The doubling time for the *dockA/B*^{null} is 31 ± 2.1 hours. Many Dictyostelium mutants that grow slowly in axenic culture have defects in cytokinesis (Noegel and Schleicher, 2000). Since cytokinesis is critically dependent on the actin cytoskeleton we investigated whether the slow growth of the *dock* mutants was due to defects in cytokinesis. Defects in cytokinesis of cells grown in suspension culture typically result in large cell sizes compared to wild type cells, since these cells become multinucleate. However nuclear staining showed that *dockB*^{null} and *dockA/B*^{null} cells did not contain more nuclei than wild type cells on average when grown in shaking suspension (Figure 3.9).

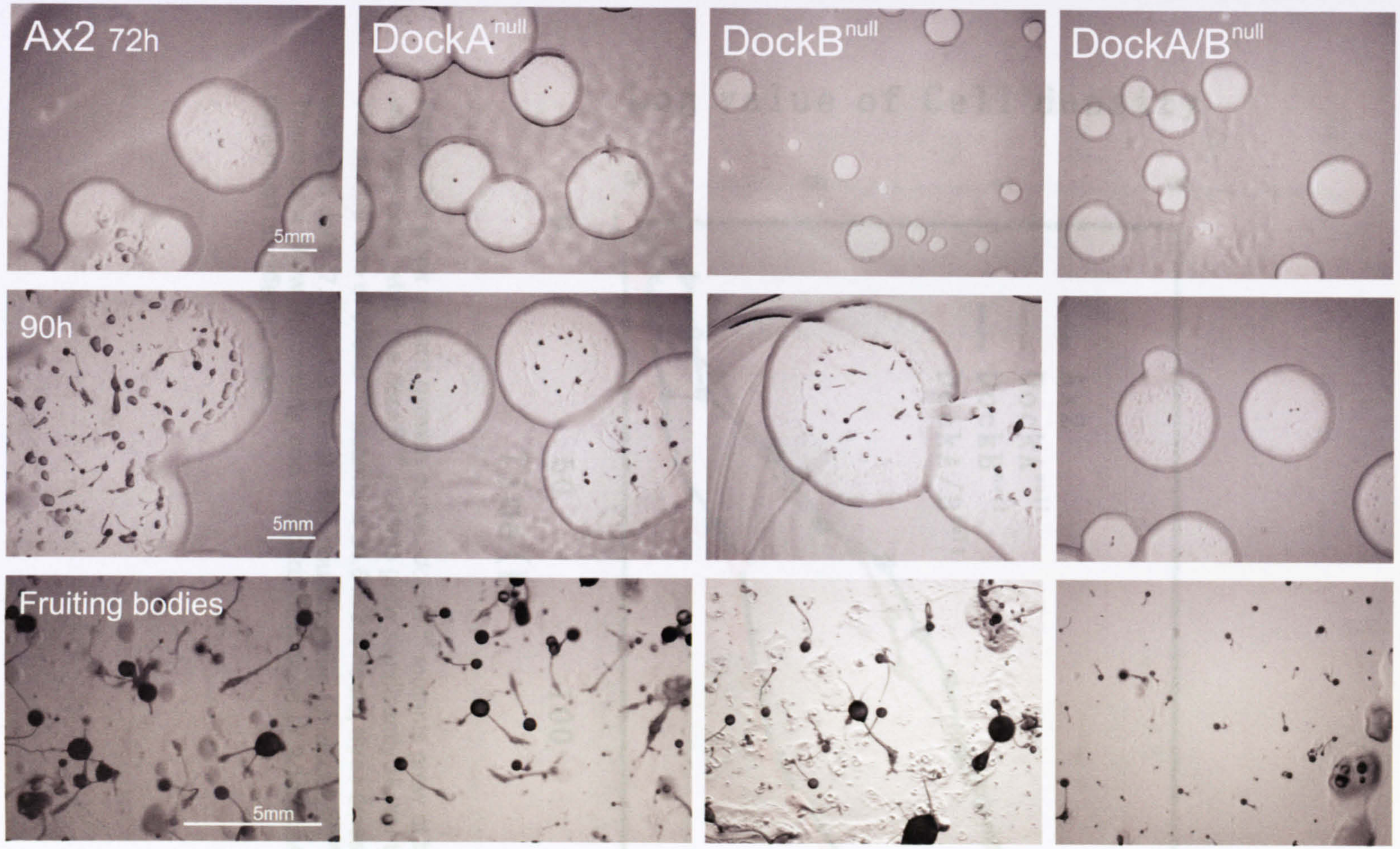

Figure 3.7 *dockA*^{null} and *dockB*^{null} phenotype. *dockA*^{null} and *dockB*^{null} mutants on bacterial lawn plates were essentially same as that of the wild type cells, including the size and shape of the every developmental stage. However *dockA/B*^{null} cells make smaller aggregates and fruiting bodies than wild type. All the experiments were repeated more than three times in independent days.

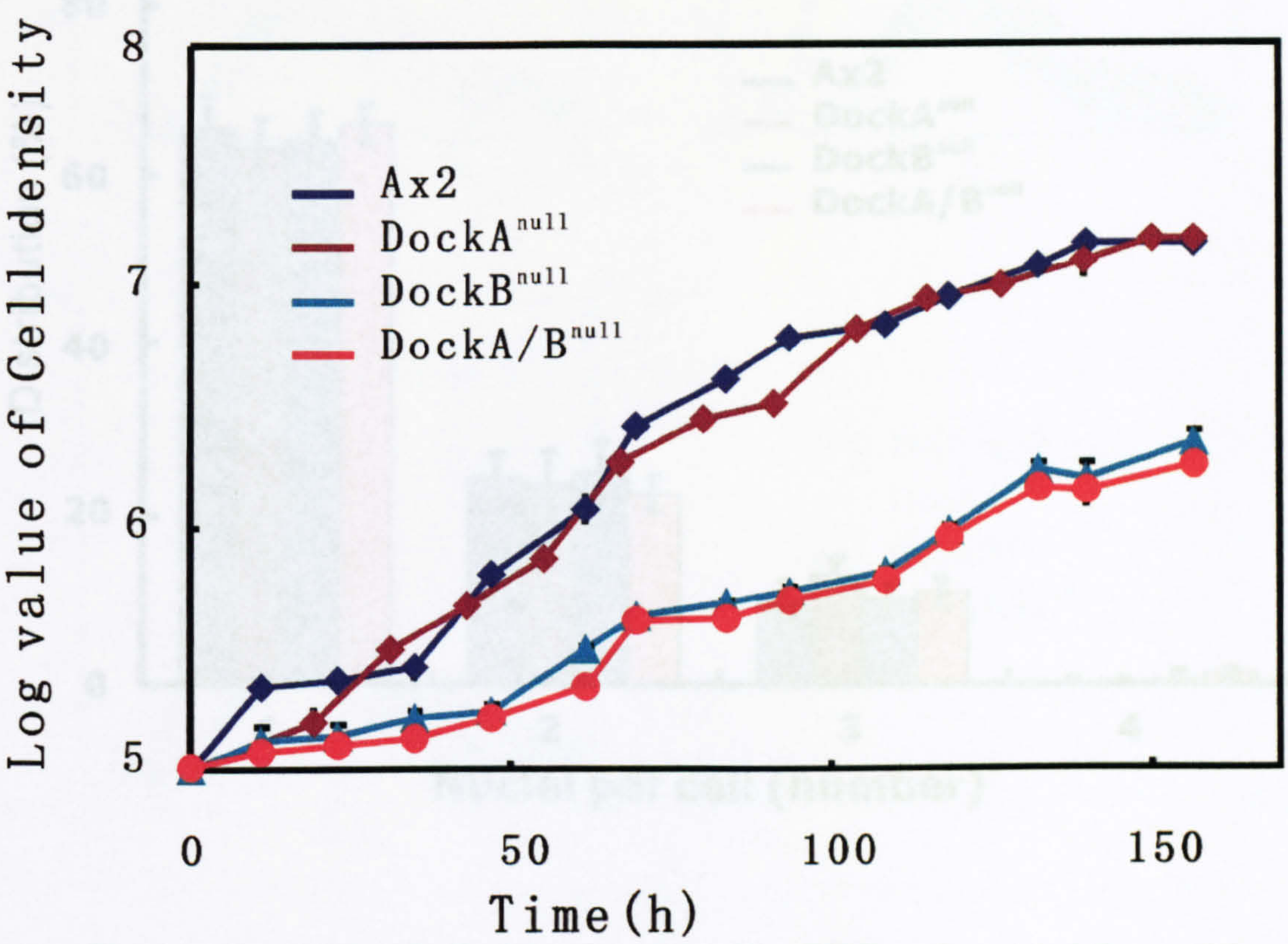

Figure 3.8 *dock* mutant growth curve. *dockA*^{null} mutants grew at the similar speed to wild type cells, while the *dockB*^{null} mutants grew significantly slower than wild type cells. The double time of *dockB*^{null} mutants is 24.6 ± 2.4 hours, three times longer than that of wild type cells (7.37 ± 1.2 hours). The doubling time for *dockA/B*^{null} is 31 ± 2.1 hours. These data show the means and standard deviations of 3 independent experiments, performed on different days.

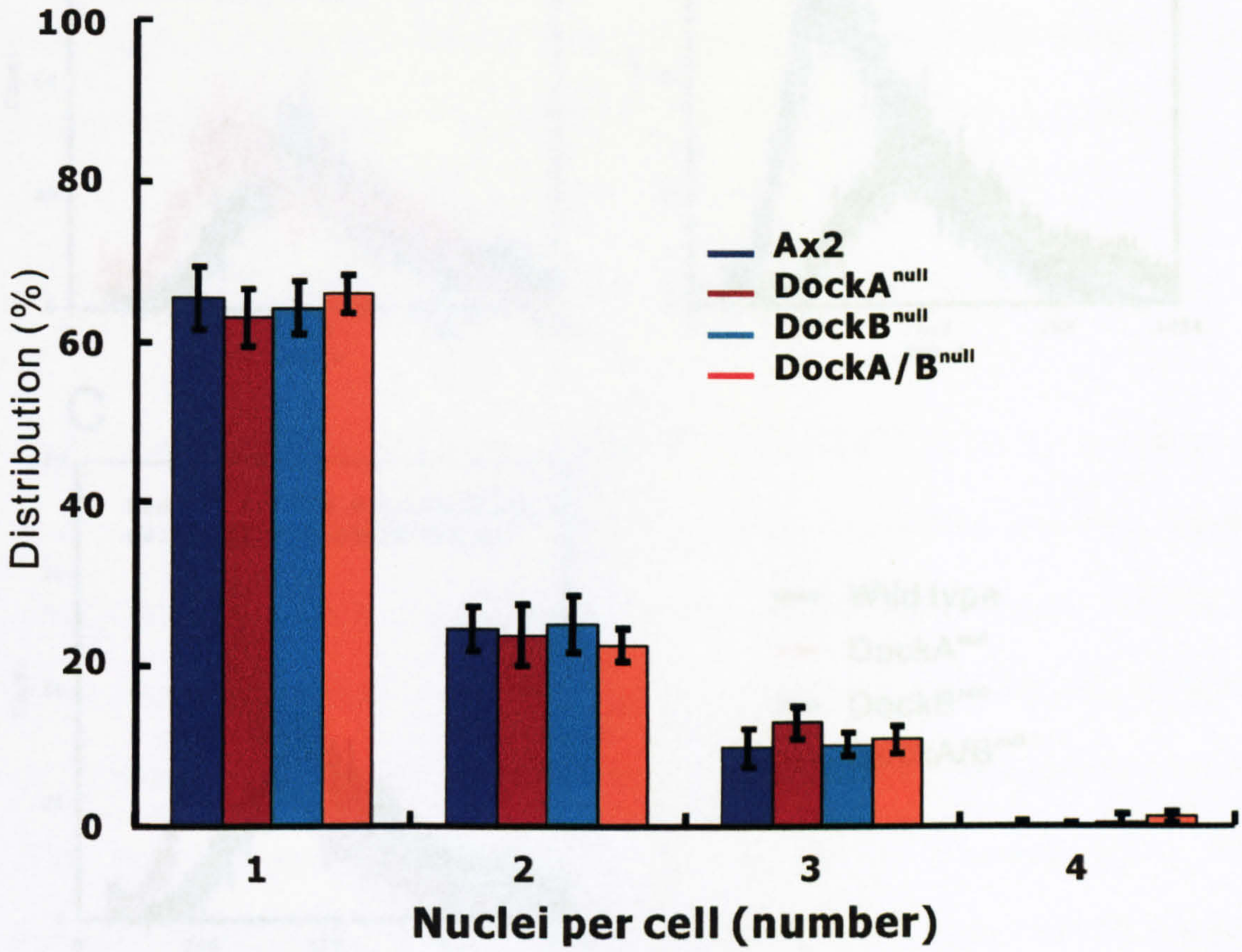

Figure 3.9 Nuclei/cell. Nuclei were stained by DAPI and counted the nuclei distribution under fluoresce microscopy. 69.4% ± 3.9% Ax2 cells in axenic medium contained one nucleus per cell. 66% ± 3.6% *dockA*^{null} cells, 65.7% ± 3.2% *dockB*^{null} cells and 64.7% ± 2.3% *dockA/B*^{null} cells contained one nucleus per cell. The distribution of more than one nucleus per cell showed no significant difference between Ax2 cells and *dockA*^{null}, *dockB*^{null} and *dockA/B*^{null} cells. These experiments were repeated three times on different days.

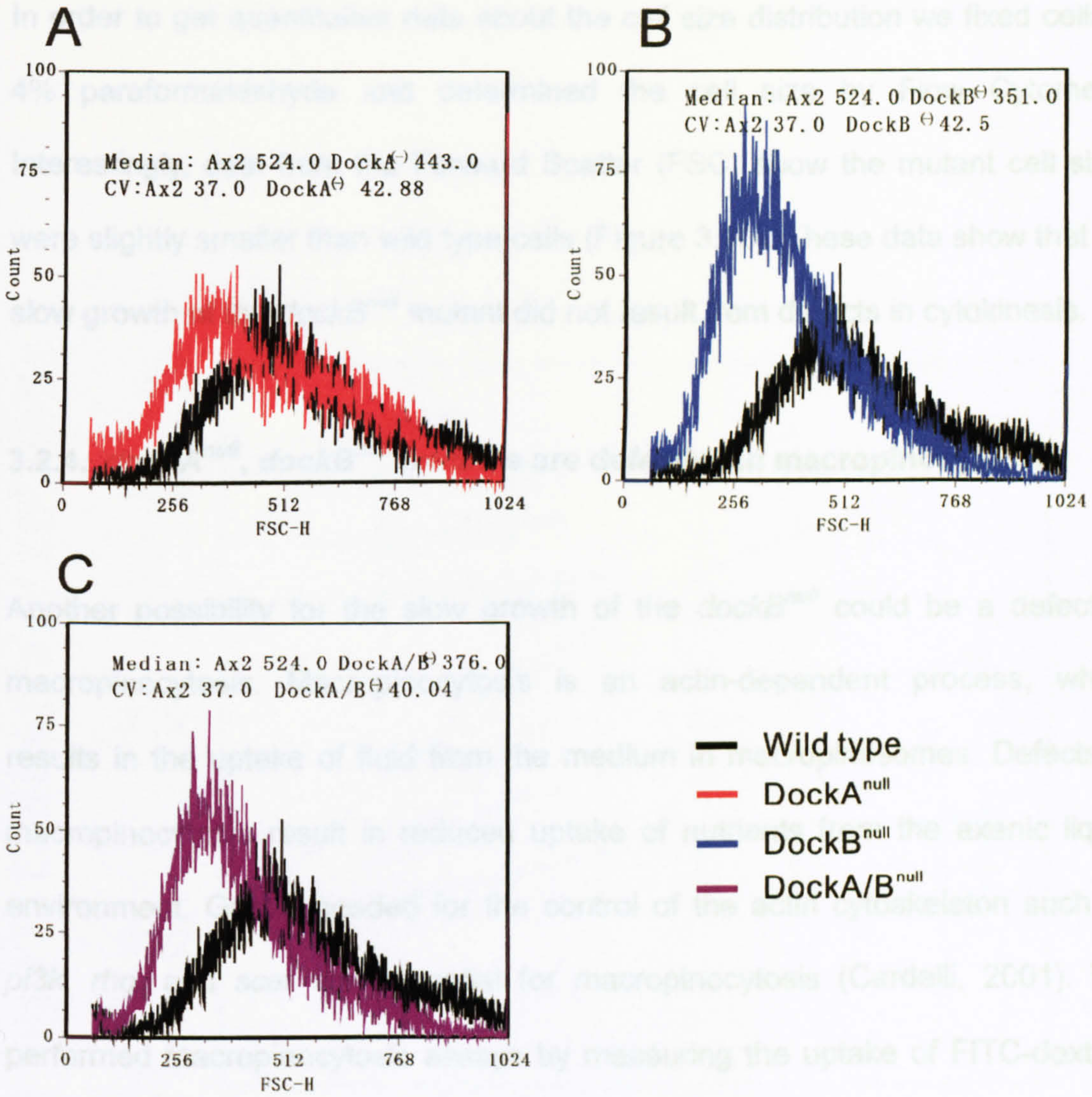

Figure 3.10 Flow cytometry data of *dockA*^{null}, *dockB*^{null} and *dockA/B*^{null}. Wildtype and mutant strains were fixed by 4% paraformaldehyde. The size distribution is shown as forward scatter. Median value of the FSC *dockA*^{null} (424 ± 6.2), *dockB*^{null} (340.3 ± 6.0) and *dockA/B*^{null} (366.3 ± 3.3) are slightly smaller than wild type cells(526 ± 1.7). These data show the means and standard deviations of 4 independent experiments, performed on different days.

In order to get quantitative data about the cell size distribution we fixed cells in 4% paraformaldehyde and determined the cell size by Flow Cytometry. Interestingly, data from the Forward Scatter (FSC) show the mutant cell sizes were slightly smaller than wild type cells (Figure 3.10). These data show that the slow growth of the *dockB*^{null} mutant did not result from defects in cytokinesis.

3.2.4. *dockA*^{null}, *dockB*^{null} mutants are defective in macropinocytosis

Another possibility for the slow growth of the *dockB*^{null} could be a defect in macropinocytosis. Macropinocytosis is an actin-dependent process, which results in the uptake of fluid from the medium in macropinosomes. Defects in macropinocytosis result in reduced uptake of nutrients from the axenic liquid environment. Genes needed for the control of the actin cytoskeleton such as *pi3k*, *rho*, and *scar* are essential for macropinocytosis (Cardelli, 2001). We performed macropinocytosis assays by measuring the uptake of FITC-dextran by *dockB*^{null} and wild type cells. Disruption of *dockA* and *dockB* genes resulted in reduced rates of macropinocytosis. d*ockB*^{null} cells showed especially strong defects in macropinocytosis (Figure 3.11). *dockA*^{null} cells also unexpectedly show considerable defects in the macropinocytosis process albeit the *dockA*^{null} grow at the similar speed as wild type cells.

The difference in fluid uptake of the *dockA*^{null} and wild type cells did not lead to a growth defect, suggesting that the growth defect observed in *dockB*^{null} cells may not be causally related to the reduced macropinocytosis. Knockout of *dockB* in the *dockA*^{null} background did not lead to a further decrease in macropinocytosis.

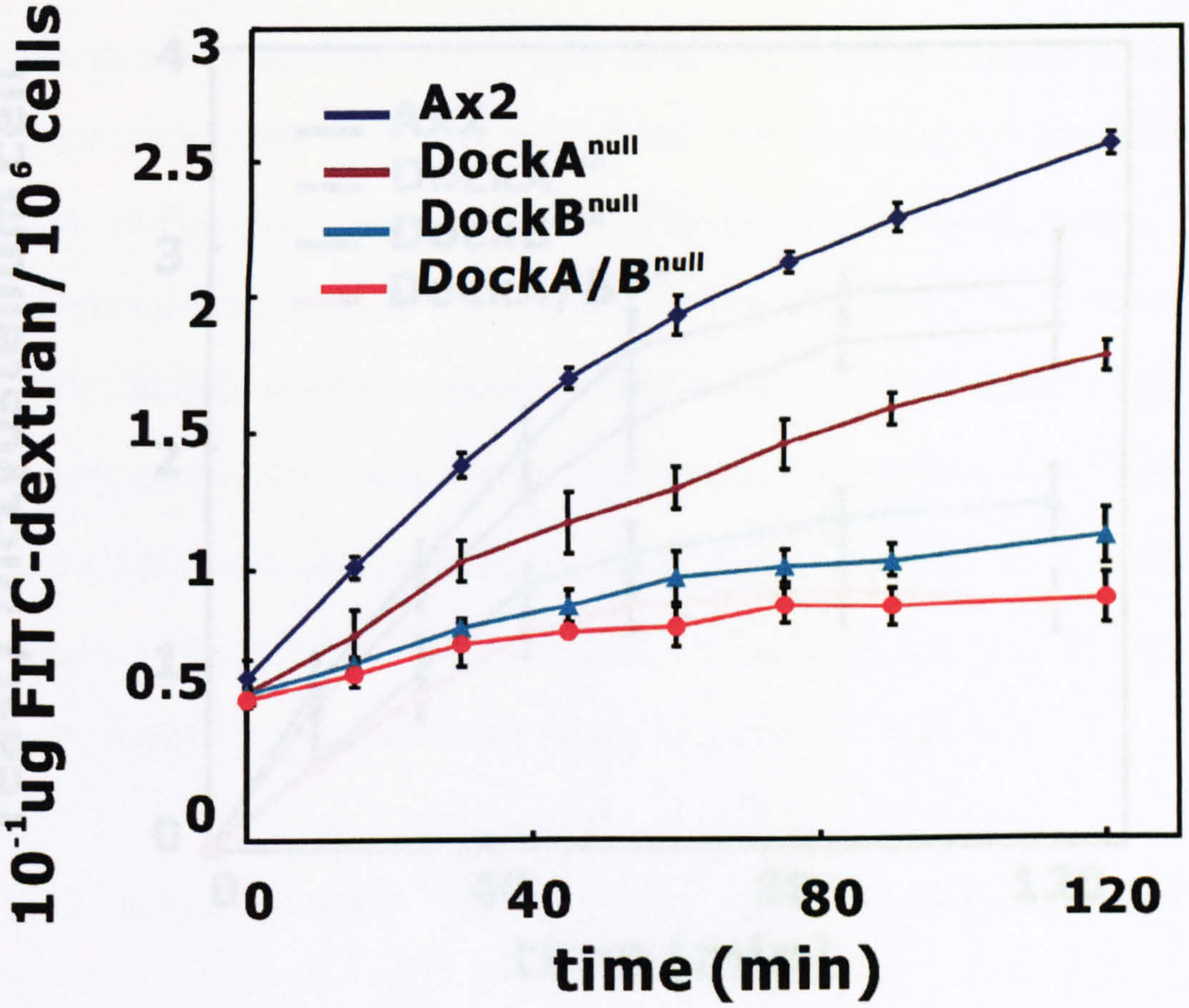

Figure 3.11 Macropinocytosis assay. Assays were performed by incubating the cells with FITC-dextran. Disruption of *dockA* and *dockB* resulted in reduced rates of macropinocytosis. *dockA/B*^{null} show similar reduced levels of macropinocytosis as those seen in *dockB*^{null}. These data show the means and standard deviations of 3 independent experiments, performed on different days.

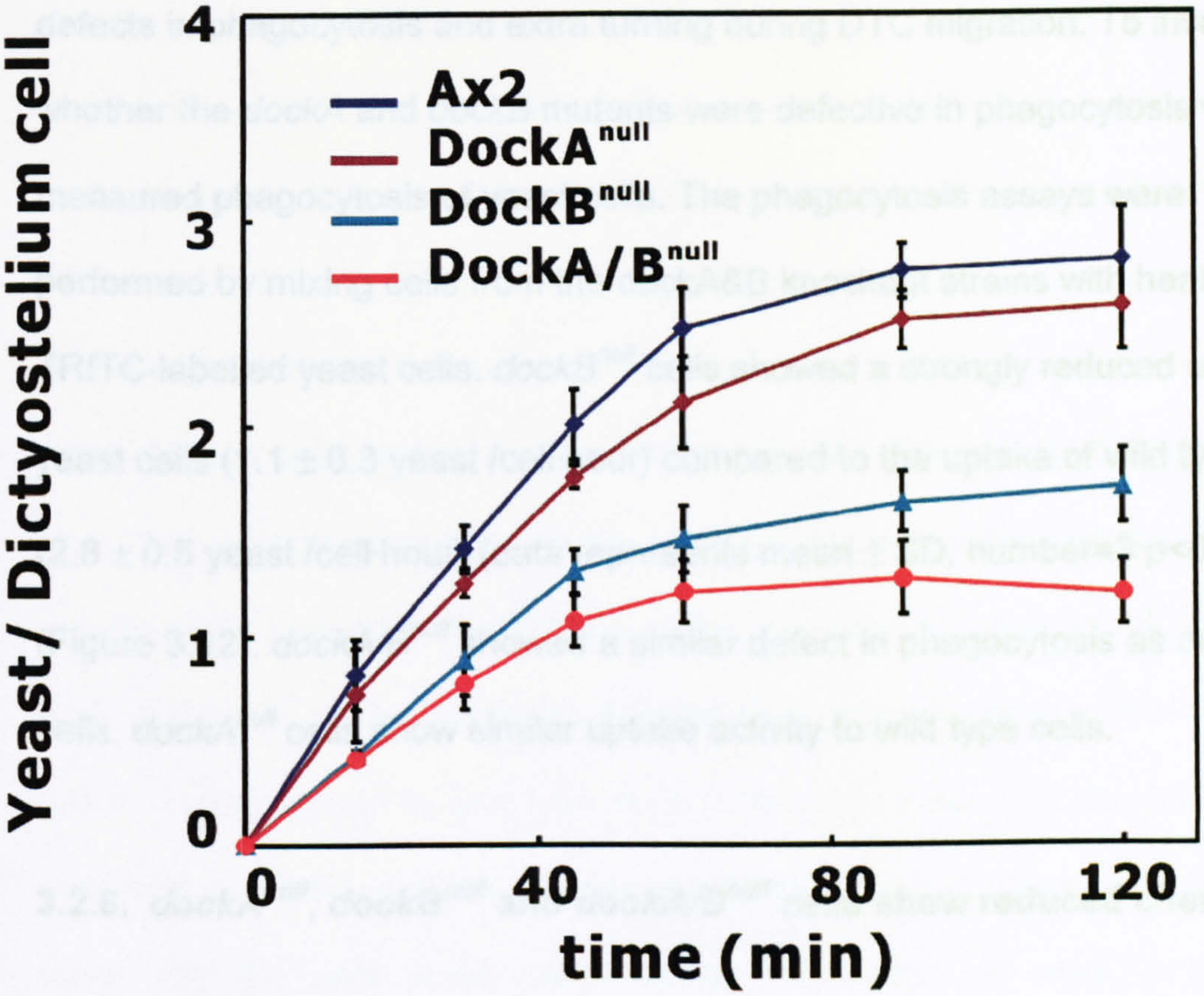

Figure 3.12 Phagocytosis of yeast. *dockB*^{null} cells showed a markedly reduced uptake of yeast cells (1.1 ± 0.3 yeast/cell·hour) compared to the uptake of wild type cells (2.8 ± 0.5 yeast cells/cell·hour) (data represents mean ± sd, number=3 $p<0.05$). *dockA/B*^{null} showed a similar defect in phagocytosis as *dockB*^{null} cells. We did not observe phagocytosis defects in *dockA*^{null} cells. These data show the means and standard deviations of 3 independent experiments, performed on different days.

3.2.5. Disruption of *dockB* results in a phagocytosis defect

The *C. elegans* Dock180 homologue, CED-5, is involved in the phagocytosis of cells corpses during apoptosis and the migration of distal tip cells (DTC) migration (Wu and Horvitz, 1998). Disruption of CED-5 in *C. elegans* results in defects in phagocytosis and extra turning during DTC migration. To investigate whether the *dockA* and *dockB* mutants were defective in phagocytosis we measured phagocytosis of yeast cells. The phagocytosis assays were performed by mixing cells from the dockA&B knockout strains with heat-killed TRITC-labelled yeast cells. $dockB^{null}$ cells showed a strongly reduced uptake of yeast cells (1.1 ± 0.3 yeast /cell·hour) compared to the uptake of wild type cells (2.8 ± 0.5 yeast /cell·hour) (data represents mean ± SD, number=3 $p<0.05$) (Figure 3.12). $dockA/B^{null}$ showed a similar defect in phagocytosis as $dockB^{null}$ cells. $dockA^{null}$ cells show similar uptake activity to wild type cells.

3.2.6. $dockA^{null}$, $dockB^{null}$ and $dockA/B^{null}$ cells show reduced chemotaxis

The Dock family of proteins have been implicated function as unconventional RacGEFs in a signalling pathway distinct from the PI3K-dependent signalling cascade (Braga, 2002; Brugnera et al., 2002; Duchek et al., 2001). $dockA/B^{null}$ cells make much smaller structures than wild type cells. One possible explanation for this phenotype is that this strain is defective in chemotaxis during the aggregation stages of development.

We tested the chemotaxis of the $dockA^{null}$ and $dockB^{null}$ mutant cells compared

to wildtype in the one drop and two drop chemotaxis assays. The cells that were used for the chemotaxis assays were pulsed with cAMP to make sure that they express all the pulsed induced genes needed for chemotaxis. In the one drop assay cells were spotted onto KK2 agar containing different concentrations of chemoattractants, such as cAMP or folate. A gradient forms across the perimeter of the spot if the cells are able to degrade the chemoattractant by extracellular membrane-associated phosphodiesterase in the case of cAMP and by folate deaminase in the case of folate (Bernstein et al., 1981). The forming gradients are detected by the cells which follow this gradient and migrate radially outward. We counted the droplets showing a positive chemotactic response as a function of time. We compared the chemotactic behaviour of starved *dock* mutant cells with wild type cells in their response to cAMP. The percentage of drops showing a positive migration response as a function of time is shown in Figure 3.13A. The results of the one drop chemotaxis assay indicated that the *dockA*^{null}, *dockB*^{null} and *dockA/B*^{null} cells showed a delayed response on plates containing 10^{-8}M cAMP in comparison to wild type cells. This could mean that the cells are less sensitive to cAMP or need steeper gradients to detect them but it could also mean that the cells move more slowly, which also will result in a delayed appearance of the outward movement response. There was no significant difference in the chemotactic response to 10^{-5}M folate between *dockA/B*^{null} cells and wildtype cells at vegetative stage (Figure 3.14). This seems to indicate that there is no intrinsic difference in the ability of the *dockA/B*^{null} cells to move. It also indicates that the chemotactic signalling pathways for cAMP and folate involve different signalling components.

In the one drop assay a failure to move chemotactically could also result from an

inability of the cells to secrete the cAMP phosphodiesterase. To rule this out we have performed further chemotaxis assays in which the formation of the gradient does not depend on the action of phosphodiesterase but is formed by diffusion. In this assay known as the two drop assay cells are challenged by a gradient of cAMP that forms by diffusion of cAMP from a localized source (a drop of cAMP placed next to the drop of cells) as described in detail in the methods section. In this assay secreted cAMP phosphodiesterase will also degrade the gradient but here a lack of cAMP phosphodiesterase secretion will result in a faster detection of the gradient. Droplets of cells were placed 4mm from the edge of drops of cAMP on 1% KK2 agar, to allow a gradient to develop, and the cells were observed for movement towards the source of the cAMP. The data in Figure 3.13B show that the *dockA*^{null}, *dockB*^{null} and *dockA/B*^{null} have a delayed response to 10^{-5}M cAMP in two drop chemotaxis assay. The effect was particularly pronounced in the *dockA/B*^{null} mutant, which showed a 40minutes delay (measured as the time it takes 50% of the population to respond).

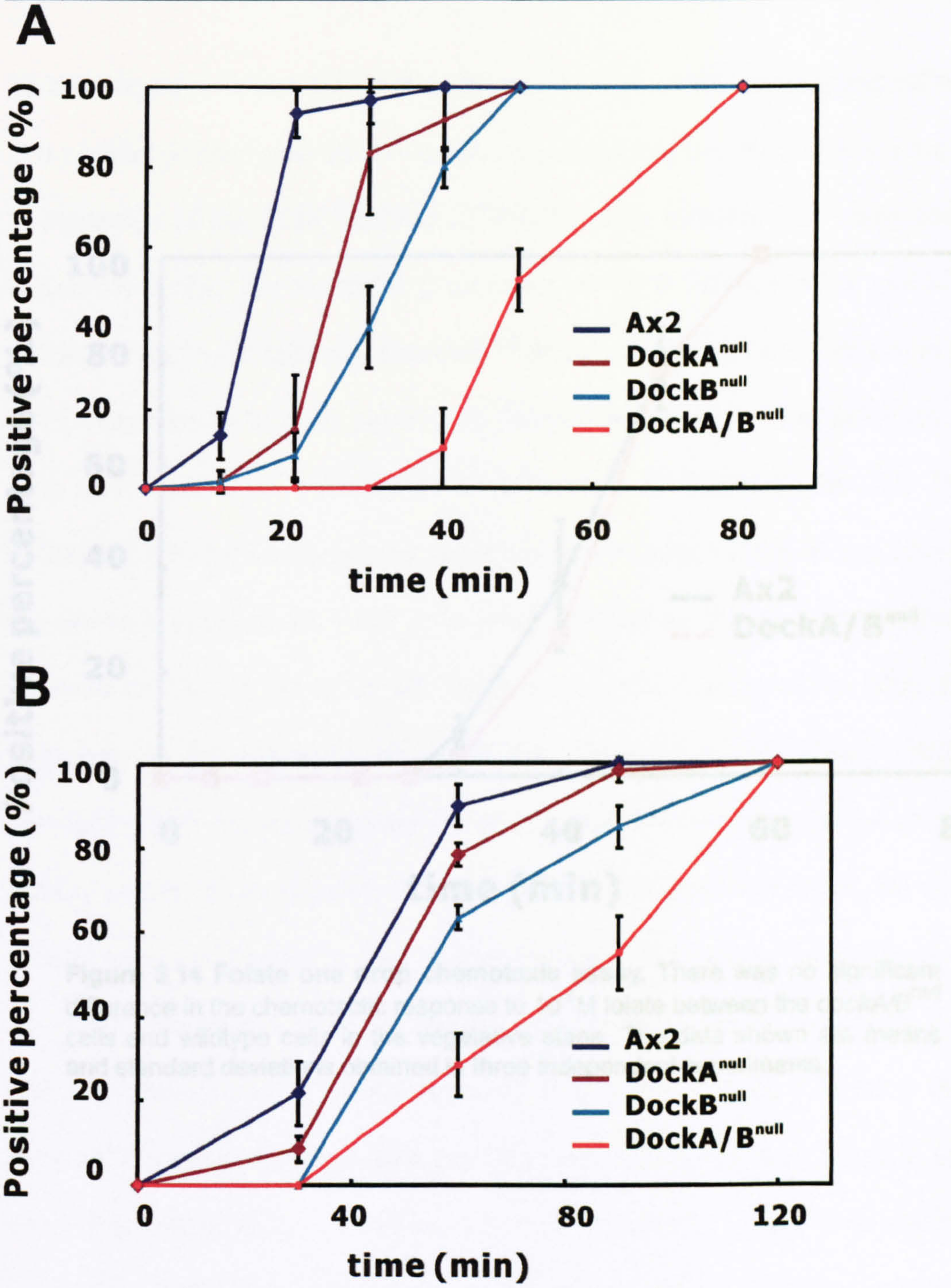

Figure 3.13 Chemotaxis assay. (A) The One Drop Chemotaxis assay indicated that the *dockA*^{null}, *dockB*^{null} and *dockA/B*^{null} cells showed a 10, 15 and 35minutes delay respectively on plates containing 10^{-8}M cAMP in comparison to that observed for Ax2 cells. **(B)** Two drop chemotaxis assay (10^{-5}M cAMP). *dockA*^{null}, *dockB*^{null} *and dockA/B*^{null} ells in two drop chemotaxis assay also show a delayed response compared to wild type cells. *dockA/B*^{null} mutant showed a 40minutes delay (measured as the time it takes 50% of the population to respond). These data shown are the means and standard deviations for results obtained in 3 independent experiments.

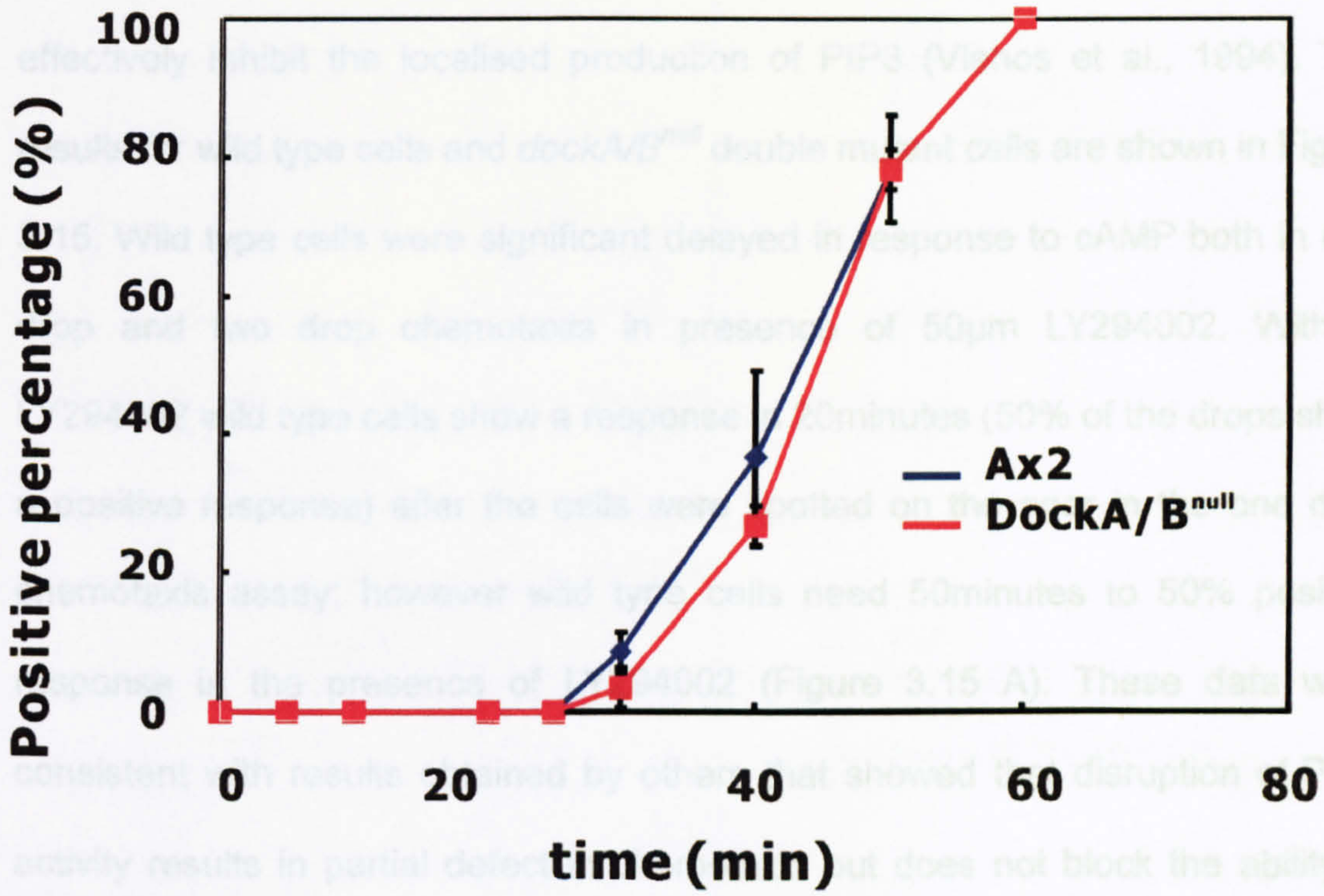

Figure 3.14 Folate one drop chemotaxis assay. There was no significant difference in the chemotactic response to 10^{-5}M folate between the *dockA/B*^{null} cells and wildtype cells in the vegetative stage. The data shown are means and standard deviations obtained in three independent experiments.

To investigate whether the Dock proteins acted in a PIP3 dependent pathway or in a parallel pathway we performed the one drop and two drop chemotaxis assay in presence of the PI3K inhibitor LY294002. This inhibitor has been shown to effectively inhibit the localised production of PIP3 (Vlahos et al., 1994). The results for wild type cells and *dockA/B*^{null} double mutant cells are shown in Figure 3.15. Wild type cells were significant delayed in response to cAMP both in one drop and two drop chemotaxis in presence of 50μm LY294002. Without LY294002 wild type cells show a response in 20minutes (50% of the drops show a positive response) after the cells were spotted on the agar in the one drop chemotaxis assay; however wild type cells need 50minutes to 50% positive response in the presence of LY294002 (Figure 3.15 A). These data were consistent with results obtained by others that showed that disruption of PI3K activity results in partial defect in chemotaxis but does not block the ability of cells to sense and orient in chemotactic gradients in *D. discoideum* (Buczynski et al., 1997; Funamoto et al., 2001). In combination with the inhibition of PI3K pathway chemotaxis is greatly reduced in *dockA/B*^{null} cells (Figure 3.15 A B). *dockA/B*^{null} cells only show 20% positive response during two hours in the one drop chemotaxis assay in the presence of LY294002. In two drop chemotaxis asay, *dockA/B*^{null} cells did not show any response to chemoattactant gradient during the two hours of observation in the presence of LY294002 (Figure 3.15B). It took up to 6 hours before the *dockA/B*^{null} cells showed a 40% positive response to cAMP in the two drop chemotaxis assay (data not shown).

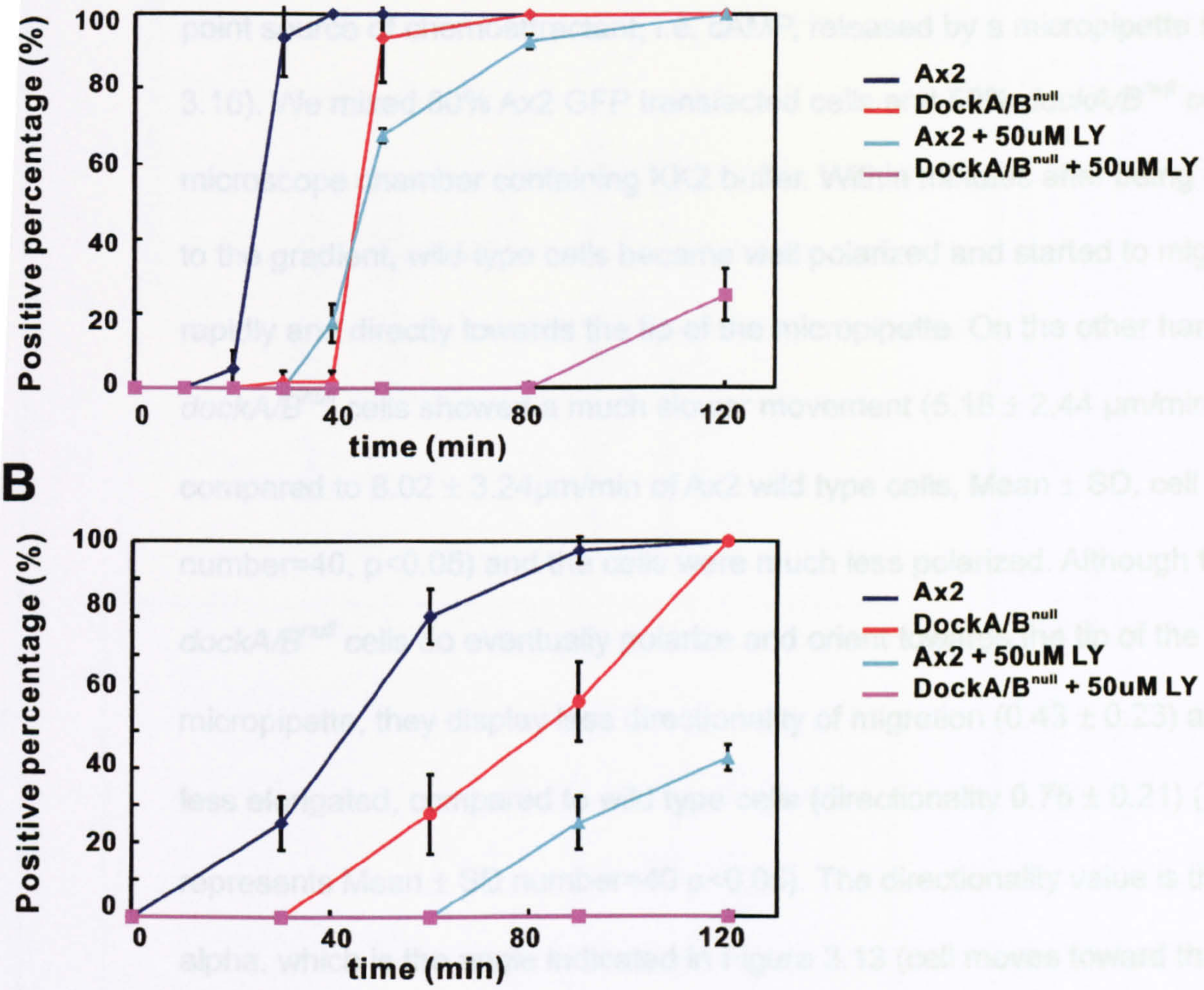

Figure 3.15 Chemotaxis assay in the presence of 50uM LY294002. (A) One drop chemotaxis assay (10^{-8}M cAMP +50μM LY294002). In the presence of LY294002, wild type cells take 90mins before showing a 100% positive response. However *dockA/B*^{null} cells only show a 20% positive response after 2 hours. **(B)** Two drop chemotaxis assay (10^{-5}M cAMP + 50μM LY294002). In the presence of LY294002, *dockA/B*^{null} cells did show any response to cAMP during 2 hours of observation. Wild type cells show a 40% positive response in this time. These data shown are the means and standard deviations obtained in three independent experiments.

To characterize the chemotactic behaviour at the individual cellular level, we visualized how cells moved in a relatively steep cAMP gradient produced by a point source of chemoattractant, i.e. cAMP, released by a micropipette (Figure 3.16). We mixed 50% Ax2 GFP transfected cells and 50% *dockA/B*^{null} cells in a microscope chamber containing KK2 buffer. Within minutes after being exposed to the gradient, wild-type cells became well polarized and started to migrate rapidly and directly towards the tip of the micropipette. On the other hand, *dockA/B*^{null} cells showed a much slower movement (5.18 ± 2.44 μm/min compared to 8.02 ± 3.24μm/min of Ax2 wild type cells, Mean ± SD, cell number=40, $p<0.05$) and the cells were much less polarized. Although the *dockA/B*^{null} cells do eventually polarize and orient towards the tip of the micropipette, they display less directionality of migration (0.43 ± 0.23) and are less elongated, compared to wild type cells (directionality 0.75 ± 0.21) (data represents Mean ± SD number=40 $p<0.05$). The directionality value is the cosine alpha, which is the angle indicated in Figure 3.13 (cell moves toward the top).

To determine whether the inability of the *dockA/B*^{null} cells to chemotaxis properly resulted from an inability to reach full aggregation competence through a failure to activate cAMP-induced aggregation stage gene expression, we examined the expression of two aggregation-stage genes, the cAMP receptor 1 (*cAR1*) and adenylyl cyclase (*aca*), which produces cAMP needed for the relay of the chemoattractant signal. Both genes were expressed to similar levels in *dockA*^{null}, *dockB*^{null}, *dockA/B*^{null} cells and wild type cells (data not shown).

Directionality parameter: Cosα

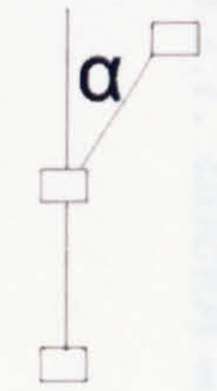

Wild type

DockA/B^{null}

	Wild type	DockA/B^{null}
Speed (μm/min)	8.02±3.24	5.18±2.44
Directionality	0.75±0.21	0.43±0.23

Figure 3.16 Needle chemotaxis Assay. Cells in the aggregation stage were allowed to settle on a glass cover-slip and stimulated with a micropipette filled with 0.1mM cAMP. Images of chemotaxing cells were captured every 5 seconds. Cell movement was analyzed with the Optimas software. Wild-type cells are well polarized, migrate fast and orientate properly toward the tip of the micropipette. *dockA/B^{null}* cells migrated less directionality (0.43+/- 0.23) and less elongate, compared to wild type cells (directionality 0.75 +/- 0.21) (data represents Mean +/- SD, number=40 $p<0.05$). Directionality is measured as cosine alpha (cell migrate toward top).

3.2.7. *dockA* and *dockB* mutant show altered actin polymerization kinetics

During chemotaxis, extracellular chemoattractants bind to receptors, which trigger the downstream signalling pathways finally resulting in actin polymerization in the leading edge of the cell to extend a pseudopod (Parent, 2004). It is well established that the Rho-family GTPases are essential regulators of cell polarity and motility by relaying signals to Arp2/3 complex, which is composed of seven proteins that function to nucleate actin polymerization from existing filaments at the leading edge (Etienne-Manneville and Hall, 2002). In *D. discoideum*, identification of the RacGEF's involved in chemotaxis should help to understand the components that link PI(3,4)P2 & PI(3,4,5)P3 and actin polymerization during chemotaxis. We performed cAMP stimulation dependent actin polymerization assay to test whether the *dockA*^{null}, *dockB*^{null}, and *dockA/B*^{null} cells are defective in cAMP induced actin polymerization.

In suspensions of *D. discoideum* cells, a temporal increase in the concentration of chemoattractants induces two phases of actin polymerization: a very brief fast large spike peak after 6 seconds, and a more prolonged smaller second peak which peaks after 60 seconds. Disruption of PTEN preferentially increases the amplitude of the second slower response (Chen et al., 2003). cAMP stimulation in the presence of inhibitors of PI3K do not significantly affect the rapid phase of chemoattractant-induced actin polymerization (own observations Figure 3.17A) and (Chen et al., 2003). These data indicate that actin polymerization is controlled by both PI3K dependent- and independent-signalling pathways upon

cAMP stimulation in *D. discoideum.* We performed cAMP induced actin polymerization assays on *dock* mutants. In *dockA*^{null}, *dockB*^{null} and the *dockA/B*^{null} mutants both the fast and slow actin polymerization responses are diminished in amplitude (Figure 3.17B). These data suggest dockA and dockB are involved in the PIP3 dependent and independent cAMP induced chemotactic signalling pathways.

In this assay actin polymerization dynamic was shown as the increased fold of the F-actin concentration in cells after cAMP stimulation. The total cellular basal polymerized actin will significant affect the final output. It's possible that the *dockA*^{null}, *dockB*^{null}, *and dockA/B*^{null} cells contain different steady state level of F-actin compared to wild type cells in their basal state. We stained the vegetative cells with fluorescent phalloidin, which specifically binds to F-actin, and examined basal cellular F-actin by flow cytometry (Figure 3.18). In unstimulated conditions we did not find a significant difference in F-actin content between *dockA*^{null}, *dockB*^{null}, *dockA/B*^{null} and wild type cells.

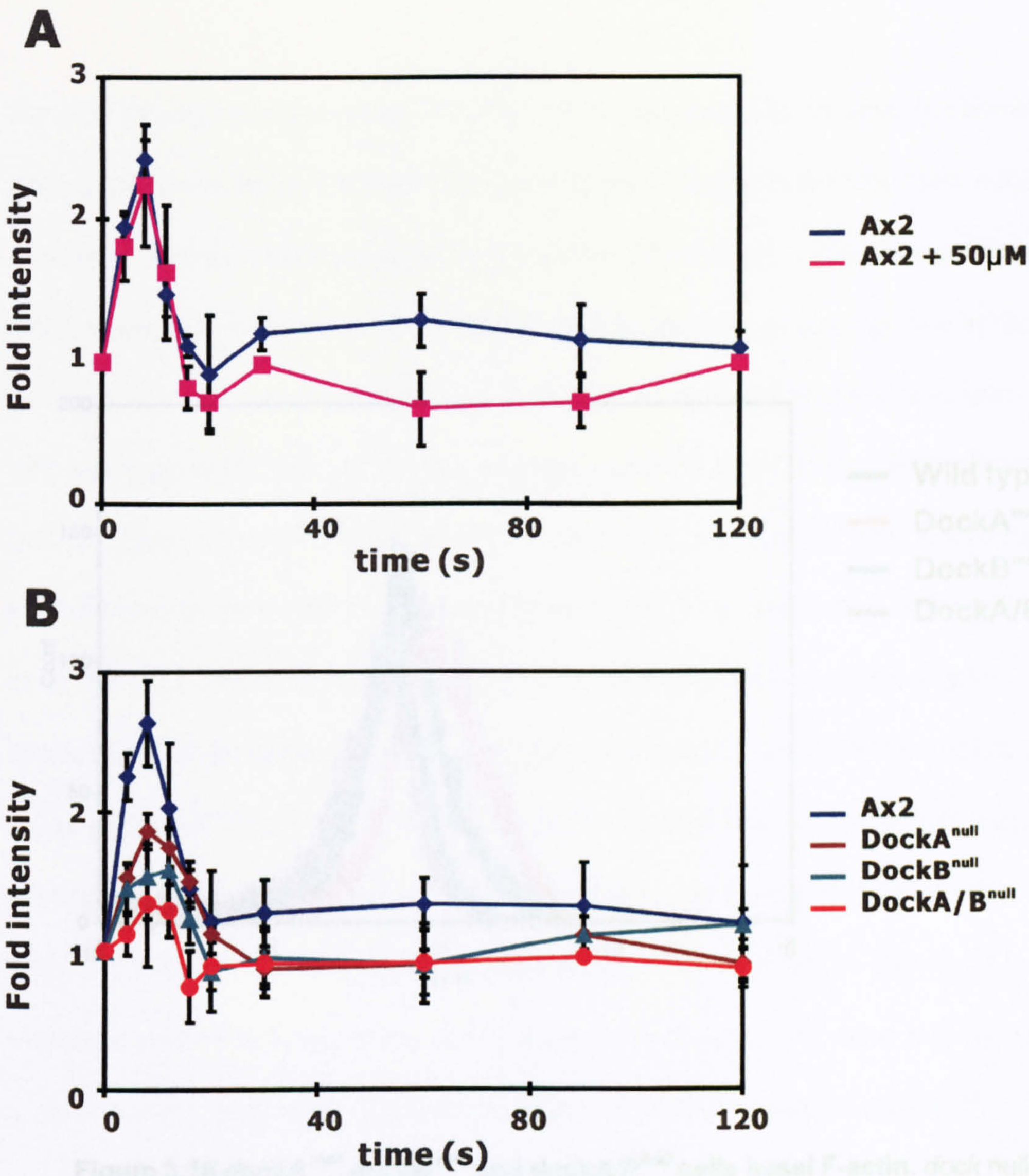

Figure 3.17 Actin polymerization assay. (A) In suspensions of *D. discoideum* cells, cAMP stimulation induces two phases of actin polymerization: a very brief fast large spike peak after 6 seconds, and a more prolonged smaller second peak which peaks after 60 seconds.PI3K inhibitor, LY294002, abolished the second peak of the actin polymerization. LY294002 did not significantly affect the rapid phase of chemoattractant-induced actin polymerization. (B) In *dockA*^{null}, *dockB*^{null} and the *dockA/B*^{null} mutants both the fast and slow actin polymerization responses are diminished. The data shown are means and standard deviation of results obtained in 9 independent experiments.

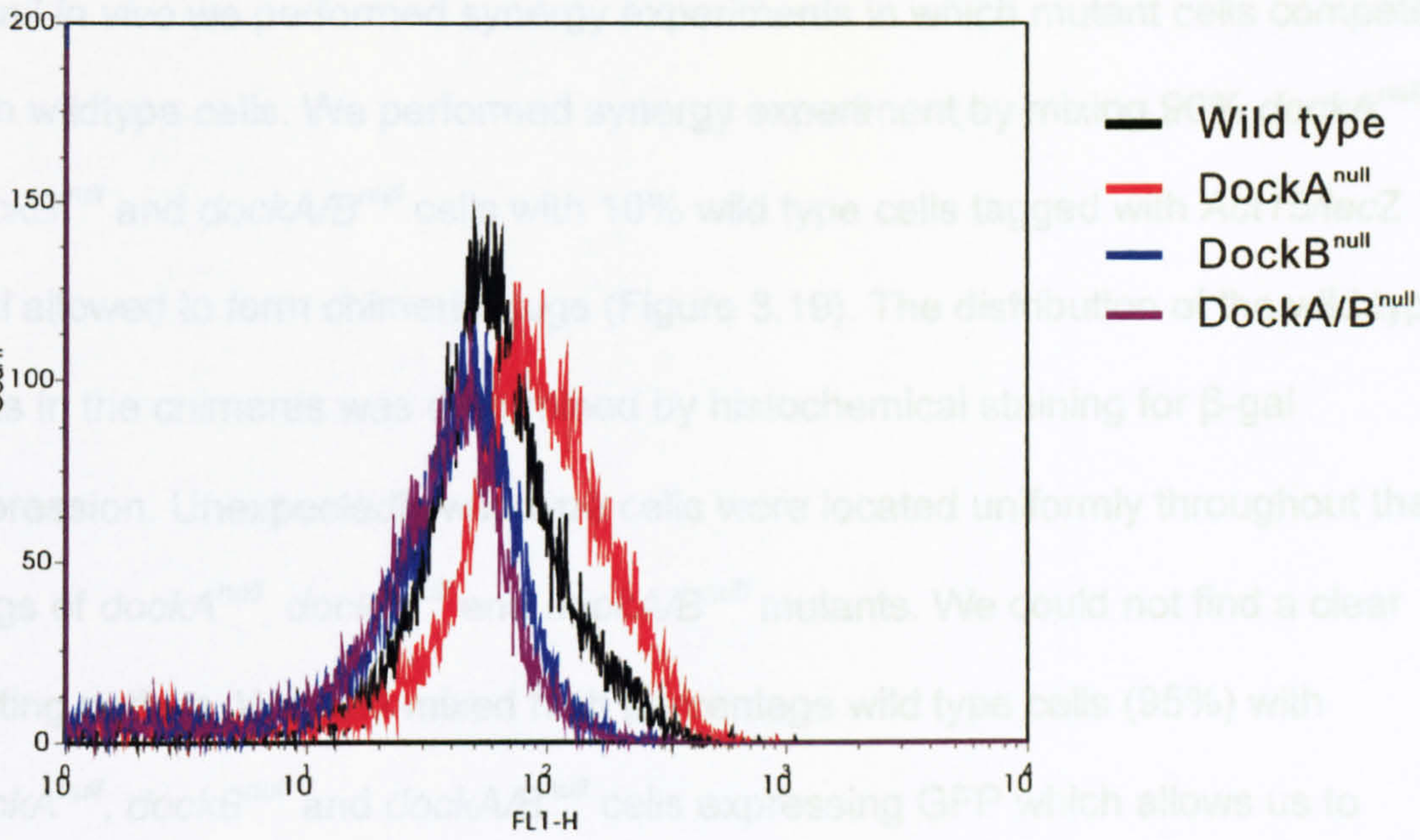

Figure 3.18 *dockA*^{null},*dockB*^{null} and dock*A/B*^{null} cells basal F-actin. *dock* null cells were stained with phalloidin to examine their basal cellular F-actin by flow cytometry. In unstimulated cells, we did not find a large difference in F-actin content between *dock* null and wild type cells. Median value of the FL1-H *dockA*^{null} (60.12 ± 2.1), *dockB*^{null} (56.12 ± 1.8) and *dockA/B*^{null} (55.13 ± 1.1) are slightly smaller than wild type cells (57.01 ± 1.1) (data present mean ± sd).

3.2.8. Synergy experiments show no sorting of *dockA*^{null}/*dockB*^{null} cells

Several experiment described thus far have implicated *dockA* and *dockB* in the control of chemotaxis. Experiments have shown *Dictyostelium* mutants defect in chemotaxis often show impaired aggregation (Meili et al., 1999; Noegel and Schleicher, 2000; Palmieri et al., 2000). To test the role of *dock* genes in more detail *in vivo* we performed synergy experiments in which mutant cells compete with wildtype cells. We performed synergy experiment by mixing 90% *dockA*^{null}, *dockB*^{null} and *dockA/B*^{null} cells with 10% wild type cells tagged with *Act15/lacZ* and allowed to form chimeric slugs (Figure 3.19). The distribution of the wild type cells in the chimeras was determined by histochemical staining for β-gal expression. Unexpectedly wild type cells were located uniformly throughout the slugs of *dockA*^{null}, *dockB*^{null} and *dockA/B*^{null} mutants. We could not find a clear sorting pattern. We next mixed high percentage wild type cells (95%) with *dockA*^{null}, *dockB*^{null} and *dockA/B*^{null} cells expressing GFP which allows us to visualize sorting in living slugs and fruiting bodies. Again we were unable to find a clear sorting pattern during all the stages of development for *dockA*^{null}, *dockB*^{null} *and dockA/B*^{null} cell mixtures (Figure 3.20).

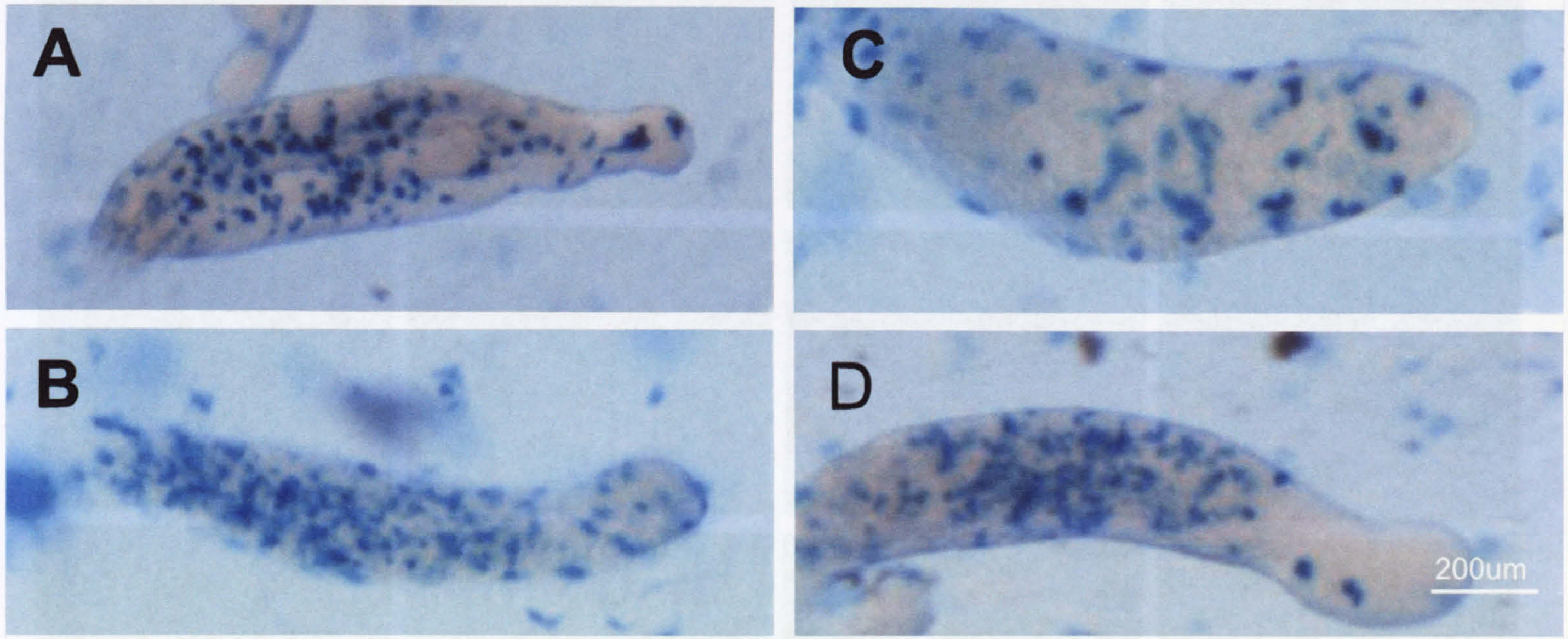

Figure 3.19 Synergy experiment (A) – (D) Mix the 10% Ax2 Lacz + Ax2, *dockA*^{null}, *dockB*^{null} and *dockA/B*^{null} respectively. Ax2 cells (blue) are located uniformly throughout the slugs with no clear sorting pattern. These data were repeated three times by independent sample in different days.

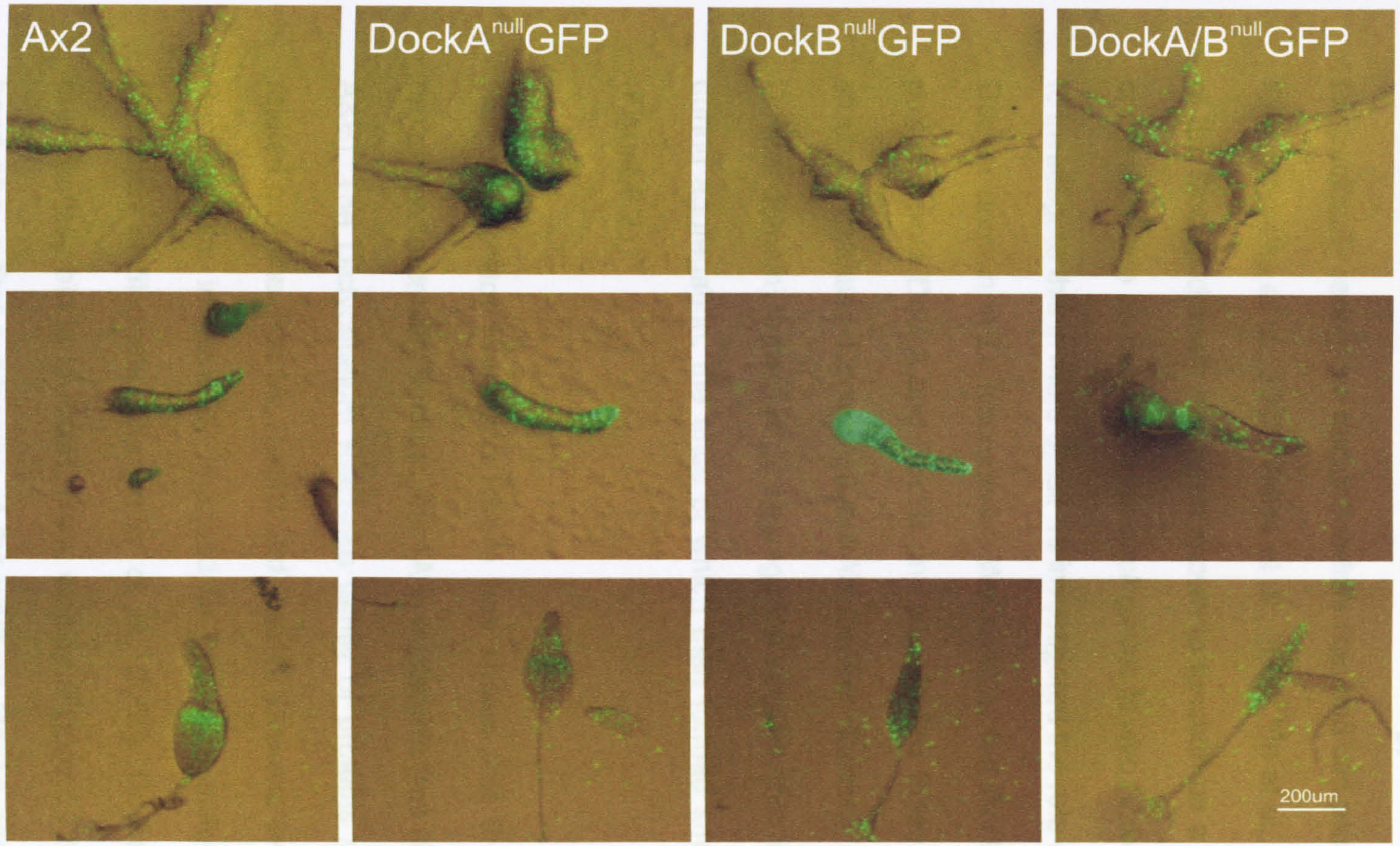

Figure 3.20 GFP synergy experiment. Mix 95% wild type cells with *dockA*^{null}, dock*B*^{null} and *dockA/B*^{null} GFP cells. No clear sorting results in different stages of development in *dockA*^{null}, *dockB*^{null} and *dockA/B*^{null} cells mixed with wildtype. These data were obtained three times on different days.

3.2.9. Phenotype caused by expression of the Docker domain

The Docker domain of Dock180 has no homology to Dbl sequences but is able to specifically recognize nucleotide-free Rac and can promote loading of GTP by Rac (Grimsley et al., 2003; Valles et al., 2004; Yin et al., 2004). Overexpression of the Docker domain has been shown to function as a dominant negative and could therefore be used to block *dock* genes *in vivo* (Valles et al., 2004). In order to investigate this in more detail we investigated the role of overexpression of the Docker domain in *D. discoideum.* We constructed Docker domain GFP fusion proteins from DockA and DockB and transfected these in *D. discoideum*. The strains expressed DockerA (DockA's Docker domain) and DockerB (DockB's Docker domain) formed large aggregation streams that broke up in smaller parts during aggregation, the ends of which then formed small aggregation centres (Figure 3.21).

Our collaborator Francisco Rivero has shown that the DockerB-GFP fusion protein preferentially binds to Rac1A in nucleotide free state *in vitro* (Figure 3.22 A&B). The Dictyostelium Rac1-like family of proteins consists of three highly related proteins, Rac1A, Rac1B and Rac1C. Overexpression of dominant active Rac1 results in severely impaired in growth, motility, endocytosis and the formation of filopodia (Dumontier et al., 2000). DockerA-GFP fusion protein preferentially binds to RacH, RacL weakly (Figure 3.22 A). Furthermore it has been shown that expression of the wildtype Rac1A and its activated form can rescue *dockB*^{null}'s phagocytosis defect (Gerti Weijer unpublished data).

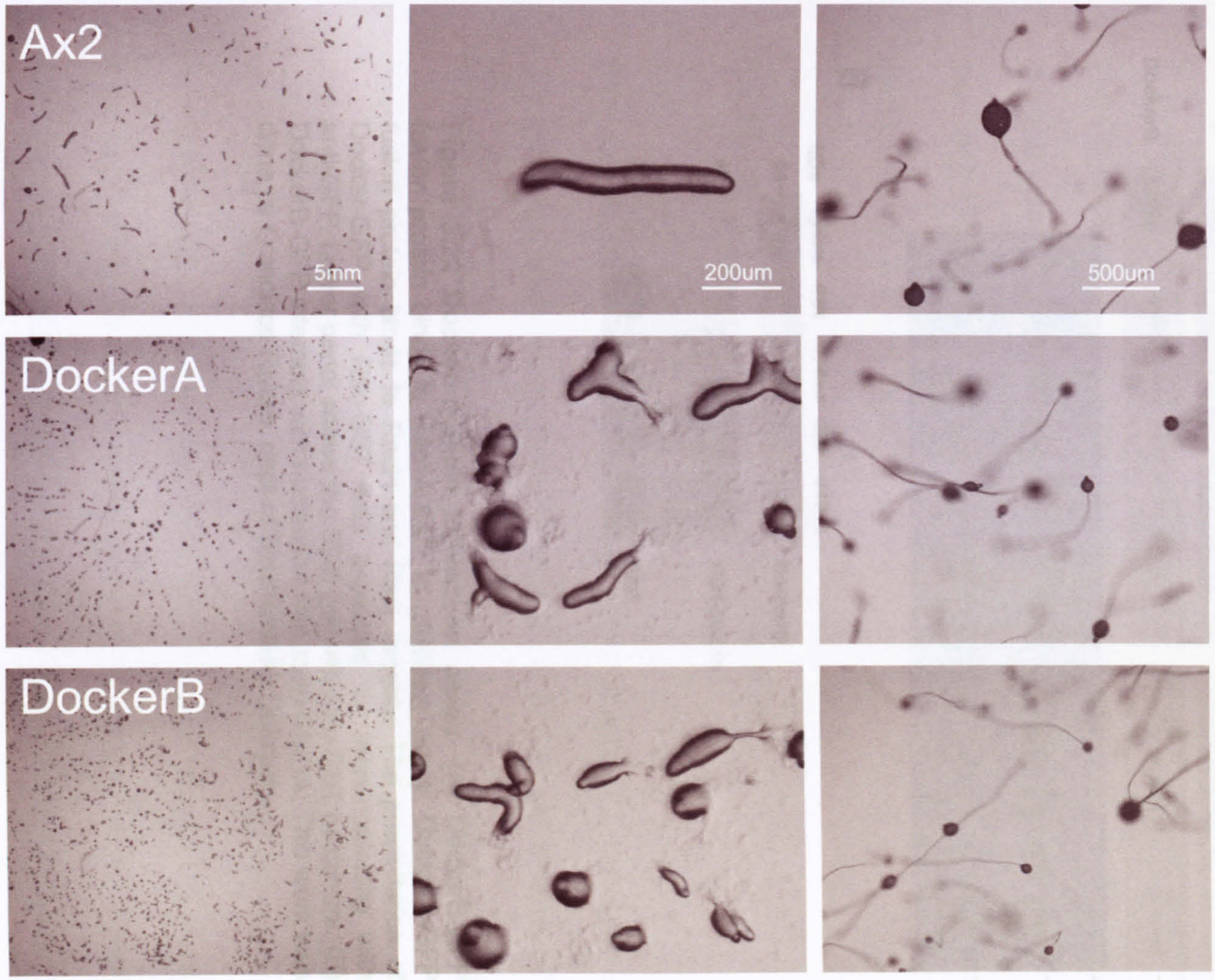

Figure 3.21 Docker expression phenotype. Aggregation streams of DockerA and DockerB strains broke up streams and formed small aggregation centres. These data were typical for results obtained in three independent experiments.

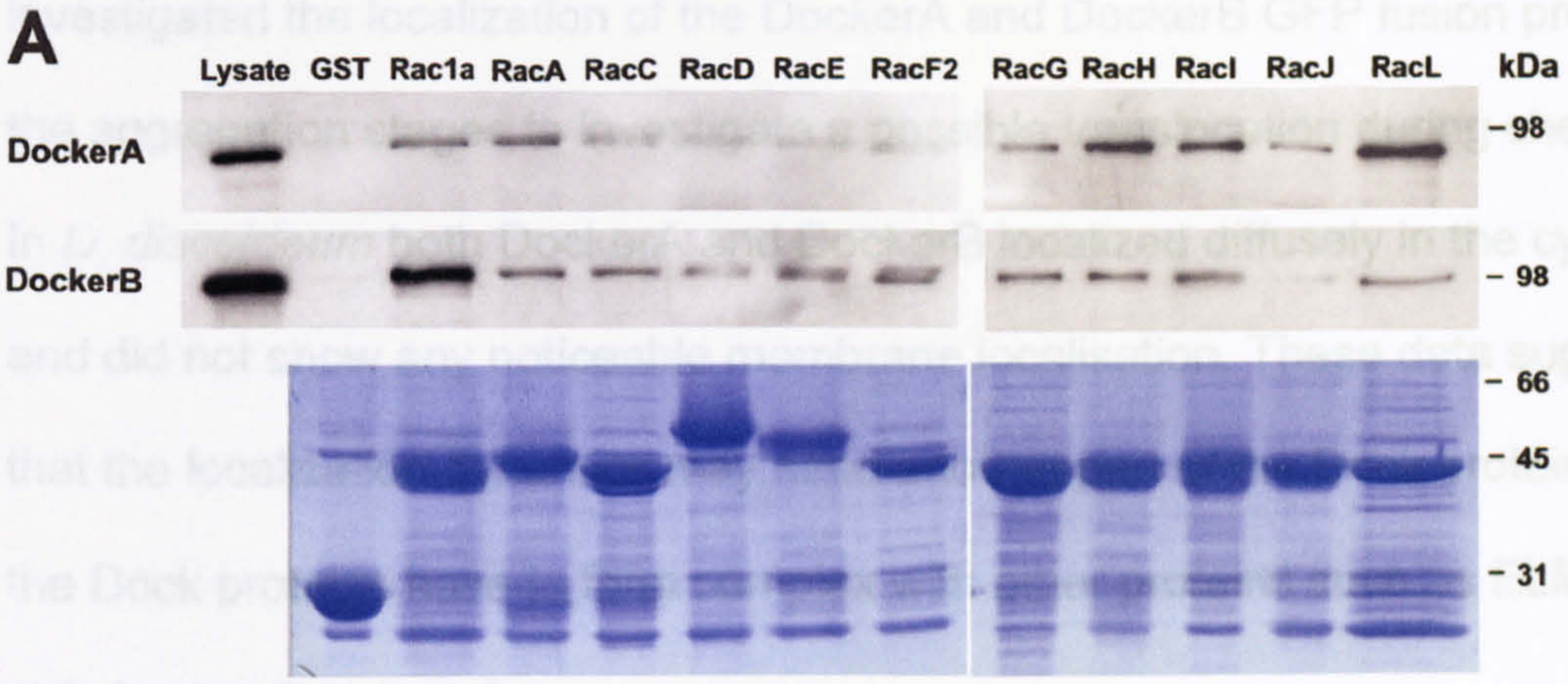

Figure 3.22 Docker domain interaction assay. (A) DockerB-GFP fusion protein binds to Rac1A-GST in pulldown assay; DockerA-GFP fusion protein binds to RacH and RacL weakly. The precipitation of Docker-GFP with Rac-GST was assessed by immunoblotting with anti-GFP. Lower panel shows the SDS gel with Rac-GST as control. (B) DockerB-GFP interacts with nucleotide free state Rac1A. This work was done by Francisco Rivero, dept of Biochemistry Cologne.

It has recently been shown that endogenous Dock180 protein can translocate to the membrane in response to PI3K activation in CHO cells(Cote et al., 2005). This membrane recruitment was blocked by pre-treatment of the cells with LY294002 and found to be dependent on the DHR-1 domain, which forms part of the Docker domain that we have described here (Cote et al., 2005). We investigated the localization of the DockerA and DockerB GFP fusion proteins in the aggregation stages to investigate a possible translocation during chemotaxis. In *D. discoideum* both DockerA and DockerB localized diffusely in the cytoplasm and did not show any noticeable membrane localisation. These data suggest that the localization dynamics may need another part of the Dock protein or that the Dock proteins have to form complex with other proteins such as ELMO to be able to recruit to membrane.

3.2.10. *dockA^{null}* slugs show poor phototaxis

Dictyostelium discoideum slugs are sensitive to light, pH, and even slight differences in temperature, which allows them to migrate towards the surface of the soil which provides an optimal location for fruiting (Fisher et al., 1981). When slugs from wild type cells are kept in the presence of lateral light, they form slugs that move almost directly towards the light source. Actin cytoskeleton proteins and related regulators were found essential for the proper phototaxis (Noegel and Schleicher, 2000) Therefore we decided to investigate the phototaxis behaviour of the *dockA* and *dockB* null strains. *dockA^{null}* slugs move toward the light source however they move much less directly compare to wild type slugs (Figure 3.23). *dockB^{null}* slugs could in general migration sense the light properly

but these slugs move shorter distances compared to wild type slugs presumably due to a defect in slug migration. *dockA/B*^{null} slugs were obviously less able to orient correctly. Phototaxis is known for more than twenty years, but the exact mechanism is still unknown.

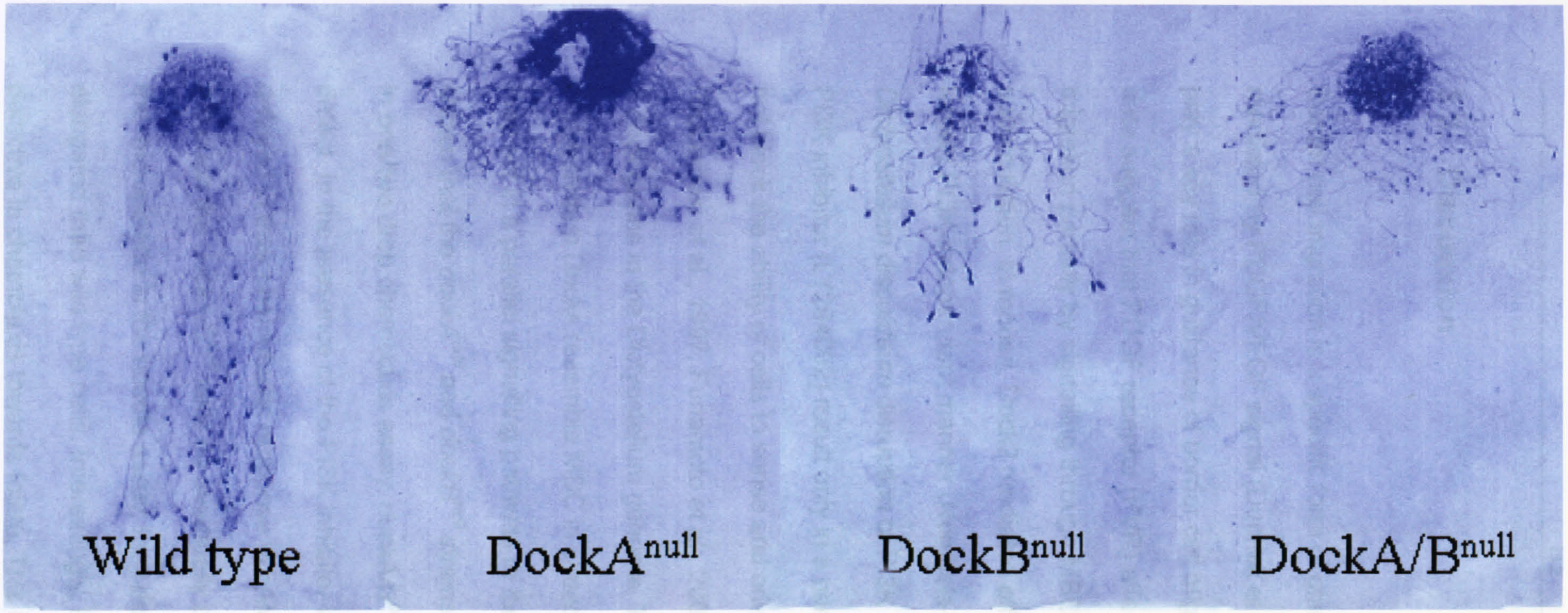

Fig.3.23 Phototaxis experiment. There was pronounced defect in phototaxis in slugs from *dockA*^{null} cells. The slugs from wild-type cells moved almost directly towards the light source. *dockA*^{null} slugs move less directed and slow while *dockB*^{null} slugs move slowly. Phototaxis of *dockA/B*^{null} slugs is like that of *dockA*^{null} slugs. These data were reproducible in more than 5 experiments.

3.3. Discussion

Border cell migration is a specific form of chemotaxis in *Drosophila*, which is mediated by PDGF/VEGF signal (Duchek et al., 2001). PI3K does not appear to play a key role in guidance of border cell migration (Duchek et al., 2001). Their data suggest that PDGF receptor (PVR) affects the guidance of border cell migration partially by signalling through MBC to Rac, which then controls F-actin accumulation. In mouse, Dock2 mediated efficient lymphocyte migration in a largely PI3K-independent manner (Nombela-Arrieta et al., 2004). In *Dictyostelium discoideum* disruption of PI3K activity and the presence of the PI3K inhibitor (LY294002) result only in a partial defect of chemotaxis but it does not block the ability of cells to sense and orient in chemotactic gradients (Buczynski et al., 1997; Funamoto et al., 2001). In this study, we have identified 8 *dock* genes in the Dictyostelium genome. Thus it's possible that the *Dictyostelium* Docks resemble MBC in *Drosophila* and Dock2 in mouse in that they act in a parallel signalling pathway to the PI3K signalling pathway. We have shown that the *dockA*^{null} and *dockB*^{null} strains show a reduced response to cAMP in one/two drop chemotaxis assay. *dockA/B*^{null} cells show an even stronger defect. In the presence of the PI3K inhibitor LY294002, *dockA/B*^{null} cells were delayed in their chemotactic response to cAMP compared to wild type cells. Although the *dockA/B*^{null} cells do eventually polarize and orient toward the tip of the micropipette in the needle assay, they display less directionality and are less elongated than wild type cells. Interestingly, the *dockA/B*^{null} double mutant is not defective in chemotaxis towards folate. This implies that there is no basic defect in motility or even in chemotaxis to some attractants; data supported further

more by the absence of a significant difference in total F-actin in vegetative stage cells measured by flow cytometry.

We examined cAMP induced actin polymerization in *dockA*^{null}, dock*B*^{null} and dock*A/B*^{null} cells. Both the fast and second slower peaks of actin polymerization were reduced. During the first peak, cells freeze and round up. During the second phase of actin polymerization, the cells extend new pseudopods from multiple regions and start to move (Chen et al., 2003; Condeelis, 1990). Interestingly, PI3K inhibitor, LY294002, did not affect the fast phase of chemoattractant-induced actin polymerization (own observations Figure 3.15A) and (Chen et al., 2003), which indicated the fast phase of actin polymerization was controlled by PI3K independent-signalling pathway upon cAMP stimulation in *Dictyostelium discoideum*. We have analyzed the localization of CRAC in *dockA*^{null}, *dockB*^{null} and *dockA/B*^{null} cells and found that it is relatively normal (data not shown), which means there is little effect of *dockA* and *dockB* on PIP3 production. Taken together, our data support the idea that *dockA* and *dockB* play important roles in the regulation of actin polymerization upon cAMP stimulation in PI3K independent pathways.

In *C. elegans* mutation of CED-5 leads to defects in the engulfing of cell corpses during apoptosis (Ellis et al., 1991). *Dictyostelium dockB*^{null} cells also show significant less phagocytosis than wild type cells. *dockB*^{null} cells grow slowly in axenic medium. Slow growth in shaking suspension normally suggests a defect in cytokinesis, which leads to multi-nucleate phenotype (Rivero et al., 2002; Tuxworth et al., 1997). However we didn't find much more multi-nucleate phenotype in *dockB*^{null} cells than wildtype cells and the mutant cells are slightly

smaller than wild type cells. It indicated there was no defect in cytokines for *dockB*^{null} cells. Disruption of *dockA* and *dockB* genes result in reduced rates of macropinocytosis, which could lead to slow growth of *dockB*^{null} and *dockA/B*^{null} cells in axenic medium.

Our collaborator Francisco Rivero has shown that the DockerB domain interacts preferentially with the Rac1A in its nucleotide-free state. DockerA preferentially binds to RacH and RacL. The Rac1-like family of proteins which consists of three highly related proteins, Rac1A, Rac1B and Rac1C. Overexpression of dominant active *rac1* were severely impaired in growth, motility, endocytosis and the formation of filopodia (Dumontier et al., 2000). These phenotype are similar to that of *dockA/B*^{null} cell's. Overexpression of the putative DockB target, Rac1A, in *dockB*^{null} background could rescue the phagocytosis defect (Gerti Weijer unpublished data). Whether Rac1A can rescue the defect in macropinocytosis need to be further examined. Thus far it suggests DockB works as the upstream of Rac1A in *Dictyostelium*.

Experiments have shown *Dictyostelium* mutants defect in chemotaxis also show impaired aggregation (Meili et al., 1999; Noegel and Schleicher, 2000; Palmieri et al., 2000). Unexpectedly, *dockA* and *dockB* null cells did not show any noticeable sorting when synergised with wild type cells. We cannot find a clear sorting pattern when we mix 5% GFP labelled *dockA*^{null}, *dockB*^{null} and *dockA/B*^{null} cells with wildtype cells on agar plates containing 100μM LY294002 (data not shown). This may be explained by the fact that the chemotaxis defect is only rather small and that we need a severe defect before the sorting pattern becomes visible, alternatively it could be that sorting does not rely primarily on

chemotaxis but on other mechanisms such as cell-cell adhesion differences.

To determine whether *dockA*^{null}, dock*B*^{null} and dock*A/B*^{null} cells are unable to chemotaxis properly due to an inability to activate cAMP-induced aggregation stage gene expression, we examined the expression of aggregation-stage genes. We found that *dockA*^{null}, dock*B*^{null} and dock*A/B*^{null} cells exhibit normal expression of two aggregation stage genes (*cAR1* and *aca*) that are representative of genes expressed during aggregation required for chemotaxis. Thus, we do not think the defects in cell movement that we have observed result from secondary effects on gene expression, although we cannot exclude the possibility that some genes required for chemosensory response are not fully expressed.

Interestingly, we observed poor slug phototaxis in *dockA*^{null}. The signalling during phototaxis is complex system, and the basis for phototaxis is not well understood. Genetic analysis of slug behaviour suggests that as many as 55 genes are involved and that several of the encoded proteins regulate signal transduction pathways (Fisher, 1997; Fisher et al., 1997). In the current model of phototaxis, light signals modulate the slug tip activation/inhibition system to cause slug turning by stimulating lateral shifts in the tip position (Fisher, 1997). Experiments have shown light affects cAMP signalling in slug stage by speeding up the movement of prestalk cells and stimulating the cAMP release (Miura and Siegert, 2000). The data from *Dictyostelium* cDNA project has shown *dockA* expressed specific in the tip of the culminant. *dockA*^{null} slugs could move toward the light source however they move much less directly compare to wild type slugs. Knockout *dockA* did not affect the slugs to sense the light source which

indicated *dockA* is possibly involved in the slug migration coordination not phototaxis. Therefore we propose that *dockA* affects cAMP signal transduction to the cytoskeleton during phototaxis especially in prestalk cells.

Chapter IV Investigation into the role of *elmo1* gene

4.1. Introduction

Members of the Elmo family of proteins are novel, evolutionarily conserved upstream regulators of the Rac signalling pathway. Elmo proteins interact with the Dock180 superfamily of proteins to form dimeric complexes which act as unconventional guanine nucleotide exchange factors (GEFs) for Rac (Brugnera et al., 2002; Gumienny et al., 2001). Through this nucleotide exchange activity Elmo proteins regulate Rac activity which then results in actin polymerisation which provides the driving force for processes such as phagocytosis and cell migration. A Blast search of the *D. discoideum* genome with the full length human Elmo1 protein sequence identified four *D. discoideum* homologous, Elmo1-4. All the *Dictyostelium discoideum* Elmo proteins have the conserved DUF609/Elmo-Ced-12 domain.

This report details the characterisation phenotype of *elmo1*^{null} strain in *D. discoideum*. The *elmo1* null cells show compromised chemotaxis, macropinocytosis, phagocytosis, cAMP induced actin polymerization, and grow significantly slower than wild type cells. The *elmo1*^{null} phenotype is very similar to that reported for *dockB*^{null} cells in *Dictyostelium discoideum*, supporting the suggestion that the Elmo-Dock complex function in the same pathway. Although the phenotype reported here implicates Elmo1 in multiple cellular processes the exact biochemical function of the Elmo1 protein remains unknown.

4.2. Results

4.2.1. Elmo in *Dictyostelium*

A Blast search of the *D. discoideum* genome with the full length human Elmo1 protein sequence identified four *D. discoideum* homologous, Elmo1 (DDB0204388), Elmo2 (DDB0206423), Elmo3 (DDB0185279) and Elmo4 (DDB0218269). *Dictyostelium* DDB0204388 shows high homology to human Elmo1, we named it Dd Elmo1 and the other Elmo homologous Dd Elmo 2-4. Dd Elmo proteins are in high varied length range from 284aa to 1267aa. *D. discoideum* Elmo amino acid sequences show high homology to Elmo's of other organism. Human Elmo has no discernible catalytic domain such as DH domain for Rac activation, but at its C-terminus it possesses a PH domain, a putative leucine zipper motif, and a proline-rich motif (Brugnera et al., 2002; Grimsley et al., 2004). The C-terminal 100 amino acids of Elmo1 are essential for the interaction with Dock180 (Brugnera et al., 2002), while the N-terminus of Elmo1 is important for mediating cell migration via the Elmo1-Dock180 complex (Grimsley et al., 2004). The domain structure of the *D. discoideum* Elmo family was determined by searching Conserved Domain Search service (CD-Search) on NCBI (Marchler-Bauer and Bryant, 2004). The Duf609/Elmo-Ced-12 is found towards the middle of the protein in the *D. discoideum* Elmo homologous. Duf609/Elmo-Ced-12 domain is a conserved domain found in a number of eukaryotic proteins including Ced-12, human Elmo1, and Elmo2. The exact role of this domain is still unknown. PH domain is not present in Ced-12 and *D. discoideum* Elmos by CD-Search (Figure 4.1). Amino-acid sequences of Elmo-related protein from mammalian, *C. elegans and Dictyostelium discoideum* were aligned by Vector NTI Clustal W package (Figure 4.2).

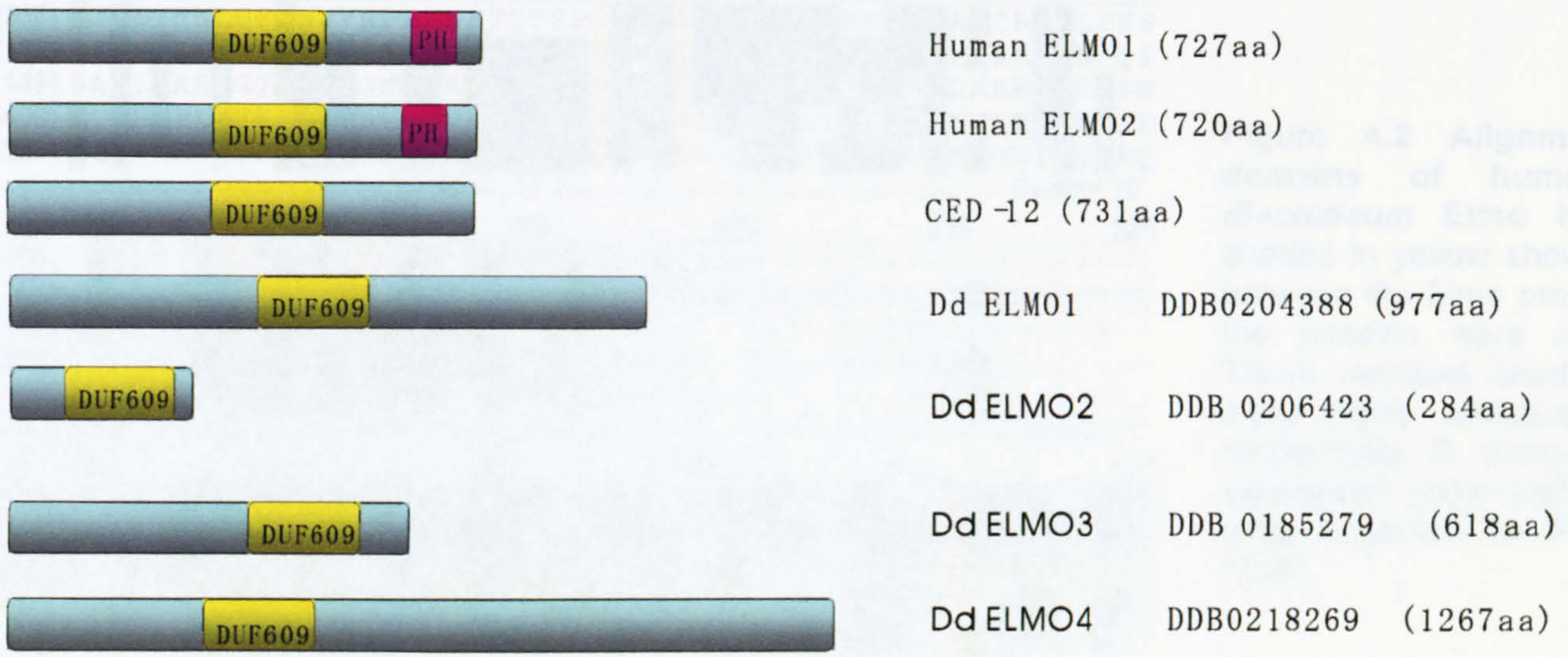

Figure 4.1 Schematic diagram of the domain structure of human Elmo1 and Elmo2 proteins, CED-12 and *D. discoideum* Elmo homologues. *Dictyostelium* Elmo proteins vary in length from 284aa to 1267aa. These Elmo homologues all contain a Duf609/Elmo-Ced-12 domain of approximately 160 amino acids which is a conserved domain found in a number of eukaryotic proteins including Ced-12, human Elmo1, and human Elmo2. Human Elmo 1&2 and Ced12 contain no discernible catalytic domains such as a DH domain for Rac activation, but at their C-termini they possess a PH domain, a putative leucine zipper motif, and a proline-rich motif (Brugnera et al., 2002; Grimsley et al., 2004). The domain structure of the *D. discoideum* Elmo family was determined by searching Conserved Domain Search service (CD-Search) on NCBI (Marchler-Bauer and Bryant, 2004). The Duf609 domain is found towards the middle of the protein in the *D. discoideum* Elmo homologues. Human Elmo1 and Elmo2 have a PH domain at its C terminus, which is not present in Ced-12 and *D. discoideum* Elmos by CD-Search.

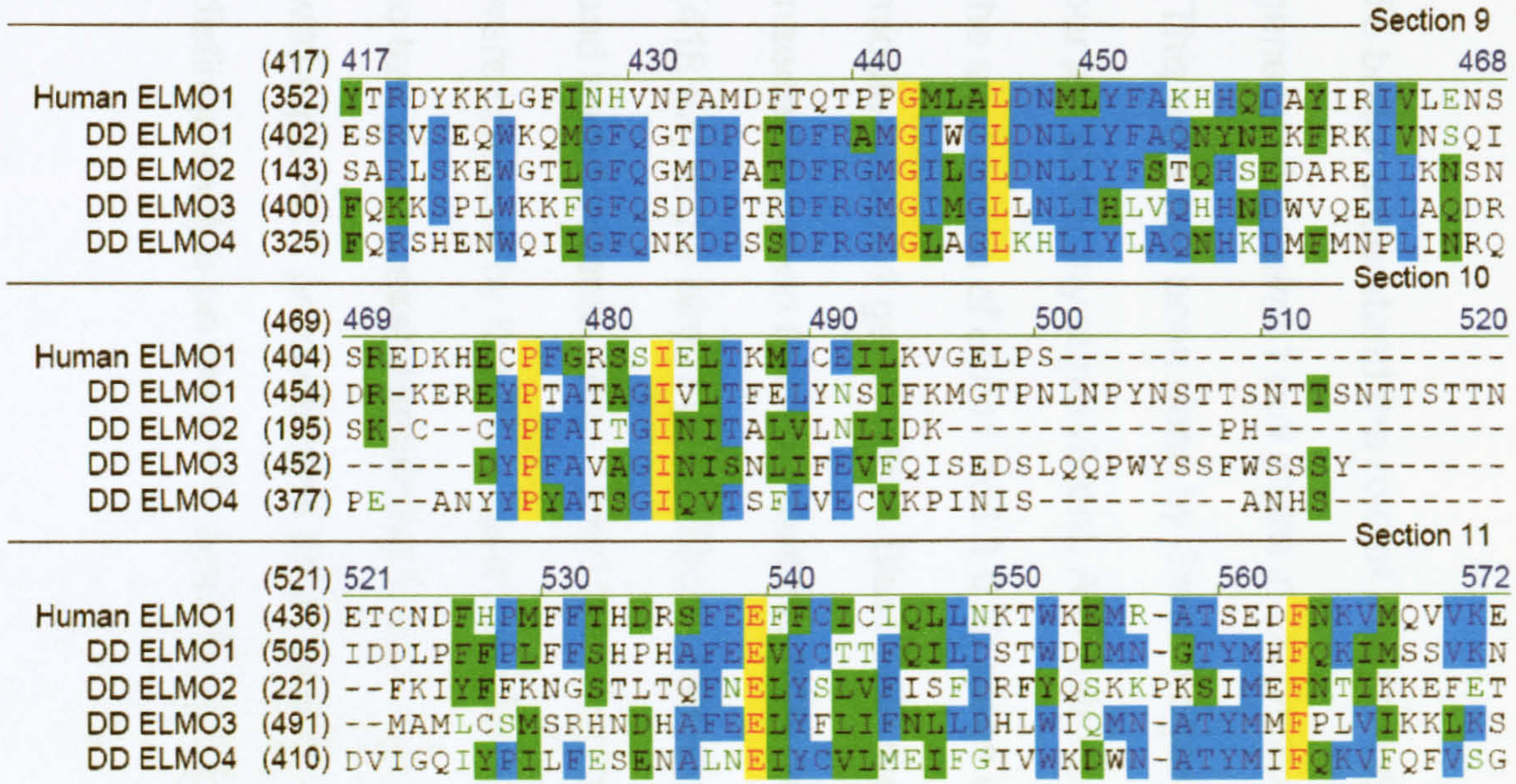

Figure 4.2 Alignment of the DUF609 domains of human Elmo1 and *D. discoideum* Elmo homologues. Residues shaded in yellow show absolute conservation between the Elmo proteins. The sequences of the proteins were aligned using Clustalw. Those residues shaded in yellow and blue show highly conserved and semi-conserved respectively. *D. discoideum* Elmo amino acid sequences show high homolog to Elmo's of other organism by Protein-Protein Blast on NCBI.

Human *elmo1* is ubiquitously expressed, although its expression was highest in the spleen, an organ rich in immune cells (Gumienny et al., 2001; Sanui et al., 2003; Scott et al., 2002). There is little known about the expression of *elmo* genes in *Dictyostelium*. We designed primers to include an intron on *elmo1* and used these to examine its expression profile. The specific fragment amplified from cDNA is 517bps, which is 86bps smaller than the transcript from genomic DNA. *elmo1* was expressed throughout the developmental cycle of Dictyostelium (data not shown).

To better understand the role of *elmo1* in the regulation of cellular behaviour, we generated an *elmo1* null strain in *Dictyostelium* by homologous recombination (This work has been done by Sarah Fogarty during her PhD rotation project in our lab under my supervision). A construct was made containing 1.0kb before the start codon of *elmo1* and 1.0 kb piece of genomic DNA derived from the middle of *emlo1* gene, with a Blasticidin resistance cassette (Faix et al., 2004) inserted between them, so that the BSR cassette replaced the N-terminal part (418 aa) of the *elmo1* gene. The construct was transfected into wild type cells, and transformants were cloned following selection in Blasticidin S. All clones were checked by the PCR using the primers to amplify gene disruption construct to test for successful knockout events. The difference between the knockout and wild-type PCR products was estimated to be 0.22kb and so is not easily distinguishable on the 0.6% agarose gel. Restriction analysis was performed on

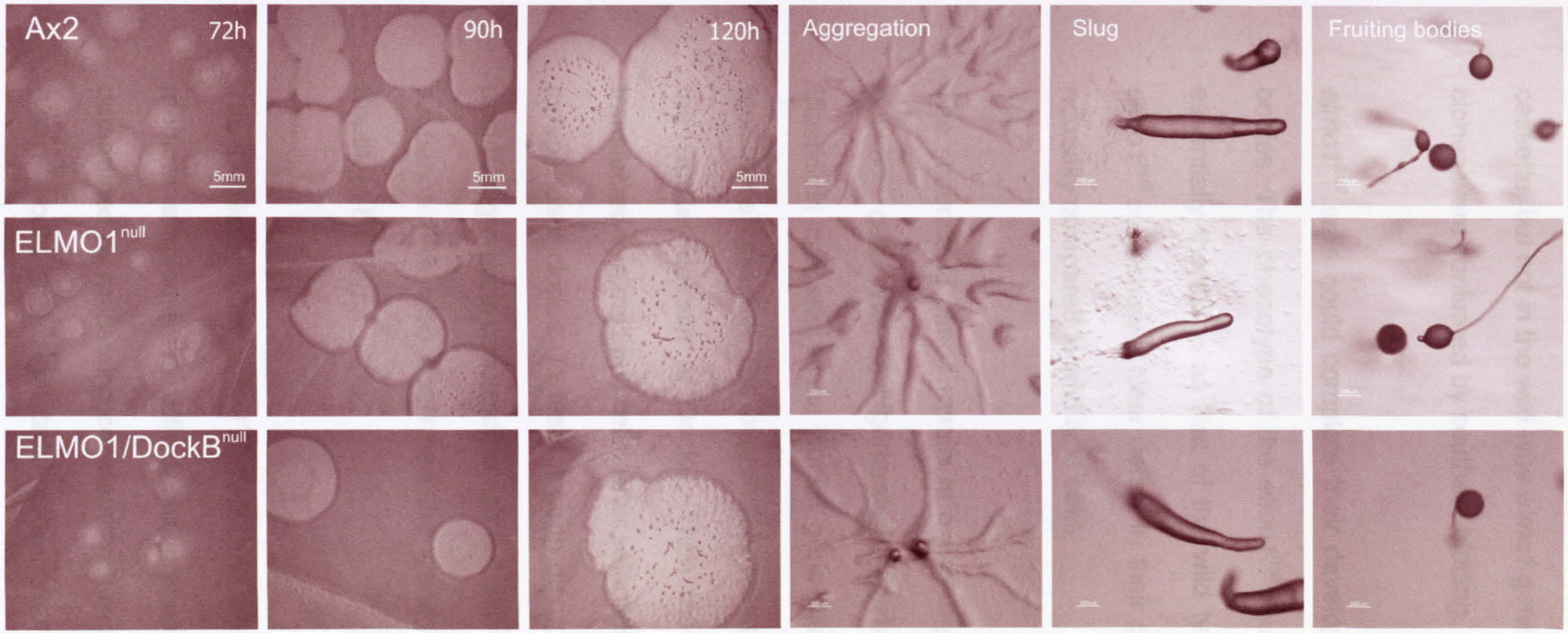

Figure 4.3 The phenotype of the *elmo1*^{null} and *elmo1*^{null}*/dockB*^{null} mutants on bacterial lawn. On the bacterial lawn plates the clones of the *elmo1*^{null} and *elmo1*^{null}*/dockB*^{null} cells were essentially the same as those of the wild type cells, including the size and shape at every developmental stage. These data were representative for results obtained in three independent experiments.

the PCR products using BglII which has a unique site within the Blasticidin cassette, but not in the wild type *elmo1* gene. The positive the independent clones were confirmed by southern blotting.

elmo1^{null} cells could complete their developmental life cycle and form fruiting bodies. The phenotype of the *elmo1*^{null} mutants on bacterial lawn plates was essentially the same as that of the wild type cells (Figure 4.3). Although the *elmo1*^{null} cells show a clear defect in their growth rate, they appear to develop normally compared to wild type cells.

The absence of *elmo1* results in a phenotype was similar to that observed in *dockB*^{null} cells. We next generated *elmo1/dockB*^{null} strains. We replaced the Blasticidin cassette in the *dockB* gene disruption construct by a hygromycin resistance cassette. The hygromycin resistance cassette was inserted before the Docker domain of DockB. Then the *dockB*/hygromycin construct was transfected to *elmo1* null cells. After selection in hygromycin, we isolated several independent clones. To test for gene disruption we expect to PCR amplify the dockB/hygromycin construct, which is 1.3kb longer than the original the genomic sequence. We also confirmed the gene disruption event in the clones by Southern blotting.

The *D. discoideum elmo1*^{null} cells and wild type cells were cultured in HL5 medium supplemented with penicillin/streptomycin at 21°C. Cell growth was determined by measuring cell density at regular time intervals (Figure 4.4). The *elmo1*^{null} cells grew significantly slower than the wild type cells with a doubling time of approximately (18 ± 2) hours compared to (8 ± 1) hours for the wild type

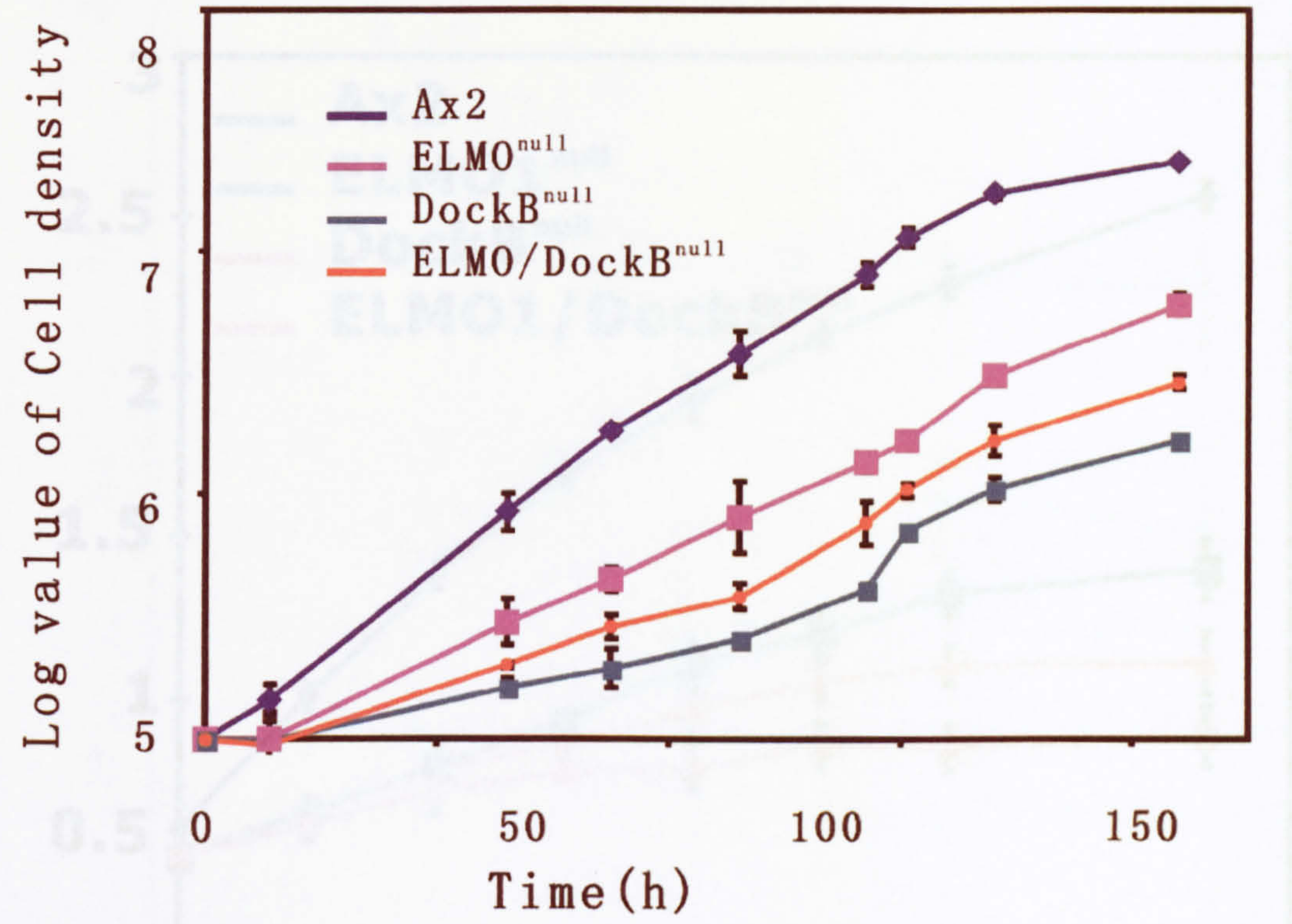

Figure 4.4 Growth curve for the *elmo1*^{null} and *elmo1*^{null}*/dockB*^{null} cells. *elmo1*^{null} and *elmo1*^{null}*/dockB*^{null} cell grow slowly in axenic medium. The doubling time of the *elmo1*^{null} cells is 18 ± 2 hours compared to 8 ± 1 hours for the wild type (Mean ± SD, $p<0.05$). These data show the means and standard deviations of 3 independent experiments, performed on different days.

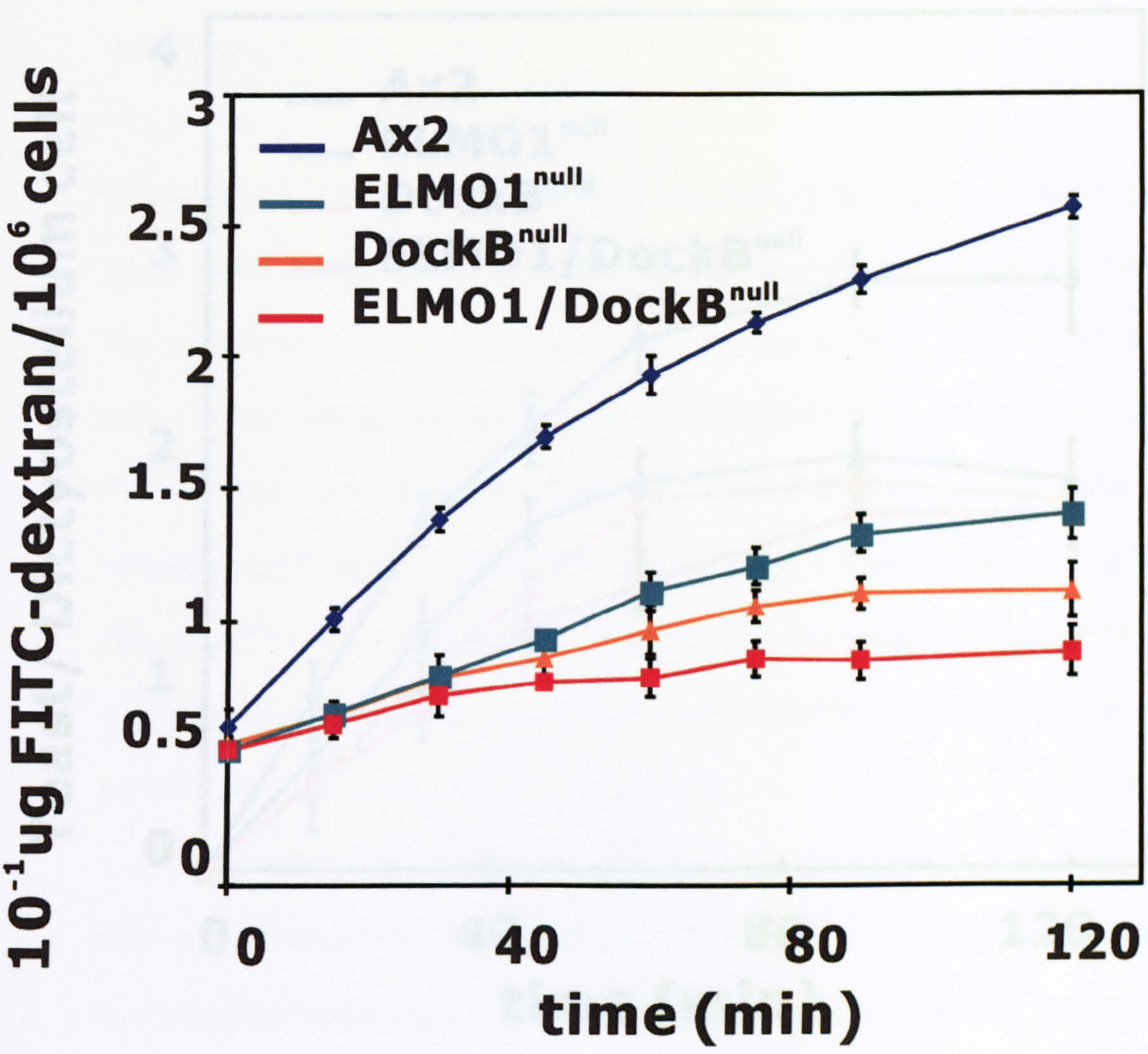

Figure 4.5 Macropinocytosis assay. Assays were performed by incubating the cells with FITC-dextran. Knockout of *elmo1* results in reduced macropinocytosis rate. *elmo1*^{null}/*dockB*^{null} cells showed a similar reduction as *dockB*^{null} cells. The data shown are the means and standard deviations of three independent experiments.

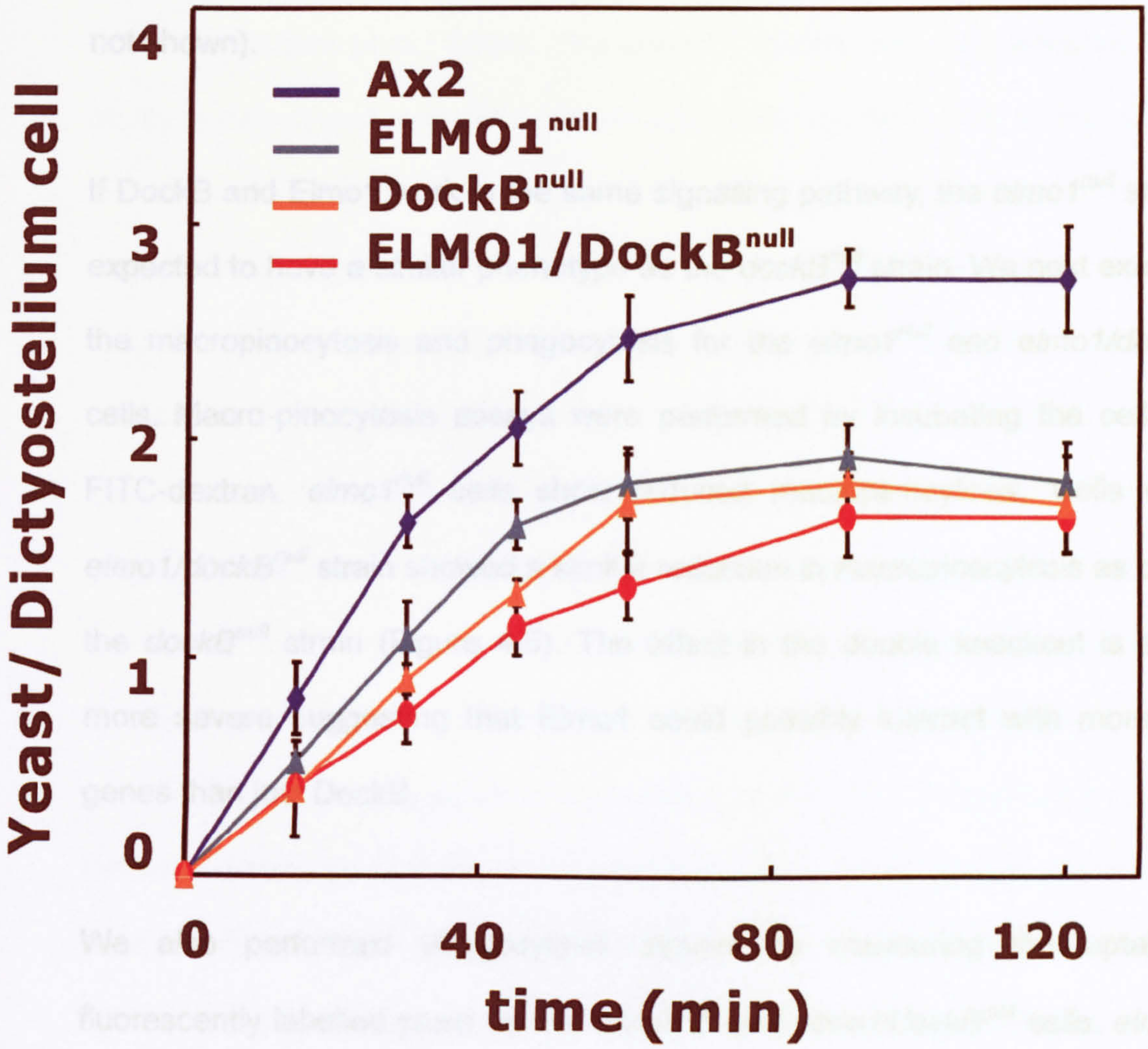

Figure 4.6 Phagocytosis assay. *elmo1*^{null} cells showed reduced uptake of yeast cells (1.3 ± 0.3 yeast cells/cell·hour) compared to the uptake speed of wild type cells (2.8 ± 0.5 yeast cells/cell·hour) (data represents mean ± sd, number=3 $p<0.05$). elmo1^{null}/*dockB*^{null} showed a similar defect in phagocytosis as elmo1^{null} cells. The data shown are the means and standard deviations of three independent experiments.

(Mean ± SD, number=3, $p<0.05$). Knockout of *dockB* in an *elmo1*^{null} background leads to a similar growth phenotype as that of *dockB*^{null} cells, which suggest that Elmo1 and DockB act possibly in the same pathways not inconsistent with the idea that they are binding partners. Despite this defect in cell growth there was no evidence of multiple nuclei/cell in *elmo1*^{null} and *elmo1*^{null} */dockB*^{null} cells (data not shown).

If DockB and Elmo1 work in the same signalling pathway, the *elmo1*^{null} strain is expected to have a similar phenotype as the *dockB*^{null} strain. We next examined the macropinocytosis and phagocytosis for the *elmo1*^{null} and *elmo1/dockB*^{null} cells. Macro-pinocytosis assays were performed by incubating the cells with FITC-dextran. *elmo1*^{null} *cells* show reduced macropinocytosis. Cells of the *elmo1/dockB*^{null} strain showed a similar reduction in macropinocytosis as cells of the *dockB*^{null} strain (Figure 4.5). The effect in the double knockout is slightly more severe suggesting that Elmo1 could possibly interact with more dock genes than just DockB.

We also performed phagocytosis assays by measuring the uptake of fluorescently labelled yeast by the *elmo1*^{null} and *elmo1/dockB*^{null} cells. *elmo1*^{null} cells showed a reduced uptake of yeast cells (1.3 ± 0.3 yeast cells/cell·hour) compared to the uptake speed of wild type cells (2.8 ± 0.5 yeast cells/cell·hour) (data represents mean ± SD, number=3 $p<0.05$). *elmo1/dockB*^{null} showed a similar defect in phagocytosis as elmo1^{null} cells (Figure 4.6).

4.2.2. Mutation of *elmo1* results defect in chemotaxis

We performed the chemotaxis assay on the *elmo1*^{null} and *elmo1/dockB*^{null} cells to examine whether *Dictyostelium* Elmo1 resemble Elmos in other organisms which mediate signal during chemotaxis (Brugnera et al., 2002; Gumienny et al., 2001; Janardhan et al., 2004). The *elmo1*^{null} mutant cells are defective in their ability to detect and respond to an external cAMP gradient both in one drop and two drop chemotaxis assay (Figure 4.7 4.8A). In one drop chemotaxis assay, *elmo1*^{null}, *elmo1/dockB*^{null} cells show 10 and 20minutes later response respectively to cAMP compared to wild type cells (measured as the time for 50% of the drops to show a response). There was no significant difference in chemotaxis to folate between the *elmo1*^{null} cells and wildtype cells at vegetative stage, which seems to indicate that there is no intrinsic difference in the ability of the *elmo1* mutant cells to move. LY294002 has been shown to inhibit the localised production of PIP3 and thus should show whether the elmo1 mutants work in the same pathway or in a parallel pathway PIP3 independent signalling pathway during chemotaxis. In the presence of moderate concentrations of the PI3K inhibitor, 50μM LY294002, *elmo1*^{null} and *elmo1/dockB*^{null} cells show a similar reduction in their chemotactic response efficiency to cAMP (Figure 4.8B).

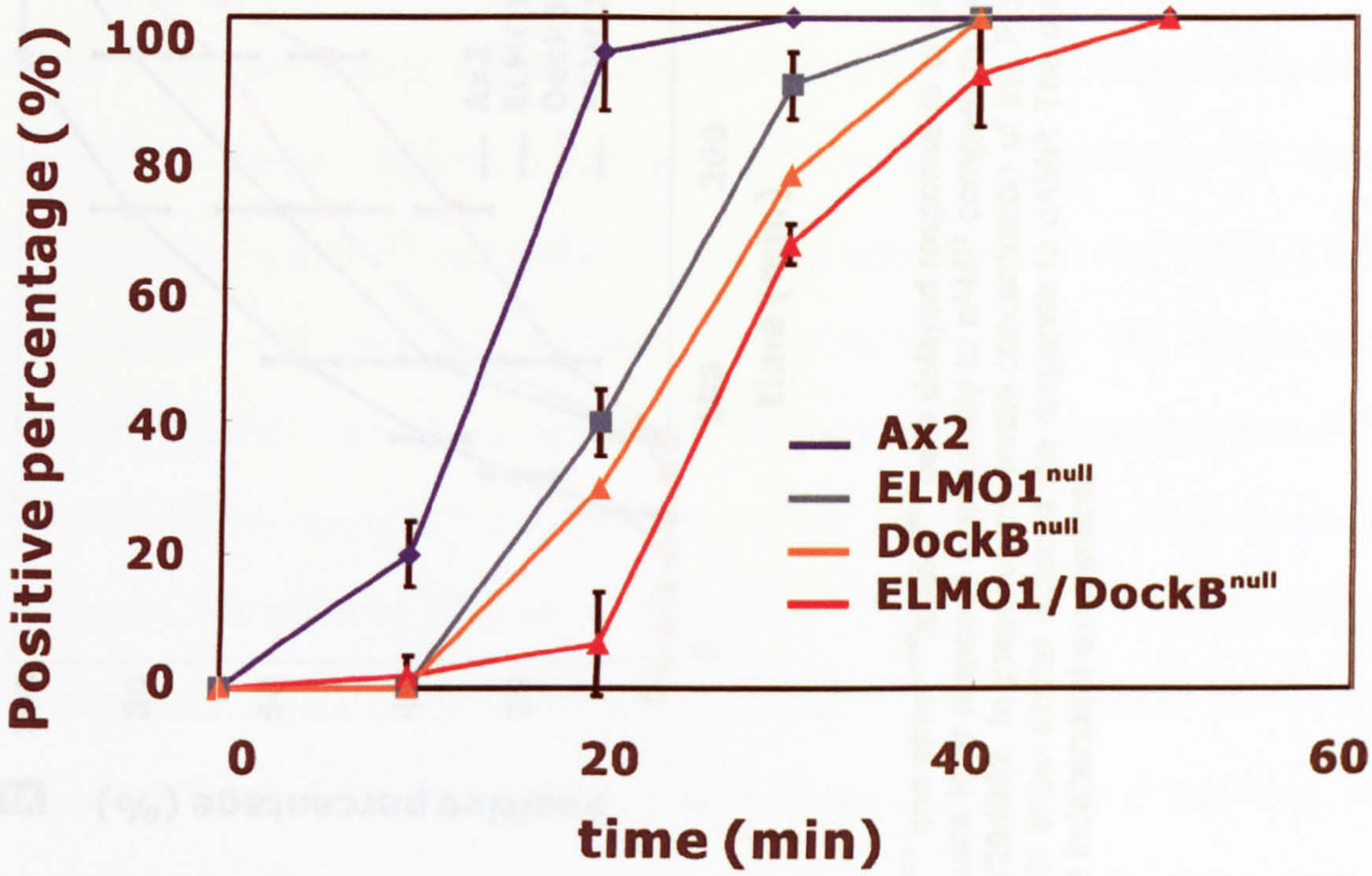

Figure 4.7 One Drop chemotaxis assay. *elmo1*^{null} and *dockB*^{null} strains show a delayed chemotactic response. *elmo1*^{null}, *elmo1*^{null}/*dockB*^{null} cells show 10 and 20minutes delayed response respectively to cAMP compared to wild type cells (measure as the time it takes 50% of the drops to show a response). The data shown are the means and standard deviations of three independent experiments.

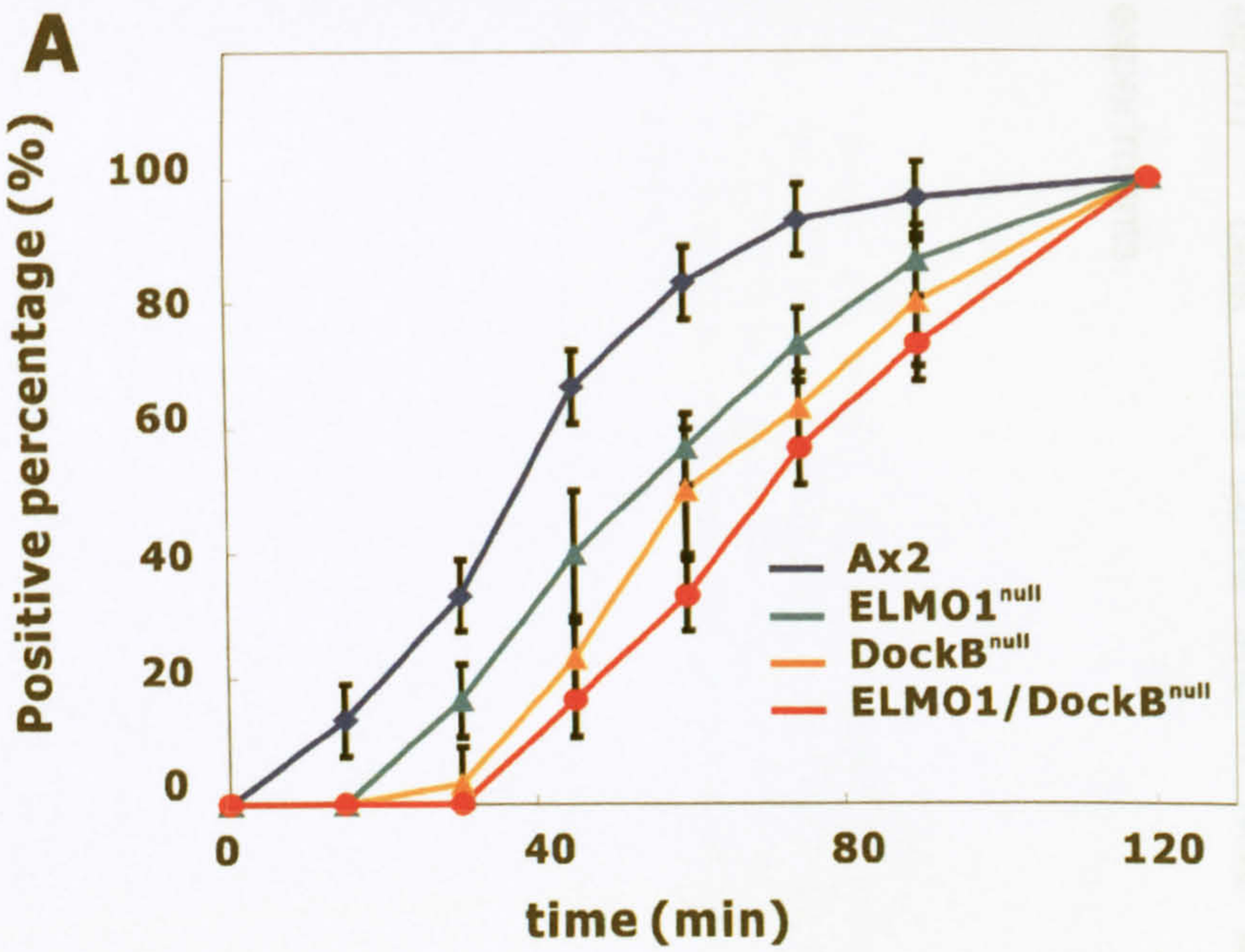

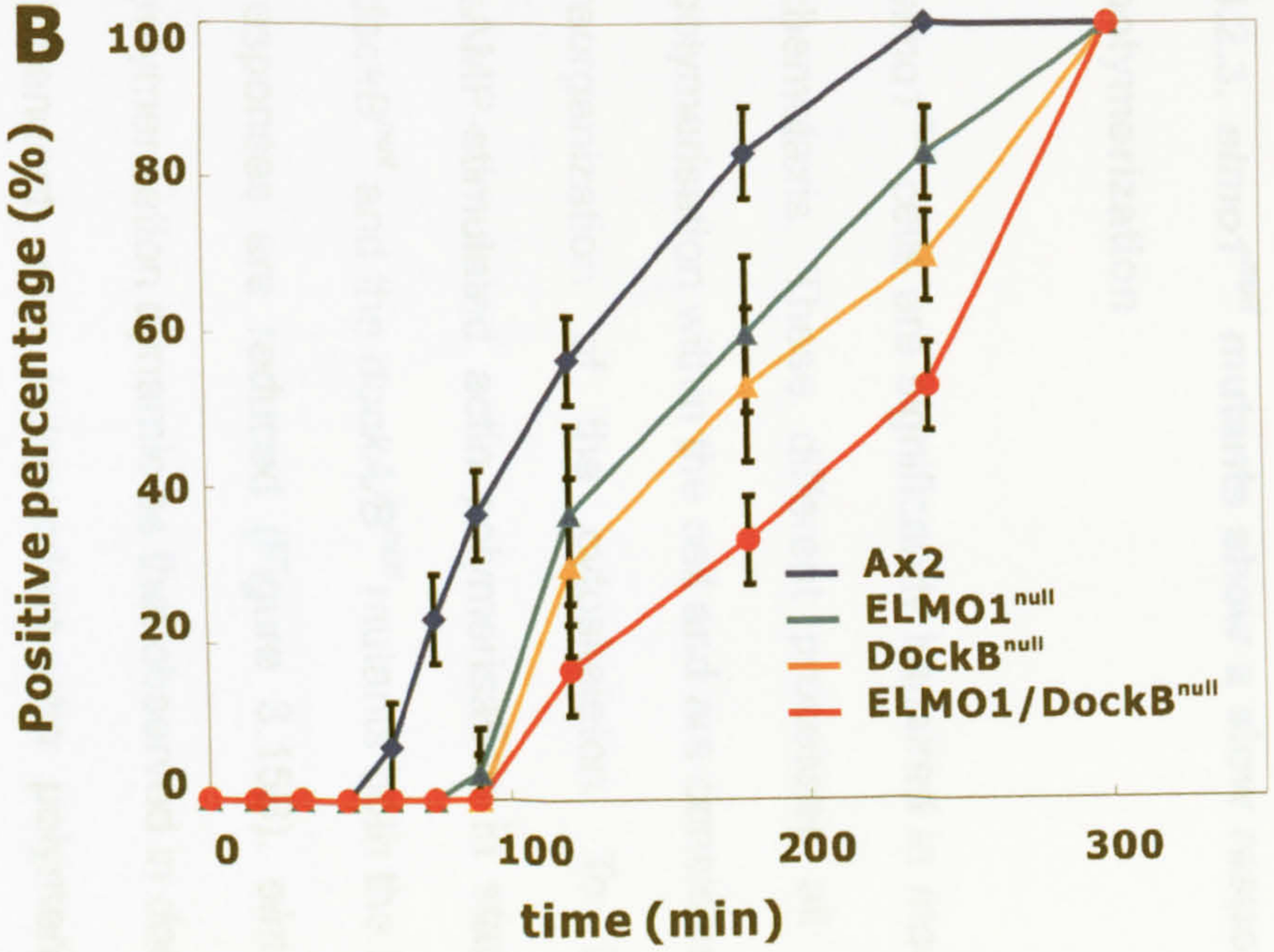

Figure 4.8 (A) Two drop chemotaxis assay. *elmo1*^{null} and *elmo1*^{null}*/dockB*^{null} cells delayed response to cAMP. *elmo1*^{null}, *elmo1*^{null}*/dockB*^{null} cells show 10 and 30minutes later response respectively to cAMP compare to wild type cells. **(B) Two drop chemotaxis assay with LY294002.** In presence moderate concentration of the PI3K inhibitor, 50μM LY294002, *elmo1*^{null} and *dockB*^{null} cells show similar reduced the response to cAMP. The data shown are the means and standard deviations of three independent experiments.

4.2.3. *elmo1*^{null} mutants show a slow response to cAMP and altered actin polymerization

elmo1^{null} cells are significantly impaired in macropinocytosis, phagocytosis and chemotaxis. These different processes all require the regulation of actin polymerisation within the cell and are consistent with Elmo1 having a role in the reorganization of the cytoskeleton. To investigate this we measured cAMP-stimulated actin polymerisation in starved *elmo1*^{null} cells. In *dockA*^{null}, *dockB*^{null} and the *dockA/B*^{null} mutants both the fast and slow actin polymerization responses are reduced (Figure 3.15B). *elmo1*^{null} cells show a similar actin polymerization dynamic as that observed in *dockB*^{null} cells (Figure 4.9). The PI3K dependent- and independent-actin polymerization peaks were reduced in *elmo1*^{null} cells. The curve shown here is the average of 9 independent experiments.

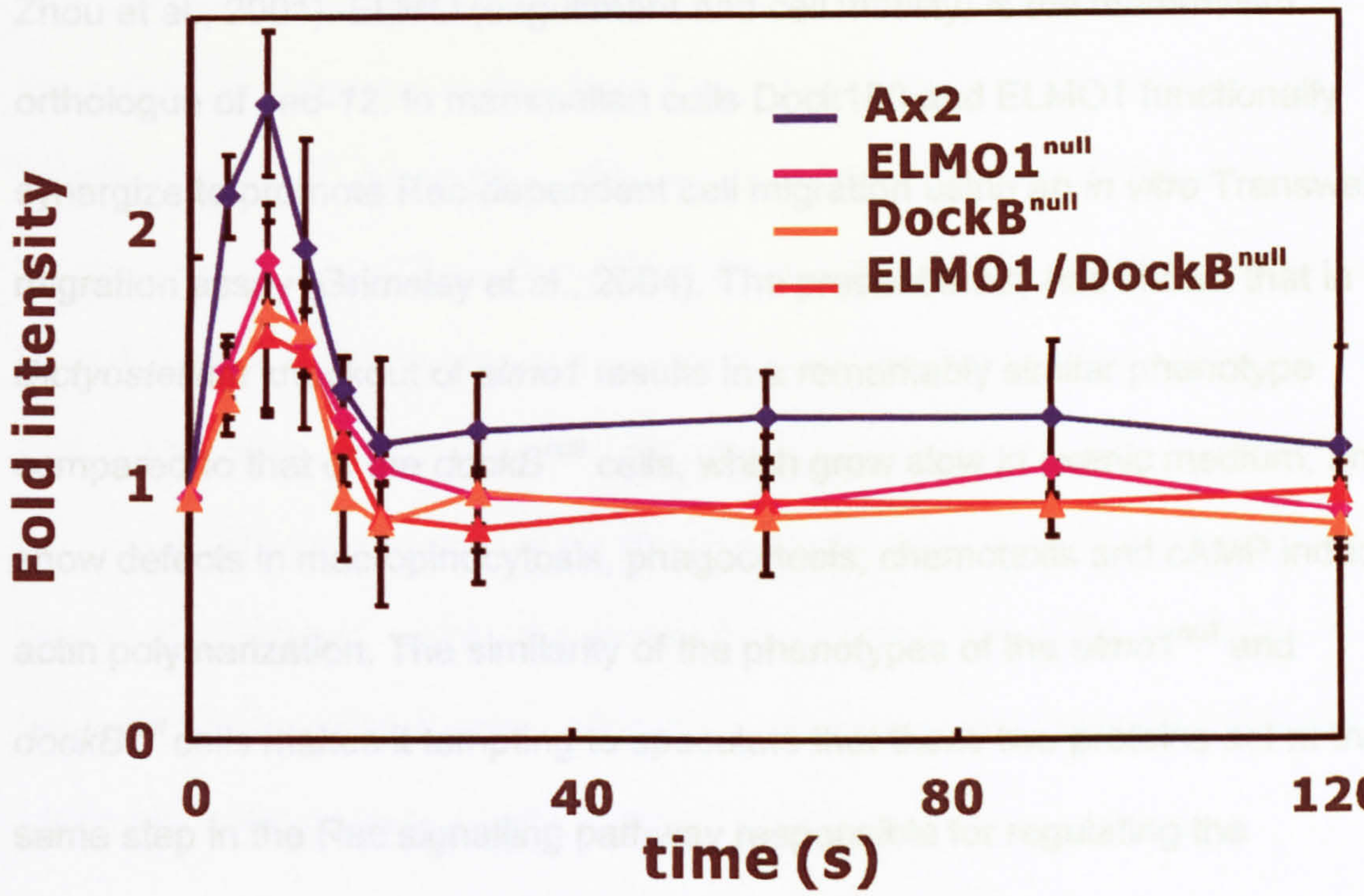

Figure 4.9 cAMP induced actin polymerization in *elmo1^{null}* mutants. *elmo1^{null}* and *elmo1/dockB^{null}* cells show similar actin polymerization dynamic as *dockB^{null}* cells. Both the fast and slow actin polymerization responses are diminished in those cells.The curve shown here is the average of 9 independent experiments.

4.3. Discussion

In *C. elegans ced-12* display defects in engulfment of apoptotic cells, and migration of the distal tip cells (DTCs) (Gumienny et al., 2001; Wu et al., 2001; Zhou et al., 2001). ELMO (engulfment and cell motility) is the mammalian orthologue of *ced-12*. In mammalian cells Dock180 and ELMO1 functionally synergize to promote Rac-dependent cell migration using an *in vitro* Transwell migration assay (Grimsley et al., 2004). The present study has shown that in *Dictyostelium* knockout of *elmo1* results in a remarkably similar phenotype compared to that of the *dockB*^{null} cells, which grow slow in axenic medium, and show defects in macropinocytosis, phagocytosis, chemotaxis and cAMP induced actin polymerization. The similarity of the phenotypes of the *elmo1*^{null} and *dockB*^{null} cells makes it tempting to speculate that these two proteins act at the same step in the Rac signalling pathway responsible for regulating the reorganization of the cytoskeleton in *Dictyostelium*. As described before DockB preferential binds to Rac1A in the nucleotide free state (unpublished data). These data strongly suggest that in *Dictyostelium* Elmo1 resemble Ced-12 and mammalian Elmos, which interacts with Dock protein and functions upstream of Rac, therefore regulating actin polymerization. However a direct interaction between DockB and Elmo1 in *D. discoideum* has yet to be established. This could be readily investigated by generating TAP-tagged constructs of these proteins *in vivo* and isolating any binding partners. The exact function of Elmo1 and its role in activating Rac when complexed with members of the Dock superfamily of proteins remains unknown. It will be interesting to show that Elmo1 could bind to DockB *in vitro* by immunoprecipitation. It would also be

useful to determine which combinations of Elmo and Dock proteins interact *in vivo* and if the different combinations of proteins produced subtle or pronounced differences in function.

Although the *elmo1*^{null} cells exhibited impaired chemotaxis, macropinocytosis and phagocytosis, they could still produce a limited response. This may be indicative of some redundancy in function between the four Elmo proteins identified in the *D. discoideum* genome. Another Elmo protein may compensate for the loss of Elmo1 by interacting with its main binding partner, presumably DockB. This is supported by work in mammals which shows that both Elmo1 and Elmo2 can form a complex with Dock180 (Brugnera et al., 2002). Alternatively the activity of conventional GEF's may be able to compensate for a decrease in the level of Elmo1 within the cells. We inserted the BSR cassette at the beginning of the *elmo1* gene, after the homologous recombination this should totally block the expression of the *elmo1* gene.

Previous reports suggest that the PH domain of mammalian Elmo proteins is required to form the Elmo/Dock180/Rac trimeric complex and is essential for the Dock180-Elmo complex to function as a Rac GEF (Lu et al., 2004). It also suggests that the Elmo PH domain function is evolutionarily conserved from *C. elegans* to humans. However while analysis of the Elmo1 proteins in *D. discoideum* identified a Duf609/Elmo-Ced-12 domain in each of the four proteins, it failed to identify a PH domain or any other recognised protein domain in any of the proteins by blast the Elmo amino acid sequence against PFAM database. This raises questions about the mechanism through which the Dock180-Elmo complex functions as unconventional GEF's. In addition a recent report suggests

that Armadillo repeats within the N-terminus of human Elmo1 mediate an interaction with activated RhoG which in turn promotes Dock180-mediated Rac activation and cytoskeletal reorganisation (Debakker et al., 2004). Although these Armadillo repeats are conserved in *C. elegans* Ced-12 they do not appear to be present in any of the Elmo proteins identified in the *D. discoideum*. This again raises questions concerning the mechanism through which the Dock180-Elmo complex is activated and how it in turn regulates nucleotide exchange on Rac. The components of this signalling pathway remain elusive at least in *D. discoideum*.

Chapter V Investigation into the role of *dockC, D, G and H* genes

5.1 Introduction

We have presented data showing that the *dockA/B^{null} cells* have reduced chemotaxis when compared to wild type cells, both in the absence and presence of a PI3K inhibitor LY294002. However LY294002 did not 100% block the *dockA/B^{null}* chemotaxis could possibly be explained by the compensation between *dock* genes in *D. discoideum* since there are still 6 *dock* genes remaining in the genome.

We generated *dockC^{null}*, *dockD^{null}*, *dockG^{null}* and *dockH^{null}* mutants in *Dictyostelium* to understand the possible role of the other dock genes in the regulation of *Dictyostelium*. *dockC^{null}* cells show poor chemotaxis. There was no clear defect in growth, macropinocytosis, phagocytosis, and phototaxis of *dockC^{null}*, *dockD^{null}*, *dockG^{null}* and *dockH^{null}* cells.

5.2 Results

5.2.1 *Dictyostelium dock* genes

As shown previously *dockA* and *dockB* are involved in growth, chemotaxis, endocytosis and phototaxis. d*ockA^{null}*, *dockB^{null}* and *dockA/B^{null}* cells show reduced chemotaxis and altered cAMP stimulated actin polymerization responses. We used the same method described before to generate *dockC^{null}*, *dockD^{null}*, *dockG^{null}* and *dockH^{null}* mutants. The phenotype of these mutants has

been studied, with an emphasis on actin dependent processes like actin polymerization, growth, endocytosis, phagocytosis, motility and chemotaxis.

5.2.2 Phenotype of *dockC^{null}*

We have used RT-PCR analysis to study the expression of the *dockC* during synchronised development on KK2 agar plates. Primers for the RT-PCR were designed to include an intron on *dockC*. The PCR fragment from RT-PCR is 281bps, which is 88bps smaller than the PCR product from contaminating genomic DNA. *dockC* is expressed during all the stages of development (data not shown).

Knockout of *dockC* did not result in obvious defects during development. *dockC^{null}* cells show similar phenotypes as wild type cells on bacterial lawns (Figure 5.1). Since the *dockA/B^{null}* double mutant showed a stronger phenotype than either single mutant, we knocked out *dockA* in the *dockC^{null}* background. However the *dockA/C^{null}* did not show any clear defect in development. *dockA/C^{null}* cells can complete development nearly as well as wild type cells (Figure 5.2).

We tested the chemotaxis ability of the *dockC^{null}* and *dockA/C^{null}* cells compared to wildtype in the one drop assay. The cells that were used for the chemotaxis assays were pulsed with cAMP to make sure that they express all the pulsed induced genes needed for chemotaxis. The percentages of drops showing a positive migration response was plotted as a function of time as shown in Figure 5.3. The results of the one drop chemotaxis assay indicated that the *dockC^{null}*

and *dockA/C*^{null} cells showed a delayed response on plates containing 10^{-8}M cAMP in comparison to wild type cells.

We also measured macropinocytosis and phagocytosis of the *dockC*^{null} cells. *dockC*^{null} strains have very similar uptake rates compared to wild type for both macropinocytosis of FITC-dextran supplemented medium (Figure 5.4) and phagocytosis of yeast cells (Figure 5.5).

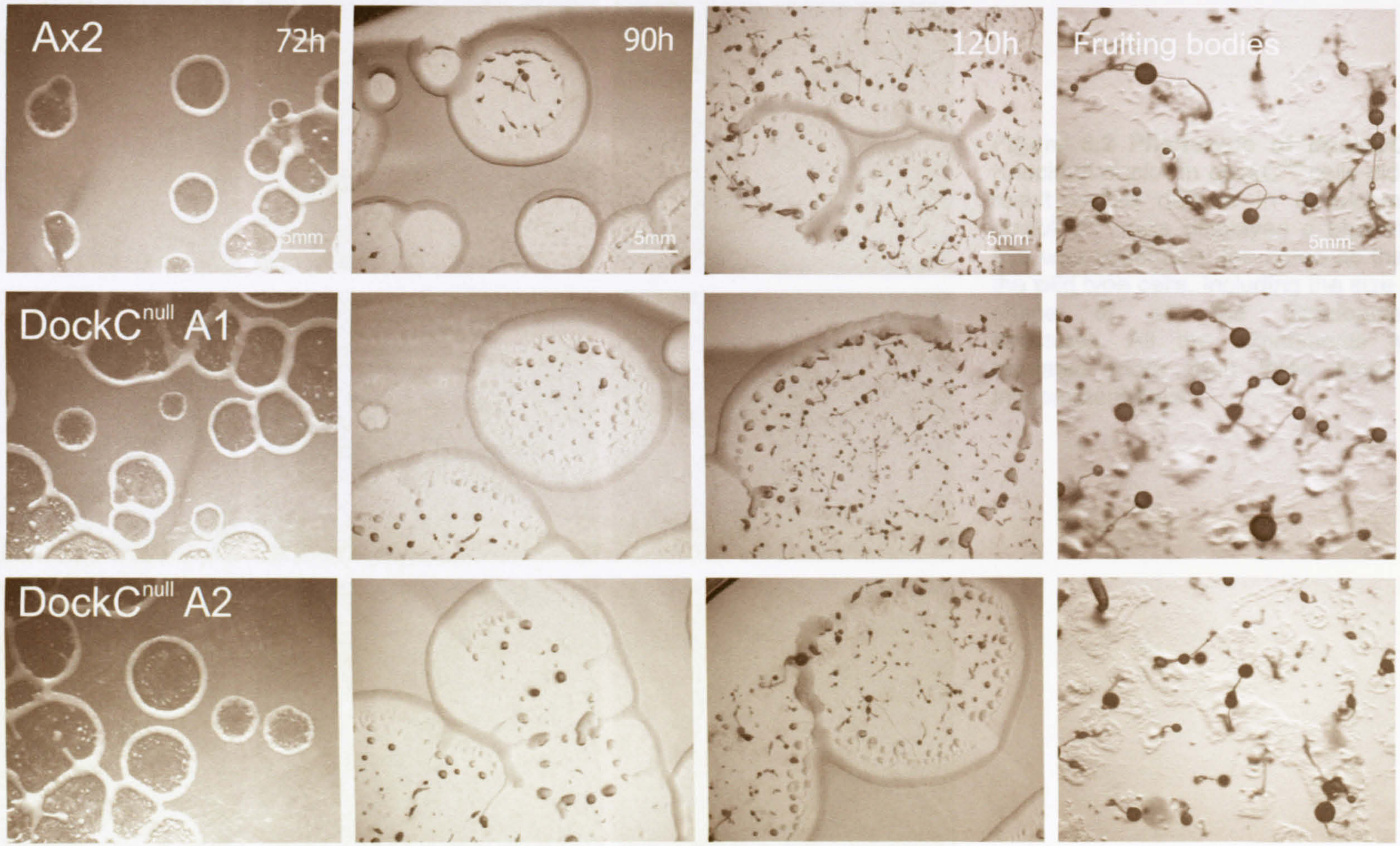

Figure 5.1 Phenotype of *dockC^{null}*. The phenotype of *dockC^{null}* strains essentially the same as that of the wild type cells, including the size and shape of all structures. All the experiments were repeated more than three times on independent days.

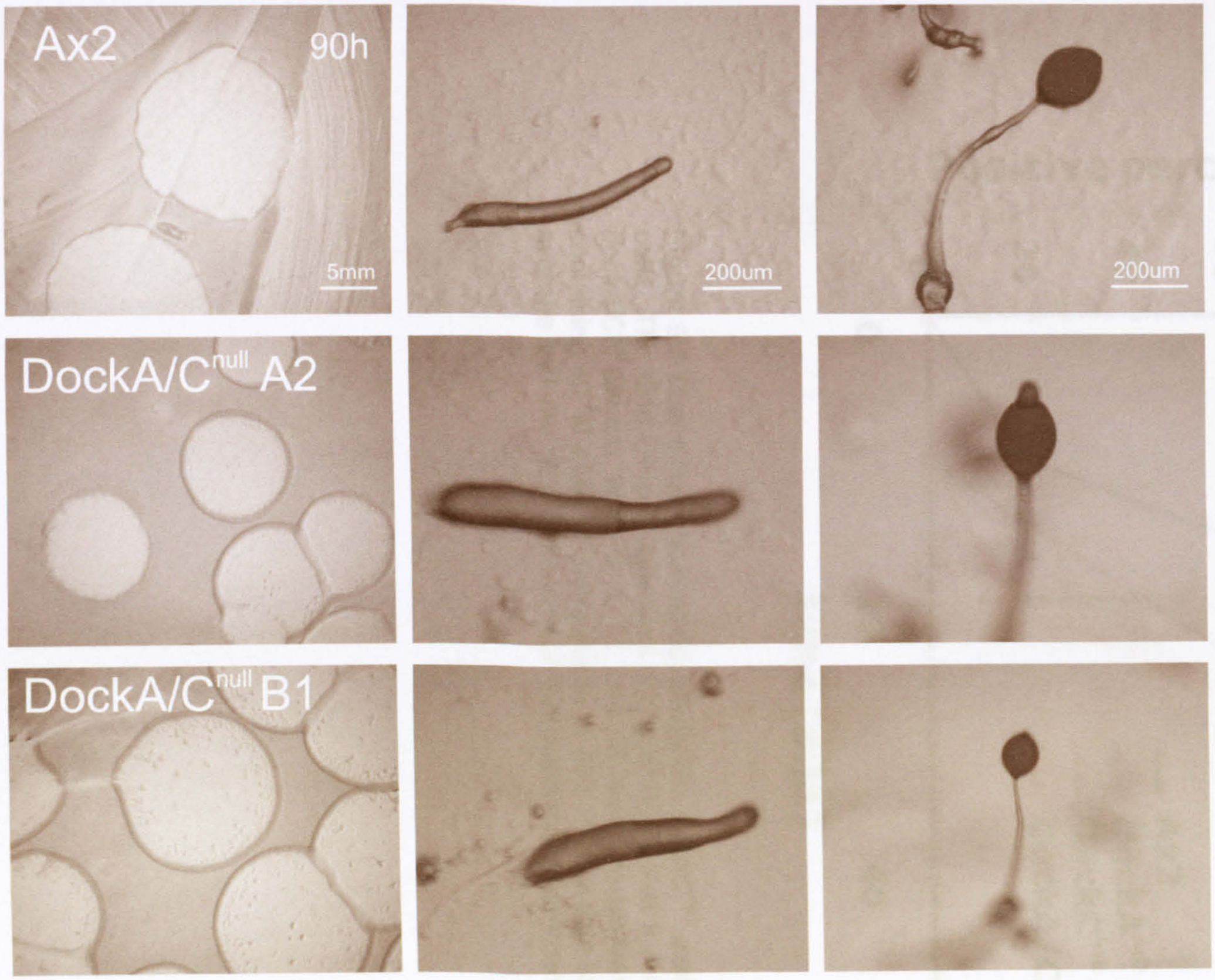

Figure 5.2 Phenotype of *dockA/C^{null}*. Knockout *dockA* in *dockC^{null}* cells did not result visible defects in development. *dockA/C^{null}* cells displayed a phenotype that was essentially the same as that of the wild type cells, including the size and shape of all the developmental structures. All the experiments were repeated more than three times on independent days.

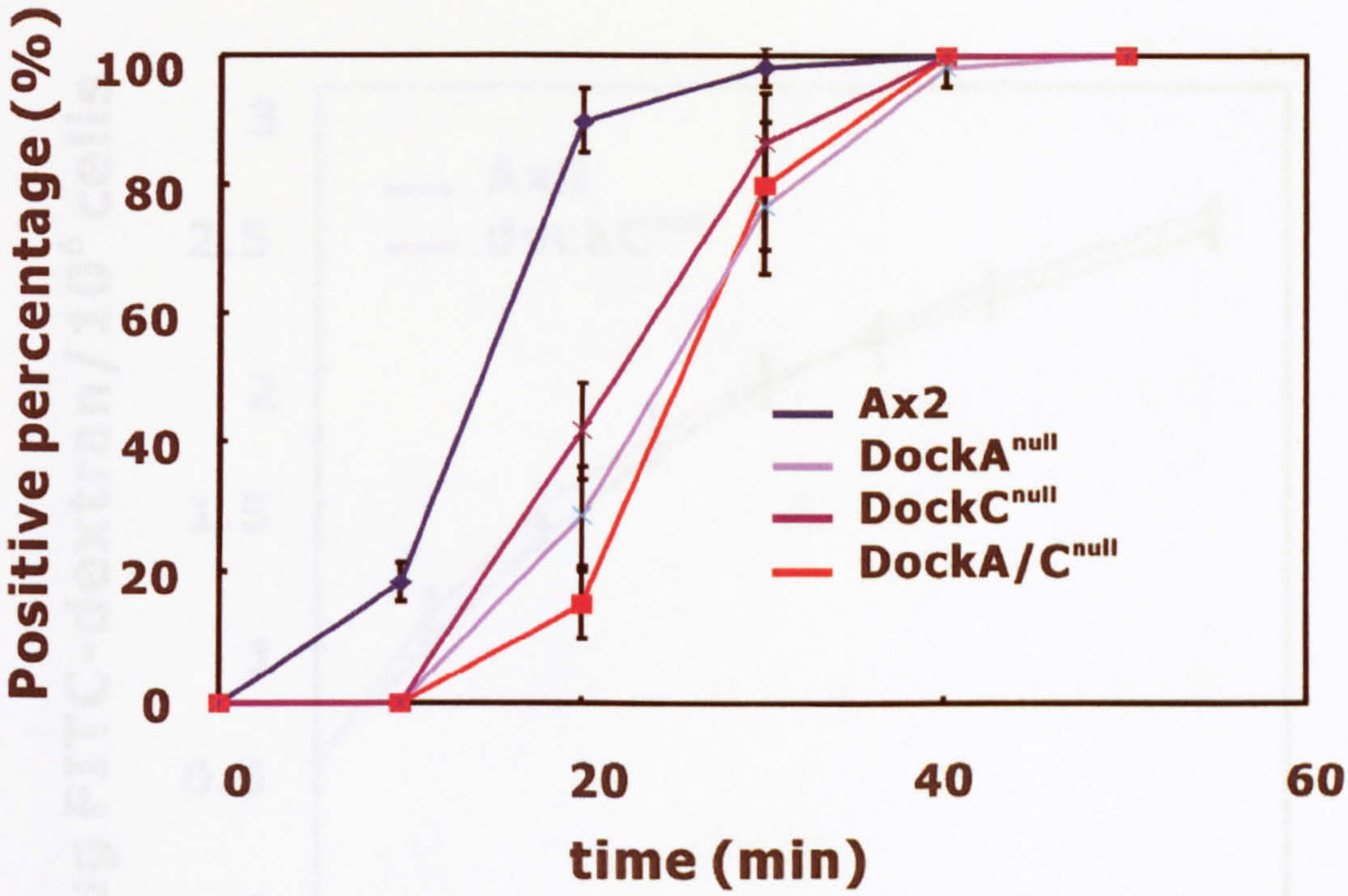

Figure 5.3 One drop chemotaxis assay for *dockC*^{null} and *dockA/C*^{null} cells. The One Drop Chemotaxis assay showed that the *dockC*^{null} and *dockA/C*^{null} strains showed a 10 and 15 delay respectively on plates containing 10^{-8}M cAMP in comparison to Ax2. These data shown are the average and standard deviations of 3 independent experiments.

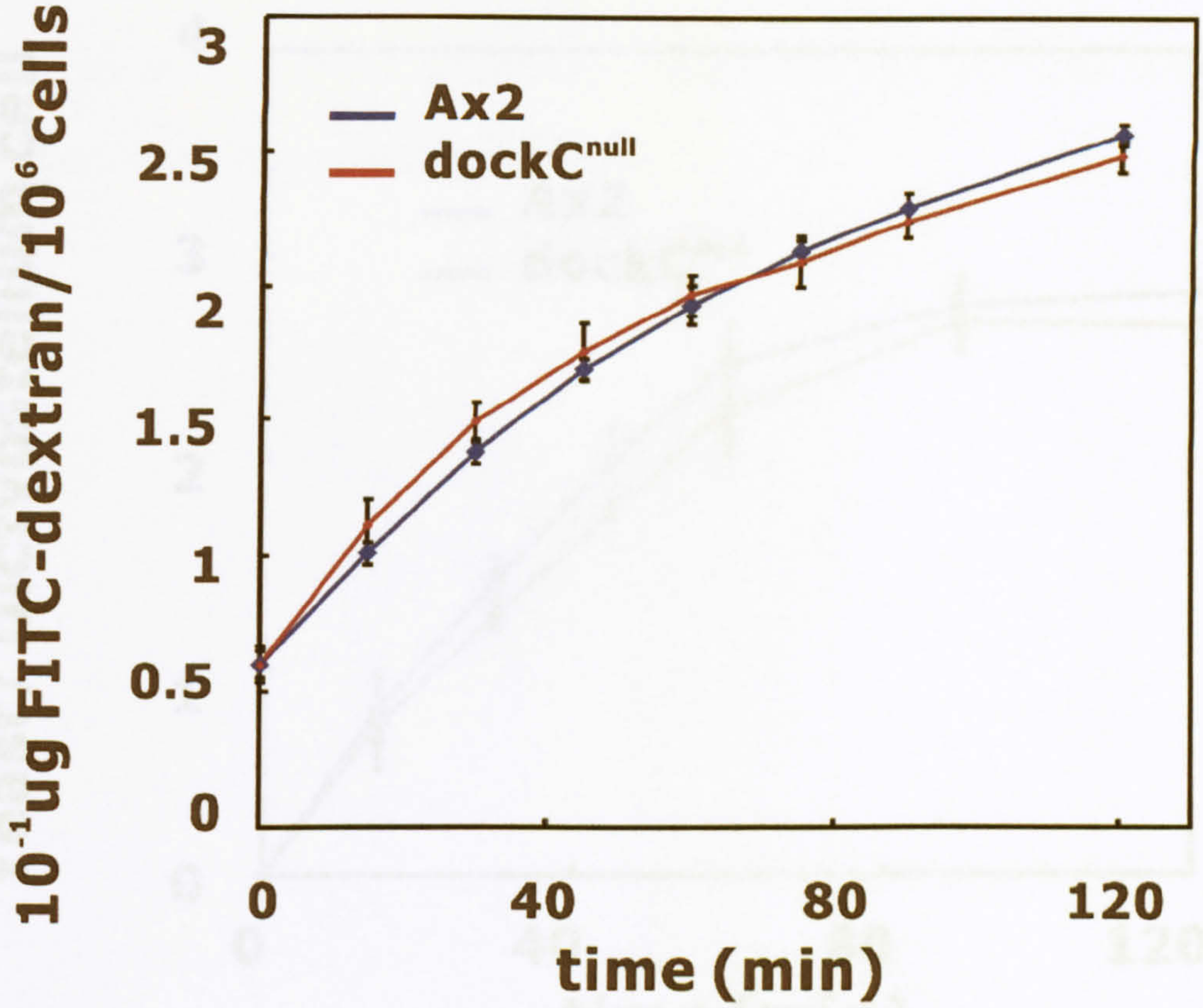

Figure 5.4 Macropinocytosis of *dockC^{null}* cells. *dockC^{null}* cells did not show a defect in macropinocytosis. These data shown are the average and standard deviations of 3 independent experiments.

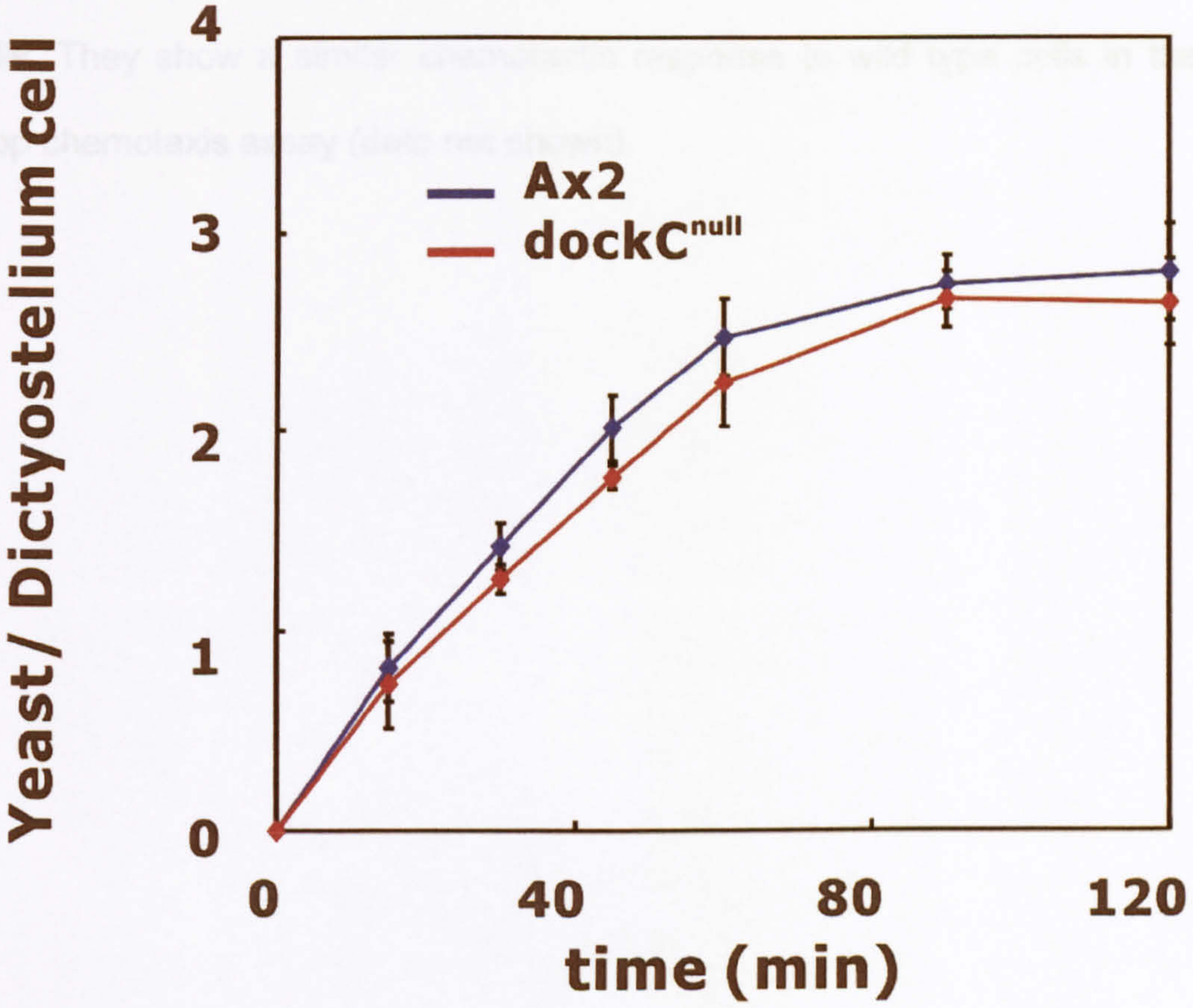

Figure 5.5 Phagocytosis of *dockC*^{null} cells. *dockC*^{null} cells did not show defect in phagocytosis with yeast. These data shown are the average and standard deviations of 3 independent experiments.

5.2.3 Phenotype of *dockD*^{null}, *dockG*^{null} *and dockH*^{null}

Knockout *dockD*, *dockG* and *dockH* did not lead to any clear defect in development. The mutant strains show similar phenotypes to wild type strains on bacterial lawns (Figure 5.6, 5.7, 5.8). They develop well on the bacterial plates without any significant morphological differences when compared to wild type cells. They show a similar chemotactic response to wild type cells in the one drop chemotaxis assay (data not shown).

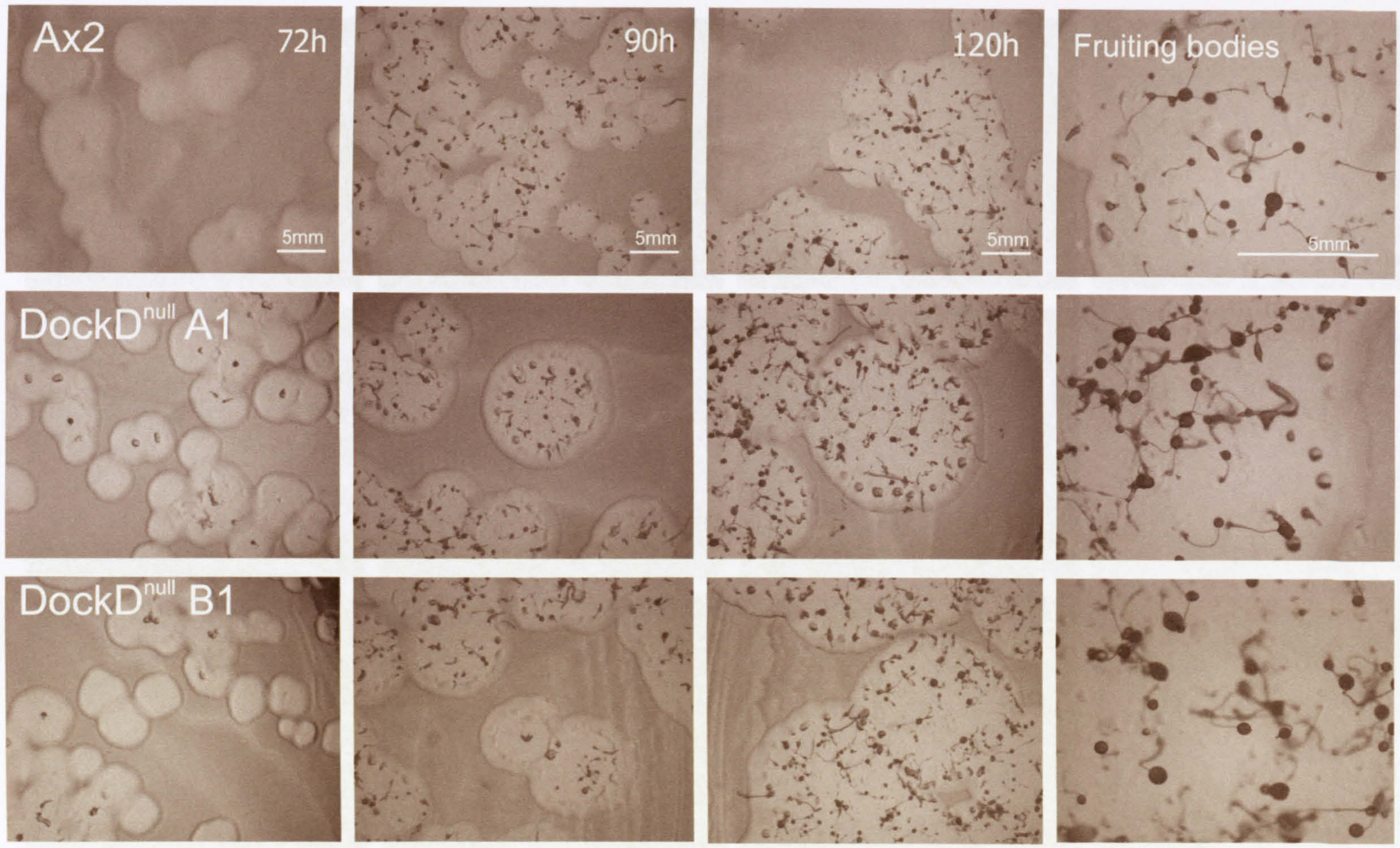

Figure 5.6 Phenotype of *dockD*^{null} cells. *dockD*^{null} cells were essentially the same as that of the wild type cells, including the size and shape of all developmental stages. All the experiments were repeated more than three

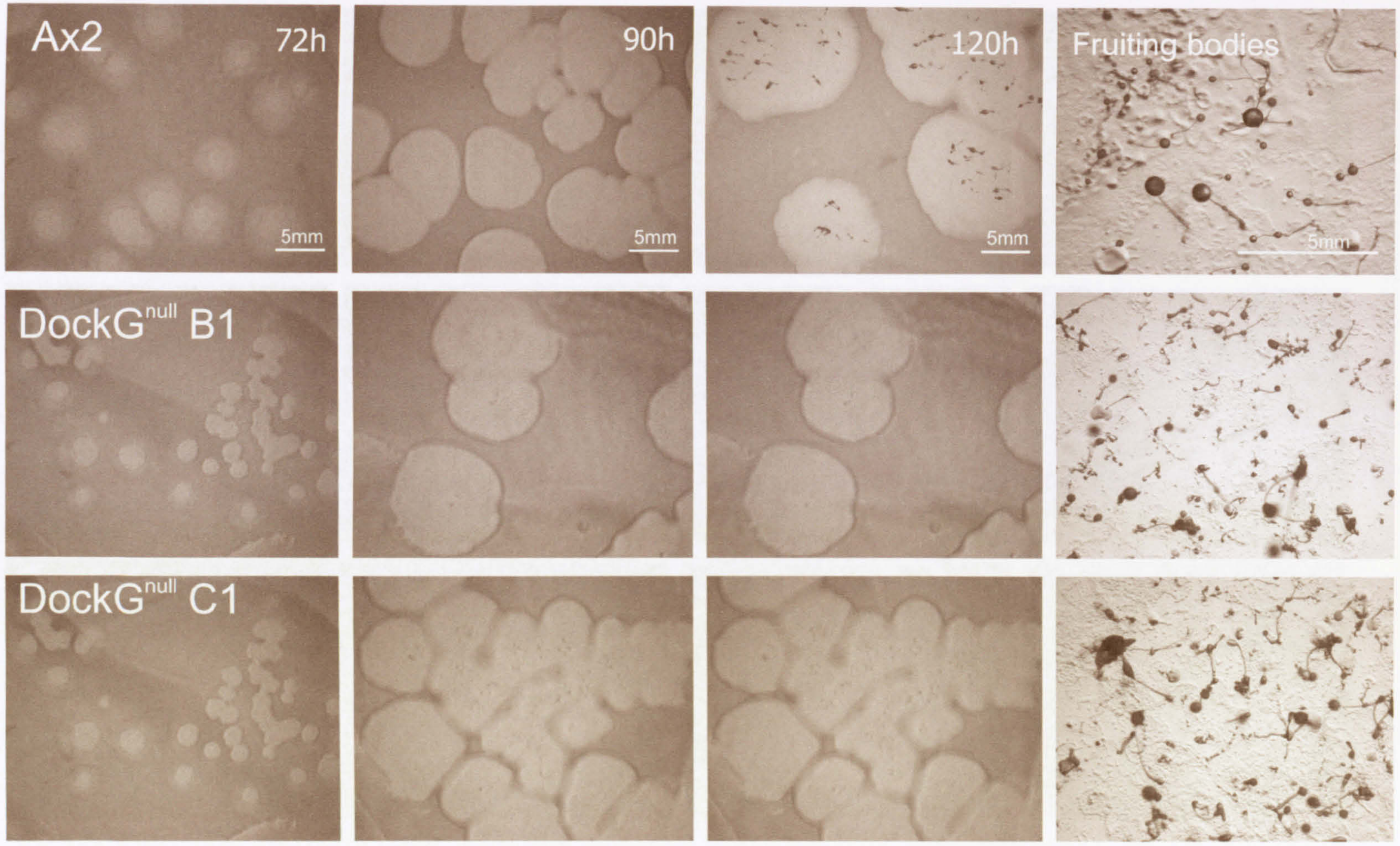

Figure 5.7 Phenotype of *dockG*^{null} cells. *dockG*^{null} cells were essentially same as that of the wild type cells, including the size and shape of all developmental stages. All the experiments were repeated more than three times

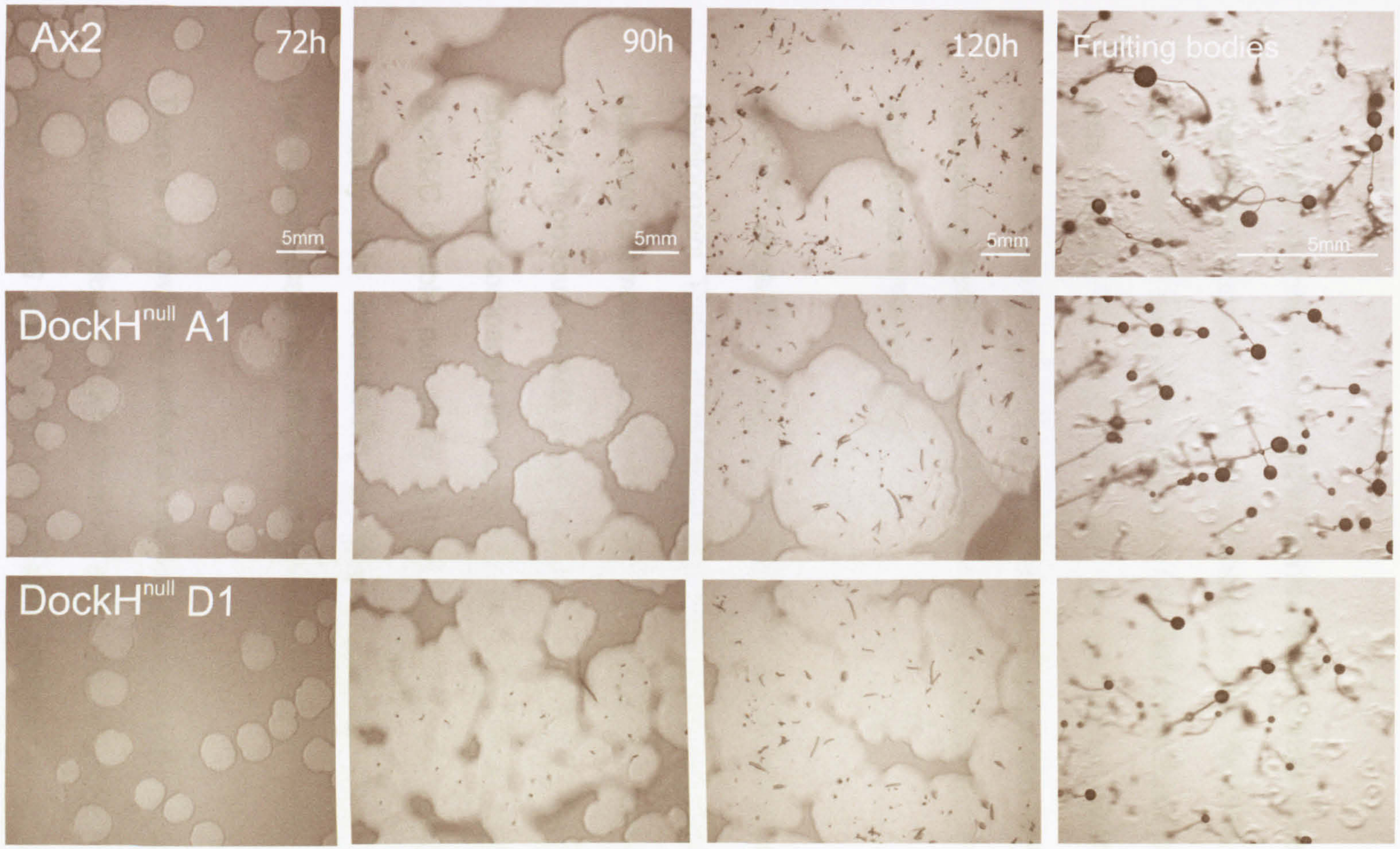

Figure 5.8 Phenotype of *dockH*^{null} cells. *dockH*^{null} cells were essentially same as that of the wild type cells, including the size and shape of all developmental stages.

5.3 Discussion

Knockout of *dockA* and *dockB* in *Dictyostelium* results in defects in endocytosis, chemotaxis and phototaxis. In combination with the PI3K inhibitor, LY294002, the *dockA/B*^{null} cells show significant reduced chemotaxis compared to wild type cells. However the *dockA/B*^{null} cells still can sense cAMP and finally migrate toward the chemotattractant. One possible explanation for this phenotype is the redundancy between *dock* genes in *D. discoideum* since there are another 6 *dock* genes in the genome.

dockC^{null}, *dockD*^{null}, *dockG*^{null} and *dockH*^{null} strains did not show clear defects in development. These strains grow at normal speed. Knockout of *dockC* results in defective chemotaxis to cAMP. Knockout of *dockA* in the *dockC*^{null} cells did not result in obvious defects in development and no significant further reduction in chemotaxis compared to *dockC*^{null} cells. We were unable to generate the *dockB/C* double null strain for unknown reasons, despite many attempts. Possibly this combination is lethal. We did not observe defects in macropinocytosis and phagocytosis for the *dockC*^{null} cells.

There is no obviously defect in chemotaxis, macropinocytosis and phagocytosis for *dockD*^{null}, *dockG*^{null}, and *dockH*^{null} cells. Thus far single mutation of the *dockC*, *dockD*, *dockG* and *dockH* has no clear phenotype. In order to have strong development defect, we may need to generate further multiple knockouts in *Dictyostelium*. Comparison of the expression profile of other *dock* genes using quantitative methods could give an indication of potential interesting *dock* genes

to knockout in *dockA/B*^{null} background. We cannot exclude the possibility that the *dockC*, *dockD*, *dockG* and *dockH* genes have other roles in the control of cell behaviour than the *dockA* and *dockB* genes'. It would be interesting to investigate the role of these *dock* genes in chemotaxis to other attractants such as folate.

Chapter VI Discussion and outlook

5.1. Role of Dock/Elmo in chemotaxis

In *Dictyostelium* inhibition of PI3K does not completely block chemotaxis; therefore there may exist several parallel signalling pathways to the actin cytoskeleton. In *Drosophila*, *C.elegans* and mouse, Docks have been shown to be involved in chemotaxis (Duchek et al., 2001; Nombela-Arrieta et al., 2004; Wu and Horvitz, 1998). We have identified 8 *dock* genes in *Dictyostelium* in this study.

Knockout of *dockA, dockB and dockC* in *Dictyostelium* results in a reduced response in chemotaxis assays to cAMP. *dockA/B*^{null} cells were greatly impaired in chemotaxis to cAMP compared to wild type cells, especially in the presence of the PI3K inhibitor LY294002. Defects were measured both in the one and two drop chemotaxis assays. The delay of the chemotactic response in the chemotaxis assays could mean that the chemotactic response is effective though cells do move more slowly. However there was no significant difference in the chemotactic response to folate between *dockA/B*^{null} cells and wildtype cells at vegetative stage. This seems to indicate that there is no intrinsic difference in the ability of the *dockA/B* mutant cells to move. To confirm this, it will be interesting to measure the speed of the random migration of the *dockA/B*^{null} cells and wild type cells. I would expect the random migrate speed of *dockA/B*^{null} is at a similar speed compare to wild type cells. Thus these data indicate that Dock mediated PI3K-independent chemotaxis signalling pathway

may exist in *Dictyostelium*. In line with our observations in *Dictyostelium* it has been reported that in mouse the PI3K inhibitor, Wortmannin, only reduced control wild type lymphocyte cell migration by 30%; however Wortmannin treatment abrogated the residual migration of Dock2-deficient cell (Nombela-Arrieta et al., 2004). In mouse Dock2 mediated efficient lymphocyte migration in a largely PI3K-independent manner, although a minor, PI3K-dependent pathway for migration exists(Nombela-Arrieta et al., 2004).

In *C.elegans*, *Drosophila* and mammalian Dock180 and its homologous has been implicated upstream of Rac activation, which then controls F-actin accumulation (Brugnera et al., 2002; Grimsley et al., 2004; Nolan et al., 1998; Wu and Horvitz, 1998). The Docker domain of Dock180 specifically recognizes nucleotide-free Rac and can mediate GTP loading of Rac *in vitro* in 293T cells (Brugnera et al., 2002). Moreover, Ced-5 (Dock180) interacts with Ced-10 (Rac) *in vitro* (Wu et al., 2001). Our collaborator Francisco Rivero has examined the possibility that *Dictyostelium* Dock interacts with Racs. We have shown DockerB interacts preferentially with the Rac1A and is bound preferentially in the nucleotide-free state; whereas DockA interacts with RacH and RacL weakly (unpublished data).

The dynamics of the actin polymerization upon chemoattractant stimulation in *dock* mutants has never been investigated before. In *Dictyostelium* chemo-attractant stimulated F-actin polymerization exhibits a biphasic response (Chen et al., 2003; Hall, 1998). There is a very brief fast large spike peak after 6 seconds and a more prolonged smaller second peak which peaks after 60 seconds. The first peak correlates with the initial cringe reaction in which the

cells round up and produce a uniform F-actin cortex. The second peak corresponds to the emergence of pseudopodia and cell movement. The first fast phase of chemoattractant-induced actin polymerization is not affected by LY294002 (Chen et al., 2003). It's intriguing that, in *dockA*^{null}, *dockB*^{null} and *dockA/B*^{null} cells both fast and prolonged peaks of actin polymerization were reduced. The analysis of CRAC localization showed that this is relatively normal in *dockA*^{null} and *dockB*^{null} cells as well as in *dockA/B*^{null} cells (data not shown). This shows that there is little effect of Dock on PIP3 production. These data clearly support the idea that Dock may be involved in a PI3K-independent signalling pathway during the cAMP induced actin polymerization.

Although *dockA/B*^{null} cells show impaired chemotaxis, the *dockA/B*^{null} cells do eventually polarize and orient toward the tip of the micropipette in needle chemotaxis assay, they display less directionality and are less elongated than wild type cells. And LY294002 did not block chemotaxis 100% in the *dockA/B*^{null} strain. This could be explained by partial functional redundancy between the *dock* genes in *D. discoideum.* It will be interesting to generate triple *dock* gene knockouts in future experiments. And we can't exclude the possibility that PI3K was not totally inhibited by LY294002 or and the existence of yet other signalling pathways.

Unexpectedly, *dockA*^{null} and *dockB*^{null} cells did not show any noticeable sorting when synergised with wild type cells. This could indicate that differences in chemotaxis are not driving sorting. The latter could be more dependent on differences in cell-cell adhesion or alternatively it might be that the differences in chemotaxis are not strong enough to result in sorting. This again has to await

further characterisation.

In other organisms Dock has been shown to regulate Rac activation and cytoskeletal reorganization through interaction with Elmo1 (Grimsley et al., 2003; Gumienny et al., 2001; Santy et al., 2005; Sanui et al., 2003). In *C.elegans* Elmo1/Ced-12 was identified as an upstream regulator of Rac that functions genetically at the same step as Dock180/Ced-5 in the engulfment of apoptotic cells and in cell migration (Brugnera et al., 2002; Gumienny et al., 2001). In mammalian fibroblasts, the Elmo1/Crk/Dock180 complex functions upstream of Rac during phagocytosis, and causes localization of Elmo1 to the membrane ruffles that are formed (Albert et al., 2000). *Dictyostelium elmo1^{null}* cells grow slowly in axenic medium, and show defects in macropinocytosis, phagocytosis, and chemotaxis. *elmo1^{null}* and *elmo1/dockB^{null}* cells have the similar phenotype to *dockB^{null}* cells. These data strongly suggest that *Dictyostelium* Elmo resemble Elmos in other organisms that work in the same signalling pathway to control the cell behaviour. However a direct interaction between Elmo1 and DockB in *D. discoideum* has yet to be established. This could be readily investigated by generating TAP-tagged constructs of these proteins *in vivo* and isolating any binding partners, or by co-immuno precipitation experiments.

How the Docks and Elmos mediate chemotaxis in *Dictyostelium* is still unknown. In mammalian cells, SH3-domain-containing adaptor protein, p130CAS (CAS), has been identified upstream of CrkII/DOCK180 (Gu et al., 2001; Kiyokawa et al., 1998b). After integrin activation, the focal adhesion kinase (FAK) becomes activated, CAS associates via its SH3 domain with proline motifs in FAK and becomes tyrosine phosphorylated, which in turn triggers the association of the

CrkII-SH2 domain with CAS and thereby the recruitment of Dock180-Elmo complex (Valles et al., 2004). Mammalian Elmo proteins contain a domain with homology to PH domains (Brugnera et al., 2002; Lu et al., 2004). Previous reports suggest that the PH domain of mammalian Elmo proteins is required to form the Elmo/Dock180/Rac trimeric complex and is essential for the Dock180-Elmo complex to function as a Rac GEF (Brugnera et al., 2002; Grimsley et al., 2003; Gumienny et al., 2001; Lu et al., 2004). It also suggests that the Elmo PH domain function is evolutionarily conserved from *C. elegans* to humans (Lu et al., 2004). However we failed to identify a PH domain in *Dictyostelium* Elmo1 protein. Moreover there is no clear CRKII homolog in *Dictyostelium* genome. Therefore it is not clear how Dictyostelium Dock/Elmo becomes recruited following engagement of surface receptors.

Recently one group reported that in LR37 cells DHR-1, which is the conserved part of the Docker domain, interacts with PI(3,4,5)P_3 *in vitro* and *in vivo*, and mediates the Dock180 signaling complex localization at sites of PI(3,4,5)P_3 accumulation in the cell's leading edge(Cote et al., 2005). In their system it seems Dock180 may work in PI3K-dependent activation. But in our hands, in presence of PI3K inhibitor, LY294002, and deletion of dockA&*B* have additive defects in chemotaxis. This data implied that both DockA&B and PI3K participate in cAMP chemotaxis in *Dictyostelium*; DockA&B involved in the PI3K parallel signaling pathway. It will be interesting to examine whether the *Dictyostelium* Docks can bind to PI(3,4,5)P_3 *in vitro*. In mouse migration to homestatic chemokines of control and Dock2 deficient T cells was almost completely abolished by pertussis toxin (PTX), a G_α inhibitor (Nombela-Arrieta et al., 2004). Dock2 play a role in heterotrimeric G-protein-dependent,

PI3K-independent manner and is the main activator of Rac in both T and B cells. Whether *Dictyostelium* Dock proteins play a role in heterotrimeric G-protein-mediated migration has not been examined.

The Rac GTPases have been implicated in actin polymerization at the leading edges of the cell, the formation of lamellipodia, and cell motility, and in Fc receptor-mediated phagocytosis (Bishop and Hall, 2000; Caron and Hall, 1998; Massol et al., 1998). Thus an important question to be addressed is whether *Dictyostelium* DockA and DockB acquire a polarized distribution responding to chemoattractant stimuli. One group has shown in LR73 cells that endogenous Dock180 translocates to the membrane in response to PI3K activation and that this can be blocked by LY294002 (Cote et al., 2005). The DHR-1 domain, which is part of the Docker domain we discussed here, is essential for the translocation (Cote et al., 2005). We expressed Docker domain GFP fusion protein (DockerA-GFP and DockerB-GFP) in wild type cells. In chemotactic cells DockerA-GFP and DockerB-GFP localized diffusely in the cytoplasm. This data suggests the localization might need other part of the Dock protein. Expression of full length Dock GFP fusion protein in *Dictyostelium* would help to discover the localization of Dock during the chemotaxis and endocytosis. It also suggests that Dock may have to form a complex with other protein such as Elmo to help its recruitment to the membrane. In LR73 cells either expression of Elmo1-GFP or Dock180-GFP alone localized primarily in the cytoplasm, while some Dock180 became localized to membrane proximal regions when co-transfected with Elmo1-GFP (Gumienny et al., 2001). Co-transfection of full length Elmo GFP with Dock GFP transfected cells would be interesting to investigate the localization of Dock/Elmo complex during the chemotaxis.

Little effect was found in *dockD*^{null}, *dockG*^{null} and *dockH*^{null} strains in cAMP mediated chemotaxis assays. Only *dockC* null cells show reduced chemotaxis to cAMP. Knockout of other *dock* genes in DockA/B^{null} background could show more severely impaired chemotaxis. Furthermore knockout of genes such as *pi3k*, *rac* in *dock* null cells will give further indications about the chemotaxis signalling pathway operative in *Dictyostelium*.

5.2. Role of Dock/Elmo in endocytosis

The Dock180-Elmo complex has been implicated in phagocytosis in C.elegans and mammalian cells (Albert et al., 2000; Gumienny et al., 2001). *Dictyostelium* *dockB*^{null} and *elmo1*^{null} cells also show significantly less phagocytic ability compared to wild type cells. Other mutants, including *dockA*^{null}, *dockC*^{null}, *dockD*^{null}, *dockG*^{null} and *dockH*^{null}, have similar rates of phagocytosis as wild type cells. It seems that *dockB* is the major determinants of phagocytosis among the Dictyostelium Dock family.

We have also shown data that disruption of both the *dockA* and *dockB* genes resulted in reduced rates of macropinocytosis. Efficient pinocytosis is important capacity for cells to grow in liquid medium (Hacker et al., 1997). *dockB*^{null} and *dockA/B*^{null} cells, which have a very strong pinocytosis defect, will be impaired in axenic growth. The *dockC*^{null}, *dockD*^{null}, *dockG*^{null} and *dockH*^{null} strains did not show defect in macropinocytosis and these cells grow at same speed as widl type cells. *elmo1*^{null} cells show similar defect in macropinocytosis to *dockB*^{null} and *dockA/B*^{null} cells.

Although it is clear that *dockA&B and elmo1* are involved in endocytosis, the detailed mechanisms by which they act are still unknown. We have expressed Rac1A in *dockB*^{null} background and shown that it very effectively rescues the phagocytosis defect (Gerti Weijer unpublished data). Whether Rac1A can rescue the defect in macropinocytosis need to be further examined.

Binding of the particle to be phagocytised to the cell surface activates an unknown signalling pathway that leads to remodelling of F-actin. This involves formation of a pseudopodial extension to engulf the particle (Cardelli, 2001). In Mammalian fibroblasts the Dock180/ Elmo1 complex functions upstream of Rac during phagocytosis, and causes localization of Dock180/Elmo1 complex from the cytoplasm to the membrane ruffles that are formed (Debakker et al., 2004). And these data suggests the specific intracellular localization of Dock180/Elmo1 enhances phagocytosis. The localization of *Dictyostelium* Dock and Elmo1 need to be further investigated. We would expect the Dock and Elmo1 will translocate from the cytoplasm to leading edge of phagocytic cup. Identification of the Interaction partners of Dock/Elmo in *Dictyostelium* will help to understand the signalling mechanism mediating endocytosis.

5.3. Other roles of Docks in the regulation of cell behaviour

Dictyostelium slugs form by aggregation of individual cells. Slugs then seek out optimal conditions for culmination by phototaxis and thermotaxis, during which the slugs move with great sensitivity towards sources of light and heat (Fisher, 1997). In *Dictyostelium* many mutants in components of the actin cytoskeleton

show defects in phototaxis (Noegel and Schleicher, 2000). We observed poor phototaxis in *dockA*^{null} slugs. There is no obvious phototaxis defect in *dockC*^{null}, *dockD*^{null}, *dockG*^{null}, *dockH*^{null} and *elmo1*^{null} strains. In the current model of the phototaxis light signal modulates the slug tip activation/inhibition system to cause slug turning by stimulating lateral shifts in the tips position (Fisher, 1997). Interestingly, *dockA* is expressed specific in the prestalk zone and tip of the culminant according to *in-situ* hybridization. The phototactic signalling pathways are complex and have not been well uncovered yet. Expression of potential DockA binding proteins, such as RacH and RacL, in *dockA*^{null} background to examine whether rescue the defect in phototaxis will help to find whether specific Rac's are involved in phototaxis signalling pathway.

Apart from chemotaxis, endocytosis and phototaxis discussed in this study of *dockA*, *dockB* and *elmo1*, it is possible that the other *dock* and *elmo* genes have other roles in the control of cell behaviour. The phenotype of these mutant cells need to be investigated in much more detail.

Abbreviations

ACA	Aggregation stage adenylyl cyclase
Arp2/3	actin-related protein 2/3
Bsr	blasticidin resistance cassette
cAMP	Cyclic adenosine 3'-5' monophosphate
cAR1-4	Dictyostelium cAMP receptor sub-types 1-4
cDNA	complementary DNA
CRAC	cytosolic regulator of adenylyl cyclase
DH	Dbl homolg domain
DMSO	dimethylsulphoxide
DNA	deoxyribonucleic acid
DNase	deoxyribonuclease
dNTP	deoxyribonucleotide triphosphate
DTT	1,4-dithiothreitol
ECL	enhanced chemiluminescence
EDTA	ethylenediaminetetraacetic acid
EGTA	ethyleneglycol-bis(2-amino-ethylene) N,N,N,N-tetraacetic acid
F-actin	Filamentous actin
GFP	Green fluorescent protein
GST	glutathione S-transferase
G-protein	Guanine nucleotide binding protein
GRP1	General Receptor for Phosphoinositides
G418	Neomycin selection marker
HEPES	N-(2-hydroxyethyl) piperazine-N.-2-ethanesulphonic acid
ISH	*In situ* hybridization
IgG	immunoglobulin G
IPTG	iso-propylthio-galactopyranoside
Kb	kilobase pairs
KD	Kilodalton
LY294002	2-(4-morpholinyl)-8-phenylchromone
Ml	Millilitres
β-ME	beta-mercaptoethanol
MOPS	Morpholinopropanesulphonic acid
mRNA	Messenger RNA
MW	molecular weight
µM	Micromolar
nM	Nanomolar
NBT	nitrobluetetrazolium
NP-40	nonylphenylpolyethyleneglyco
OD	optical density
PCR	polymerase chain reaction
PH	pleckstrin homology domain
PIPES	piperazine-N,N.-bis(2-ethanesulphonic acid)
PIP3	phosphatidyl inositol (3,4,5) tris phosphate
PI3K	Phosphatidylinositol 3-kinase
PKB	Protein kinase B
PLC	Phospholipase C

PMSF	Phenylmethylsulphonylfluoride
PTEN	Phosphatase and Tensin homolog
REMI	Restriction enzyme mediated intergation
RNA	ribonucleic acid
Rnase	Ribonuclease
Rpm	rotations per minute
SDS	sodium dodecyl sulphate
TEMED	N,N,N.,N.-tetramethyl-ethylendiamine
TRITC	tetramethylrhodamine isothiocyanate
SCAR	Suppresser of cAR
SH2/3	src homology domain 2/3
UV	ultraviolet
vol.	volume
v/v	volume by volume
w/v	weight by volume
WASP	Wiskott-Aldrich syndrome protein
X-gal	5-bromo-4-chloro-3-indolyl-D-galactopyranoside

Units of Measure

Unit	Name
°C	degree Celsius
D	Dalton
G	gram
h	hour
L	litre
m	meter
min	minute
s	sec
V	volt

References

Albert, M.L., Kim, J.I. and Birge, R.B. (2000) alphavbeta5 integrin recruits the CrkII-Dock180-rac1 complex for phagocytosis of apoptotic cells. *Nat Cell Biol*, **2**, 899-905.

Altschul, S.F., Gish, W., Miller, W., Myers, E.W. and Lipman, D.J. (1990) Basic local alignment search tool. *J Mol Biol*, **215**, 403-410.

Aoki, K., Nakamura, T., Fujikawa, K. and Matsuda, M. (2005) Local PIP3 Accumulation Recruits Vav2 and Vav3 to Activate Rac1/Cdc42 and Initiate Neurite Outgrowth in Nerve Growth Factor-stimulated PC12 Cells. *Mol Biol Cell.*

Ascough, K.R. (2004) Endocytosis: Actin in the driving seat. *Curr Biol*, **14**, R124-126.

Bailly, M., Macaluso, F., Cammer, M., Chan, A., Segall, J.E. and Condeelis, J.S. (1999) Relationship between Arp2/3 complex and the barbed ends of actin filaments at the leading edge of carcinoma cells after epidermal growth factor stimulation. *J Cell Biol*, **145**, 331-345.

Bear, J.E., Rawls, J.F. and Saxe, C.L., 3rd. (1998) SCAR, a WASP-related protein, isolated as a suppressor of receptor defects in late Dictyostelium development. *J Cell Biol*, **142**, 1325-1335.

Bernstein, R.L., Rossier, C., van Driel, R., Brunner, M. and Gerisch, G. (1981) Folate deaminase and cyclic AMP phosphodiesterase in Dictyostelium discoideum: their regulation by extracellular cyclic AMP and folic acid. *Cell Differ*, **10**, 79-86.

Bishop, A.L. and Hall, A. (2000) Rho GTPases and their effector proteins. *Biochem J*, **348 Pt 2**, 241-255.

Blagg, S.L., Stewart, M., Sambles, C. and Insall, R.H. (2003) PIR121 regulates pseudopod dynamics and SCAR activity in Dictyostelium. *Curr Biol*, **13**, 1480-1487.

Bokoch, G.M. (2005) Regulation of innate immunity by Rho GTPases. *Trends Cell Biol*, **15**, 163-171.

Braga, V.M. (2002) GEF without a Dbl domain? *Nat Cell Biol*, **4**, E188-190.

Brugnera, E., Haney, L., Grimsley, C., Lu, M., Walk, S.F., Tosello-Trampont, A.C., Macara, I.G., Madhani, H., Fink, G.R. and Ravichandran, K.S. (2002) Unconventional Rac-GEF activity is mediated through the Dock180-ELMO complex. *Nat Cell Biol*, **4**, 574-582.

Buczynski, G., Grove, B., Nomura, A., Kleve, M., Bush, J., Firtel, R.A. and Cardelli, J. (1997) Inactivation of two Dictyostelium discoideum genes, DdPIK1 and DdPIK2, encoding proteins related to mammalian phosphatidylinositide 3-kinases, results in defects in endocytosis, lysosome to postlysosome transport, and actin cytoskeleton organization. *J Cell Biol*, **136**, 1271-1286.

Cardelli, J. (2001) Phagocytosis and macropinocytosis in Dictyostelium: phosphoinositide-based processes, biochemically distinct. *Traffic*, **2**, 311-320.

Caron, E. and Hall, A. (1998) Identification of two distinct mechanisms of phagocytosis controlled by different Rho GTPases. *Science*, **282**, 1717-1721.

Chen, L., Janetopoulos, C., Huang, Y.E., Iijima, M., Borleis, J. and Devreotes, P.N. (2003) Two Phases of Actin Polymerization Display Different Dependences on PI(3,4,5)P3 Accumulation and Have Unique Roles during Chemotaxis. *Mol Biol Cell.*

Cheresh, D.A., Leng, J. and Klemke, R.L. (1999) Regulation of cell contraction and membrane ruffling by distinct signals in migratory cells. *J Cell Biol*, **146**, 1107-1116.

Chimini, G. and Chavrier, P. (2000) Function of Rho family proteins in actin dynamics during phagocytosis and engulfment. *Nat Cell Biol*, **2**, E191-196.

Chisholm, R.L. and Firtel, R.A. (2004) Insights into morphogenesis from a simple developmental system. *Nat Rev Mol Cell Biol*, **5**, 531-541.

Chung, C.Y., Funamoto, S. and Firtel, R.A. (2001) Signaling pathways controlling cell polarity and chemotaxis. *Trends Biochem Sci*, **26**, 557-566.

Comer, F.I., Lippincott, C.K., Masbad, J.J. and Parent, C.A. (2005) The PI3K-Mediated Activation of CRAC Independently Regulates Adenylyl Cyclase Activation and Chemotaxis. *Curr Biol*, **15**, 134-139.

Condeelis, J. (1990) Molecular analysis of amoeboid chemotaxis. *Cancer Invest*, **8**, 659-660.

Condeelis, J., Hall, A., Bresnick, A., Warren, V., Hock, R., Bennett, H. and Ogihara, S. (1988) Actin polymerization and pseudopod extension during amoeboid chemotaxis. *Cell Motil Cytoskeleton*, **10**, 77-90.

Cote, J.F., Motoyama, A.B., Bush, J.A. and Vuori, K. (2005) A novel and evolutionarily conserved PtdIns(3,4,5)P(3)-binding domain is necessary for DOCK180 signalling. *Nat Cell Biol.*

Cote, J.F. and Vuori, K. (2002) Identification of an evolutionarily conserved superfamily of DOCK180-related proteins with guanine nucleotide exchange activity. *J Cell Sci*, **115**, 4901-4913.

de Hostos, E.L., Rehfuess, C., Bradtke, B., Waddell, D.R., Albrecht, R., Murphy, J. and Gerisch, G. (1993) Dictyostelium mutants lacking the cytoskeletal protein coronin are defective in cytokinesis and cell motility. *J Cell Biol*, **120**, 163-173.

de Oliveira, C.A. and Mantovani, B. (1988) Latrunculin A is a potent inhibitor of phagocytosis by macrophages. *Life Sci*, **43**, 1825-1830.

Debakker, C.D., Haney, L.B., Kinchen, J.M., Grimsley, C., Lu, M., Klingele, D., Hsu, P.K., Chou, B.K., Cheng, L.C., Blangy, A., Sondek, J., Hengartner, M.O., Wu, Y.C. and Ravichandran, K.S. (2004) Phagocytosis of Apoptotic Cells Is Regulated by a UNC-73/TRIO-MIG-2/RhoG Signaling Module and Armadillo Repeats of CED-12/ELMO. *Curr Biol*, **14**, 2208-2216.

Devreotes, P.N. and Zigmond, S.H. (1988) Chemotaxis in eukaryotic cells: a focus on leukocytes and Dictyostelium. *Annu Rev Cell Biol*, **4**, 649-686.

Dolfi, F., Garcia-Guzman, M., Ojaniemi, M., Nakamura, H., Matsuda, M. and Vuori, K. (1998) The adaptor protein Crk connects multiple cellular stimuli to the JNK signaling pathway. *Proc Natl Acad Sci U S A*, **95**, 15394-15399.

Dormann, D., Weijer, G., Dowler, S. and Weijer, C.J. (2004) In vivo analysis of 3-phosphoinositide dynamics during Dictyostelium phagocytosis and chemotaxis. *J Cell Sci*, **117**, 6497-6509.

Dormann, D., Weijer, G., Parent, C.A., Devreotes, P.N. and Weijer, C.J. (2002) Visualizing PI3 kinase-mediated cell-cell signaling during Dictyostelium development. *Curr Biol*, **12**, 1178-1188.

Duchek, P., Somogyi, K., Jekely, G., Beccari, S. and Rorth, P. (2001) Guidance of cell migration by the Drosophila PDGF/VEGF receptor. *Cell*, **107**, 17-26.

Dumontier, M., Hocht, P., Mintert, U. and Faix, J. (2000) Rac1 GTPases control filopodia formation, cell motility, endocytosis, cytokinesis and development in Dictyostelium. *J Cell Sci*, **113 (Pt 12)**, 2253-2265.

Eden, S., Rohatgi, R., Podtelejnikov, A.V., Mann, M. and Kirschner, M.W. (2002) Mechanism of regulation of WAVE1-induced actin nucleation by Rac1 and Nck. *Nature*, **418**, 790-793.

Egelhoff, T.T. and Spudich, J.A. (1991) Molecular genetics of cell migration: Dictyostelium as a model system. *Trends Genet*, **7**, 161-166.

Eichinger, L., Pachebat, J.A., Glockner, G., Rajandream, M.A., Sucgang, R., Berriman, M., Song, J., Olsen, R., Szafranski, K., Xu, Q., Tunggal, B., Kummerfeld, S., Madera, M., Konfortov, B.A., Rivero, F., Bankier, A.T., Lehmann, R., Hamlin, N., Davies, R., Gaudet, P., Fey, P., Pilcher, K., Chen, G., Saunders, D., Sodergren, E., Davis, P., Kerhornou, A., Nie, X., Hall, N., Anjard, C., Hemphill, L., Bason, N., Farbrother, P., Desany, B., Just, E., Morio, T., Rost, R., Churcher, C., Cooper, J., Haydock, S., van Driessche, N., Cronin, A., Goodhead, I., Muzny, D., Mourier, T., Pain, A., Lu, M., Harper, D., Lindsay, R., Hauser, H., James, K., Quiles, M., Madan Babu, M., Saito, T., Buchrieser, C., Wardroper, A., Felder, M., Thangavelu, M., Johnson, D., Knights, A., Loulseged, H., Mungall, K., Oliver, K., Price, C., Quail, M.A., Urushihara, H., Hernandez, J., Rabbinowitsch, E., Steffen, D., Sanders, M., Ma, J., Kohara, Y., Sharp, S., Simmonds, M., Spiegler, S., Tivey, A., Sugano, S., White, B., Walker, D., Woodward, J., Winckler, T., Tanaka, Y., Shaulsky, G., Schleicher, M., Weinstock, G., Rosenthal, A., Cox, E.C., Chisholm, R.L., Gibbs, R., Loomis, W.F., Platzer, M., Kay, R.R., Williams, J., Dear, P.H., Noegel, A.A., Barrell, B. and Kuspa, A. (2005) The genome of the social amoeba Dictyostelium discoideum. *Nature*, **435**, 43-57.

Ellis, R.E., Jacobson, D.M. and Horvitz, H.R. (1991) Genes required for the engulfment of cell corpses during programmed cell death in Caenorhabditis elegans. *Genetics*, **129**, 79-94.

Engqvist-Goldstein, A.E. and Drubin, D.G. (2003) Actin assembly and endocytosis: from yeast to mammals. *Annu Rev Cell Dev Biol*, **19**, 287-332.

Erickson, M.R., Galletta, B.J. and Abmayr, S.M. (1997) Drosophila myoblast city encodes a conserved protein that is essential for myoblast fusion, dorsal closure, and cytoskeletal organization. *J Cell Biol*, **138**, 589-603.

Etienne-Manneville, S. and Hall, A. (2002) Rho GTPases in cell biology. *Nature*, **420**, 629-635.

Faix, J., Kreppel, L., Shaulsky, G., Schleicher, M. and Kimmel, A.R. (2004) A rapid and efficient method to generate multiple gene disruptions in Dictyostelium discoideum using a single selectable marker and the Cre-loxP system. *Nucleic Acids Res*, **32**, e143.

Firtel, R.A. and Chung, C.Y. (2000) The molecular genetics of chemotaxis: sensing and responding to chemoattractant gradients. *Bioessays*, **22**, 603-615.

Fisher, P.R. (1997) Genetics of phototaxis in a model eukaryote, Dictyostelium discoideum. *Bioessays*, **19**, 397-407.

Fisher, P.R., Noegel, A.A., Fechheimer, M., Rivero, F., Prassler, J. and Gerisch, G. (1997) Photosensory and thermosensory responses in Dictyostelium slugs are specifically impaired by absence of the F-actin cross-linking gelation factor (ABP-120). *Curr Biol*, **7**, 889-892.

Fisher, P.R., Smith, E. and Williams, K.L. (1981) An extracellular chemical signal controlling phototactic behavior by D. discoideum slugs. *Cell*, **23**, 799-807.

Fukui, Y., Hashimoto, O., Sanui, T., Oono, T., Koga, H., Abe, M., Inayoshi, A., Noda, M., Oike, M., Shirai, T. and Sasazuki, T. (2001) Haematopoietic cell-specific CDM family protein DOCK2 is essential for lymphocyte migration. *Nature*, **412**, 826-831.

Funamoto, S., Meili, R., Lee, S., Parry, L. and Firtel, R.A. (2002) Spatial and temporal regulation of 3-phosphoinositides by PI 3-kinase and PTEN mediates chemotaxis. *Cell*, **109**, 611-623.

Funamoto, S., Milan, K., Meili, R. and Firtel, R.A. (2001) Role of phosphatidylinositol 3' kinase and a downstream pleckstrin homology domain-containing protein in controlling chemotaxis in dictyostelium. *J Cell Biol*, **153**, 795-810.

Gardiner, E.M., Pestonjamasp, K.N., Bohl, B.P., Chamberlain, C., Hahn, K.M. and Bokoch, G.M. (2002) Spatial and temporal analysis of Rac activation during live neutrophil chemotaxis. *Curr Biol*, **12**, 2029-2034.

Gerisch, G., Hulser, D., Malchow, D. and Wick, U. (1975) Cell communication by periodic cyclic-AMP pulses. *Philos Trans R Soc Lond B Biol Sci*, **272**, 181-192.

Glotzer, M. (2005) The molecular requirements for cytokinesis. *Science*, **307**, 1735-1739.

Grimsley, C.M., Kinchen, J.M., Tosello-Trampont, A.C., Brugnera, E., Haney, L.B., Lu, M., Chen, Q., Klingele, D., Hengartner, M.O. and Ravichandran, K.S. (2004) Dock180 and ELMO1 proteins cooperate to promote evolutionarily conserved Rac-dependent cell migration. *J Biol Chem*, **279**, 6087-6097.

Grimsley, C.M., Kinchen, J.M., Tosello-Trampont, A.C., Brugnera, E., Haney, L.B., Lu, M., Chen, Q., Schubert, D., Klingele, D., Hengartner, M.O. and Ravichandran, K.S. (2003) Dock180 and ELMO1 proteins cooperate to promote evolutionarily conserved Rac-dependent cell migration. *J Biol Chem*.

Gu, J., Sumida, Y., Sanzen, N. and Sekiguchi, K. (2001) Laminin-10/11 and fibronectin differentially regulate integrin-dependent Rho and Rac activation via p130(Cas)-CrkII-DOCK180 pathway. *J Biol Chem*, **276**, 27090-27097.

Gumienny, T.L., Brugnera, E., Tosello-Trampont, A.C., Kinchen, J.M., Haney, L.B., Nishiwaki, K., Walk, S.F., Nemergut, M.E., Macara, I.G., Francis, R., Schedl, T., Qin, Y., Van Aelst, L., Hengartner, M.O. and Ravichandran, K.S. (2001) CED-12/ELMO, a novel member of the CrkII/Dock180/Rac pathway, is required for phagocytosis and cell migration. *Cell*, **107**, 27-41.

Hacker, U., Albrecht, R. and Maniak, M. (1997) Fluid-phase uptake by macropinocytosis in Dictyostelium. *J Cell Sci*, **110 (Pt 2)**, 105-112.

Hall, A. (1998) Rho GTPases and the actin cytoskeleton. *Science*, **279**, 509-514.

Hedgecock, E.M., Sulston, J.E. and Thomson, J.N. (1983) Mutations affecting programmed cell deaths in the nematode Caenorhabditis elegans. *Science*, **220**, 1277-1279.

Higgs, H.N. and Pollard, T.D. (2001) Regulation of actin filament network formation through ARP2/3 complex: activation by a diverse array of proteins. *Annu Rev Biochem*, **70**, 649-676.

Hirsch, E., Katanaev, V.L., Garlanda, C., Azzolino, O., Pirola, L., Silengo, L., Sozzani, S., Mantovani, A., Altruda, F. and Wymann, M.P. (2000) Central role for G protein-coupled phosphoinositide 3-kinase gamma in inflammation. *Science*, **287**, 1049-1053.

Hoppe, A.D. and Swanson, J.A. (2004) Cdc42, Rac1, and Rac2 display distinct patterns of activation during phagocytosis. *Mol Biol Cell*, **15**, 3509-3519.

Huang, Y.E., Iijima, M., Parent, C.A., Funamoto, S., Firtel, R.A. and Devreotes, P. (2003) Receptor-mediated Regulation of PI3Ks Confines PI(3,4,5)P3 to the Leading Edge of Chemotaxing Cells. *Mol Biol Cell*, **14**, 1913-1922.

Iijima, M. and Devreotes, P. (2002) Tumor suppressor PTEN mediates sensing of chemoattractant gradients. *Cell*, **109**, 599-610.

Iijima, M., Huang, Y.E. and Devreotes, P. (2002) Temporal and spatial regulation of chemotaxis. *Dev Cell*, **3**, 469-478.

Janardhan, A., Swigut, T., Hill, B., Myers, M.P. and Skowronski, J. (2004) HIV-1 Nef Binds the DOCK2-ELMO1 Complex to Activate Rac and Inhibit Lymphocyte Chemotaxis. *PLoS Biol*, **2**, E6.

Jin, T., Amzel, M., Devreotes, P.N. and Wu, L. (1998) Selection of gbeta subunits with point mutations that fail to activate specific signaling pathways in vivo: dissecting cellular responses mediated by a heterotrimeric G protein in Dictyostelium discoideum. *Mol Biol Cell*, **9**, 2949-2961.

Jin, T., Zhang, N., Long, Y., Parent, C.A. and Devreotes, P.N. (2000) Localization of the G protein betagamma complex in living cells during chemotaxis. *Science*, **287**, 1034-1036.

Jones, G.E., Allen, W.E. and Ridley, A.J. (1998) The Rho GTPases in macrophage motility and chemotaxis. *Cell Adhes Commun*, **6**, 237-245.

Katanaev, V.L. (2001) Signal transduction in neutrophil chemotaxis. *Biochemistry (Mosc)*, **66**, 351-368.

Kim, C., Marchal, C.C., Penninger, J. and Dinauer, M.C. (2003) The hemopoietic Rho/Rac guanine nucleotide exchange factor Vav1 regulates N-formyl-methionyl-leucyl-phenylalanine-activated neutrophil functions. *J Immunol*, **171**, 4425-4430.

Kim, J.Y., Caterina, M.J., Milne, J.L., Lin, K.C., Borleis, J.A. and Devreotes, P.N. (1997) Random

mutagenesis of the cAMP chemoattractant receptor, cAR1, of Dictyostelium. Mutant classes that cause discrete shifts in agonist affinity and lock the receptor in a novel activational intermediate. *J Biol Chem*, **272**, 2060-2068.

Kimble, J. (1981) Alterations in cell lineage following laser ablation of cells in the somatic gonad of Caenorhabditis elegans. *Dev Biol*, **87**, 286-300.

Kiyokawa, E., Hashimoto, Y., Kobayashi, S., Sugimura, H., Kurata, T. and Matsuda, M. (1998a) Activation of Rac1 by a Crk SH3-binding protein, DOCK180. *Genes Dev*, **12**, 3331-3336.

Kiyokawa, E., Hashimoto, Y., Kurata, T., Sugimura, H. and Matsuda, M. (1998b) Evidence that DOCK180 up-regulates signals from the CrkII-p130(Cas) complex. *J Biol Chem*, **273**, 24479-24484.

Kozma, R., Ahmed, S., Best, A. and Lim, L. (1995) The Ras-related protein Cdc42Hs and bradykinin promote formation of peripheral actin microspikes and filopodia in Swiss 3T3 fibroblasts. *Mol Cell Biol*, **15**, 1942-1952.

Kriebel, P.W., Barr, V.A. and Parent, C.A. (2003) Adenylyl cyclase localization regulates streaming during chemotaxis. *Cell*, **112**, 549-560.

Krishnan, J. and Iglesias, P.A. (2004) A modeling framework describing the enzyme regulation of membrane lipids underlying gradient perception in Dictyostelium cells. *J Theor Biol*, **229**, 85-99.

Kuspa, A. and Loomis, W.F. (1992) Tagging developmental genes in Dictyostelium by restriction enzyme-mediated integration of plasmid DNA. *Proc Natl Acad Sci U S A*, **89**, 8803-8807.

Lee, E., Seastone, D.J., Harris, E., Cardelli, J.A. and Knecht, D.A. (2003) RacB regulates cytoskeletal function in Dictyostelium spp. *Eukaryot Cell*, **2**, 474-485.

Lemmon, M.A., Ferguson, K.M. and Abrams, C.S. (2002) Pleckstrin homology domains and the cytoskeleton. *FEBS Lett*, **513**, 71-76.

Li, Z., Hannigan, M., Mo, Z., Liu, B., Lu, W., Wu, Y., Smrcka, A.V., Wu, G., Li, L., Liu, M., Huang, C.K. and Wu, D. (2003) Directional sensing requires G beta gamma-mediated PAK1 and PIX alpha-dependent activation of Cdc42. *Cell*, **114**, 215-227.

Lim, M.A., Yang, L., Zheng, Y., Wu, H., Dong, L.Q. and Liu, F. (2004) Roles of PDK-1 and PKN in regulating cell migration and cortical actin formation of PTEN-knockout cells. *Oncogene*, **23**, 9348-9358.

Lu, M., Kinchen, J.M., Rossman, K.L., Grimsley, C., DeBakker, C., Brugnera, E., Tosello-Trampont, A.C., Haney, L.B., Klingele, D., Sondek, J., Hengartner, M.O. and Ravichandran, K.S. (2004) PH domain of ELMO functions in trans to regulate Rac activation via Dock180. *Nat Struct Mol Biol*.

Lu, M., Kinchen, J.M., Rossman, K.L., Grimsley, C., Hall, M., Sondek, J., Hengartner, M.O., Yajnik, V. and Ravichandran, K.S. (2005) A Steric-Inhibition Model for Regulation of Nucleotide Exchange via the Dock180 Family of GEFs. *Curr Biol*, **15**, 371-377.

Machesky, L.M. and Insall, R.H. (1998) Scar1 and the related Wiskott-Aldrich syndrome protein, WASP, regulate the actin cytoskeleton through the Arp2/3 complex. *Curr Biol*, **8**, 1347-1356.

Maehama, T. and Dixon, J.E. (1998) The tumor suppressor, PTEN/MMAC1, dephosphorylates the lipid second messenger, phosphatidylinositol 3,4,5-trisphosphate. *J Biol Chem*, **273**, 13375-13378.

Maghazachi, A.A. (2003) G protein-coupled receptors in natural killer cells. *J Leukoc Biol*, **74**, 16-24.

Manahan, C.L., Iglesias, P.A., Long, Y. and Devreotes, P.N. (2004) Chemoattractant signaling in dictyostelium discoideum. *Annu Rev Cell Dev Biol*, **20**, 223-253.

Maniak, M. (2001) Fluid-phase uptake and transit in axenic Dictyostelium cells. *Biochim Biophys Acta*, **1525**, 197-204.

Maniak, M. (2002) Conserved features of endocytosis in Dictyostelium. *Int Rev Cytol*, **221**, 257-287.

Marchler-Bauer, A. and Bryant, S.H. (2004) CD-Search: protein domain annotations on the fly. *Nucleic Acids Res*, **32**, W327-331.

Massol, P., Montcourrier, P., Guillemot, J.C. and Chavrier, P. (1998) Fc receptor-mediated phagocytosis requires CDC42 and Rac1. *Embo J*, **17**, 6219-6229.

May, R.C., Caron, E., Hall, A. and Machesky, L.M. (2000) Involvement of the Arp2/3 complex in phagocytosis mediated by FcgammaR or CR3. *Nat Cell Biol*, **2**, 246-248.

May, R.C. and Machesky, L.M. (2001) Phagocytosis and the actin cytoskeleton. *J Cell Sci*, **114**, 1061-1077.

Meili, R., Ellsworth, C., Lee, S., Reddy, T.B., Ma, H. and Firtel, R.A. (1999) Chemoattractant-mediated transient activation and membrane localization of Akt/PKB is required for efficient chemotaxis to cAMP in Dictyostelium. *Embo J*, **18**, 2092-2105.

Meller, N., Irani-Tehrani, M., Ratnikov, B.I., Paschal, B.M. and Schwartz, M.A. (2004) The novel Cdc42 guanine nucleotide exchange factor, zizimin1, dimerizes via the Cdc42-binding CZH2 domain. *J Biol Chem*.

Miki, H., Suetsugu, S. and Takenawa, T. (1998) WAVE, a novel WASP-family protein involved in actin reorganization induced by Rac. *Embo J*, **17**, 6932-6941.

Miura, K. and Siegert, F. (2000) Light affects cAMP signaling and cell movement activity in Dictyostelium discoideum. *Proc Natl Acad Sci U S A*, **97**, 2111-2116.

Moon, S.Y. and Zheng, Y. (2003) Rho GTPase-activating proteins in cell regulation. *Trends Cell Biol*, **13**, 13-22.

Myers, M.P., Pass, I., Batty, I.H., Van der Kaay, J., Stolarov, J.P., Hemmings, B.A., Wigler, M.H., Downes, C.P. and Tonks, N.K. (1998) The lipid phosphatase activity of PTEN is critical for its tumor supressor function. *Proc Natl Acad Sci U S A*, **95**, 13513-13518.

Nellen, W., Datta, S., Reymond, C., Sivertsen, A., Mann, S., Crowley, T. and Firtel, R.A. (1987) Molecular biology in Dictyostelium: tools and applications. *Methods Cell Biol*, **28**, 67-100.

Neuhaus, E.M. and Soldati, T. (1999) Molecular mechanisms of membrane trafficking. What do we learn from Dictyostelium discoideum? *Protist*, **150**, 235-243.

Nishikimi, A., Meller, N., Uekawa, N., Isobe, K., Schwartz, M.A. and Maruyama, M. (2005) Zizimin2: a novel, DOCK180-related Cdc42 guanine nucleotide exchange factor expressed predominantly in lymphocytes. *FEBS Lett*, **579**, 1039-1046.

Nobes, C.D. and Hall, A. (1995) Rho, rac, and cdc42 GTPases regulate the assembly of multimolecular focal complexes associated with actin stress fibers, lamellipodia, and filopodia. *Cell*, **81**, 53-62.

Noegel, A.A., Blau-Wasser, R., Sultana, H., Muller, R., Israel, L., Schleicher, M., Patel, H. and Weijer, C.J. (2004) The cyclase-associated protein CAP as regulator of cell polarity and cAMP signaling in Dictyostelium. *Mol Biol Cell*, **15**, 934-945.

Noegel, A.A. and Schleicher, M. (2000) The actin cytoskeleton of Dictyostelium: a story told by mutants. *J Cell Sci*, **113 (Pt 5)**, 759-766.

Nolan, K.M., Barrett, K., Lu, Y., Hu, K.Q., *Vincent, S. and Settleman, J. (1998) Myoblast city, the* Drosophila homolog of DOCK180/CED-5, is required in a Rac signaling pathway utilized for multiple developmental processes. *Genes Dev*, **12**, 3337-3342.

Nombela-Arrieta, C., Lacalle, R.A., Montoya, M.C., Kunisaki, Y., Megias, D., Marques, M., Carrera, A.C., Manes, S., Fukui, Y., Martinez, A.C. and Stein, J.V. (2004) Differential requirements for DOCK2 and phosphoinositide-3-kinase gamma during T and B lymphocyte homing. *Immunity*, **21**, 429-441.

Palmieri, S.J., Nebl, T., Pope, R.K., Seastone, D.J., Lee, E., Hinchcliffe, E.H., Sluder, G., Knecht, D., Cardelli, J. and Luna, E.J. (2000) Mutant Rac1B expression in Dictyostelium: effects on morphology, growth, endocytosis, development, and the actin cytoskeleton. *Cell Motil Cytoskeleton*, **46**, 285-304.

Pang, K.M., Lee, E. and Knecht, D.A. (1998) Use of a fusion protein between GFP and an actin-binding domain to visualize transient filamentous-actin structures. *Curr Biol*, **8**, 405-408.

Parent, C.A. (2004) Making all the right moves: chemotaxis in neutrophils and Dictyostelium. *Curr Opin Cell Biol*, **16**, 4-13.

Parent, C.A., Blacklock, B.J., Froehlich, W.M., Murphy, D.B. and Devreotes, P.N. (1998) G protein signaling events are activated at the leading edge of chemotactic cells. *Cell*, **95**, 81-91.

Paululat, A., Holz, A. and Renkawitz-Pohl, R. (1999) Essential genes for myoblast fusion in Drosophila embryogenesis. *Mech Dev*, **83**, 17-26.

Peracino, B., Borleis, J., Jin, T., Westphal, M., Schwartz, J.M., Wu, L., Bracco, E., Gerisch, G., Devreotes, P. and Bozzaro, S. (1998) G protein beta subunit-null mutants are impaired in phagocytosis and chemotaxis due to inappropriate regulation of the actin cytoskeleton. *J Cell Biol*, **141**, 1529-1537.

Pitt, G.S., Gundersen, R.E. and Devreotes, P.N. (1990) Mechanisms of excitation and adaptation in Dictyostelium. *Semin Cell Biol*, **1**, 99-104.

Pollard, T.D., Blanchoin, L. and Mullins, R.D. (2000) Molecular mechanisms controlling actin filament dynamics in nonmuscle cells. *Annu Rev Biophys Biomol Struct*, **29**, 545-576.

Pollard, T.D. and Borisy, G.G. (2003) Cellular motility driven by assembly and disassembly of actin filaments. *Cell*, **112**, 453-465.

Postma, M., Bosgraaf, L., Loovers, H.M. and Van Haastert, P.J. (2004) Chemotaxis: signalling modules join hands at front and tail. *EMBO Rep*, **5**, 35-40.

Postma, M., Roelofs, J., Goedhart, J., Gadella, T.W., Visser, A.J. and Van Haastert, P.J. (2003) Uniform cAMP stimulation of Dictyostelium cells induces localized patches of signal transduction and pseudopodia. *Mol Biol Cell*, **14**, 5019-5027.

Pring, M., Evangelista, M., Boone, C., Yang, C. and Zigmond, S.H. (2003) Mechanism of formin-induced nucleation of actin filaments. *Biochemistry*, **42**, 486-496.

Raftopoulou, M. and Hall, A. (2004) Cell migration: Rho GTPases lead the way. *Dev Biol*, **265**, 23-32.

Reddien, P.W. and Horvitz, H.R. (2000) CED-2/CrkII and CED-10/Rac control phagocytosis and cell migration in Caenorhabditis elegans. *Nat Cell Biol*, **2**, 131-136.

Reif, K. and Cyster, J. (2002) The CDM protein DOCK2 in lymphocyte migration. *Trends Cell Biol*, **12**, 368-373.

Ridley, A.J., Schwartz, M.A., Burridge, K., Firtel, R.A., Ginsberg, M.H., Borisy, G., Parsons, J.T. and Horwitz, A.R. (2003) Cell migration: integrating signals from front to back. *Science*, **302**, 1704-1709.

Rivero, F., Albrecht, R., Dislich, H., Bracco, E., Graciotti, L., Bozzaro, S. and Noegel, A.A. (1999) RacF1, a novel member of the Rho protein family in Dictyostelium discoideum, associates transiently with cell contact areas, macropinosomes, and phagosomes. *Mol Biol Cell*, **10**, 1205-1219.

Rivero, F., Dislich, H., Glockner, G. and Noegel, A.A. (2001) The Dictyostelium discoideum family of Rho-related proteins. *Nucleic Acids Res*, **29**, 1068-1079.

Rivero, F., Illenberger, D., Somesh, B.P., Dislich, H., Adam, N. and Meyer, A.K. (2002) Defects in cytokinesis, actin reorganization and the contractile vacuole in cells deficient in RhoGDI. *Embo J*, **21**, 4539-4549.

Rogers, S.L. and Gelfand, V.I. (2000) Membrane trafficking, organelle transport, and the cytoskeleton. *Curr Opin Cell Biol*, **12**, 57-62.

Rupper, A. and Cardelli, J. (2001) Regulation of phagocytosis and endo-phagosomal trafficking pathways in Dictyostelium discoideum. *Biochim Biophys Acta*, **1525**, 205-216.

Santy, L.C., Ravichandran, K.S. and Casanova, J.E. (2005) The DOCK180/Elmo Complex Couples ARNO-Mediated Arf6 Activation to the Downstream Activation of Rac1. *Curr Biol*, **15**, 1749-1754.

Sanui, T., Inayoshi, A., Noda, M., Iwata, E., Stein, J.V., Sasazuki, T. and Fukui, Y. (2003) DOCK2 regulates Rac activation and cytoskeletal reorganization through interaction with ELMO1. *Blood*, **102**, 2948-2950.

Schiestl, R.H. and Petes, T.D. (1991) Integration of DNA fragments by illegitimate recombination in Saccharomyces cerevisiae. *Proc Natl Acad Sci U S A*, **88**, 7585-7589.

Schmidt, A. and Hall, A. (2002) Guanine nucleotide exchange factors for Rho GTPases: turning on the switch. *Genes Dev*, **16**, 1587-1609.

Scott, M.P., Zappacosta, F., Kim, E.Y., Annan, R.S. and Miller, W.T. (2002) Identification of novel SH3 domain ligands for the Src family kinase Hck. Wiskott-Aldrich syndrome protein (WASP), WASP-interacting protein (WIP), and ELMO1. *J Biol Chem*, **277**, 28238-28246.

Seastone, D.J., Harris, E., Temesvari, L.A., Bear, J.E., Saxe, C.L. and Cardelli, J. (2001) The WASp-like protein scar regulates macropinocytosis, phagocytosis and endosomal membrane flow in Dictyostelium. *J Cell Sci*, **114**, 2673-2683.

Seastone, D.J., Lee, E., Bush, J., Knecht, D. and Cardelli, J. (1998) Overexpression of a novel rho family GTPase, RacC, induces unusual actin-based structures and positively affects phagocytosis in Dictyostelium discoideum. *Mol Biol Cell*, **9**, 2891-2904.

Servant, G., Weiner, O.D., Herzmark, P., Balla, T., Sedat, J.W. and Bourne, H.R. (2000) Polarization of chemoattractant receptor signaling during neutrophil chemotaxis. *Science*, **287**, 1037-1040.

Sherr, C.J. (2004) Principles of tumor suppression. *Cell*, **116**, 235-246.

Southern, E.M. (1975) Detection of specific sequences among DNA fragments separated by gel electrophoresis. *J Mol Biol*, **98**, 503-517.

Srinivasan, S., Wang, F., Glavas, S., Ott, A., Hofmann, F., Aktories, K., Kalman, D. and Bourne, H.R. (2003) Rac and Cdc42 play distinct roles in regulating PI(3,4,5)P3 and polarity during neutrophil chemotaxis. *J Cell Biol*, **160**, 375-385.

Stramer, B., Wood, W., Galko, M.J., Redd, M.J., Jacinto, A., Parkhurst, S.M. and Martin, P. (2005) Live imaging of wound inflammation in Drosophila embryos reveals key roles for small GTPases during in vivo cell migration. *J Cell Biol*, **168**, 567-573.

Sussman, M. (1987) Cultivation and synchronous morphogenesis of Dictyostelium under controlled experimental conditions. *Methods Cell Biol*, **28**, 9-29.

Svitkina, T.M. and Borisy, G.G. (1999) Arp2/3 complex and actin depolymerizing factor/cofilin in dendritic organization and treadmilling of actin filament array in lamellipodia. *J Cell Biol*, **145**, 1009-1026.

Tuxworth, R.I., Cheetham, J.L., Machesky, L.M., Spiegelmann, G.B., Weeks, G. and Insall, R.H. (1997) Dictyostelium RasG is required for normal motility and cytokinesis, but not growth. *J Cell Biol*, **138**, 605-614.

Valles, A.M., Beuvin, M. and Boyer, B. (2004) Activation of Rac1 by paxillin-Crk-DOCK180 signaling complex is antagonized by Rap1 in migrating NBT-II cells. *J Biol Chem*, **279**, 44490-44496.

Van Haastert, P.J. and Devreotes, P.N. (2004) Chemotaxis: signalling the way forward. *Nat Rev Mol Cell Biol*, **5**, 626-634.

Van Haastert, P.J., Jastorff, B., Pinas, J.E. and Konijn, T.M. (1982) Analogs of cyclic AMP as chemoattractants and inhibitors of Dictyostelium chemotaxis. *J Bacteriol*, **149**, 99-105.

Vlahos, C.J., Matter, W.F., Hui, K.Y. and Brown, R.F. (1994) A specific inhibitor of phosphatidylinositol 3-kinase, 2-(4-morpholinyl)-8-phenyl-4H-1-benzopyran-4-one (LY294002). *J Biol Chem*, **269**, 5241-5248.

Weijer, C.J. (1999) Morphogenetic cell movement in Dictyostelium. *Semin Cell Dev Biol*, **10**, 609-619.

Weijer, C.J. (2004) Dictyostelium morphogenesis. *Curr Opin Genet Dev*, **14**, 392-398.

Weiner, O.D. (2002) Regulation of cell polarity during eukaryotic chemotaxis: the chemotactic compass. *Curr Opin Cell Biol*, **14**, 196-202.

Welch, H.C., Coadwell, W.J., Ellson, C.D., Ferguson, G.J., Andrews, S.R., Erdjument-Bromage, H., Tempst, P., Hawkins, P.T. and Stephens, L.R. (2002) P-Rex1, a PtdIns(3,4,5)P3- and Gbetagamma-regulated guanine-nucleotide exchange factor for Rac. *Cell*, **108**, 809-821.

Wu, L., Valkema, R., Van Haastert, P.J. and Devreotes, P.N. (1995) The G protein beta subunit is essential for multiple responses to chemoattractants in Dictyostelium. *J Cell Biol*, **129**, 1667-1675.

Wu, Y.C. and Horvitz, H.R. (1998) C. elegans phagocytosis and cell-migration protein CED-5 is similar to human DOCK180. *Nature*, **392**, 501-504.

Wu, Y.C., Tsai, M.C., Cheng, L.C., Chou, C.J. and Weng, N.Y. (2001) C. elegans CED-12 acts in the conserved crkII/DOCK180/Rac pathway to control cell migration and cell corpse engulfment. *Dev Cell*, **1**, 491-502.

Yamauchi, A., Kim, C., Li, S., Marchal, C.C., Towe, J., Atkinson, S.J. and Dinauer, M.C. (2004) Rac2-deficient murine macrophages have selective defects in superoxide production and phagocytosis of opsonized particles. *J Immunol*, **173**, 5971-5979.

Yin, J., Haney, L., Walk, S., Zhou, S., Ravichandran, K.S. and Wang, W. (2004) Nuclear localization of the DOCK180/ELMO complex. *Arch Biochem Biophys*, **429**, 23-29.

Zegers, M.M., Forget, M.A., Chernoff, J., Mostov, K.E., ter Beest, M.B. and Hansen, S.H. (2003) Pak1 and PIX regulate contact inhibition during epithelial wound healing. *Embo J*, **22**, 4155-4165.

Zheng, Y. (2004) G protein control of microtubule assembly. *Annu Rev Cell Dev Biol*, **20**, 867-894.

Zhou, K., Takegawa, K., Emr, S.D. and Firtel, R.A. (1995) A phosphatidylinositol (PI) kinase gene family in Dictyostelium discoideum: biological roles of putative mammalian p110 and yeast Vps34p PI 3-kinase homologs during growth and development. *Mol Cell Biol*, **15**, 5645-5656.

Zhou, Z., Caron, E., Hartwieg, E., Hall, A. and Horvitz, H.R. (2001) The C. elegans PH domain protein CED-12 regulates cytoskeletal reorganization via a Rho/Rac GTPase signaling pathway. *Dev Cell*, **1**, 477-489.

Zigmond, S.H. (2004) Formin-induced nucleation of actin filaments. *Curr Opin Cell Biol*, **16**, 99-105.